UNIVERSITY OF MILAN

DEPARTMENT OF CHEMISTRY

DOCTORAL COURSE IN ORGANIC CHEMISTRY
XXXI cycle

Rational Design and Synthesis of a Glycoconjugate Vaccine Against Group A *Streptococcus*

PhD student: Olimpia Pitirollo

Tutor: Prof. Luigi Lay

Co-tutors: Dott.ssa Francesca Micoli
Dott. Roberto Adamo

Coordinator: Prof.ssa Emanuela Licandro

A.A. 2017/2018

UNIVERSITÀ DEGLI STUDI DI MILANO

DIPARTIMENTO DI CHIMICA

CORSO DI DOTTORATO DI RICERCA IN CHIMICA
XXXI ciclo

Rational Design and Synthesis of a Glycoconjugate Vaccine Against Group A *Streptococcus*

Dottorando: Olimpia Pitirollo

Tutor: Prof. Luigi Lay

CO-tutors: Dott.ssa Francesca Micoli
Dott. Roberto Adamo

Coordinatore: Prof.ssa Emanuela Licandro

A.A. 2017/2018

Riassunto

I vaccini glicoconiugati sono uno degli strumenti più efficaci per la prevenzione delle infezioni batteriche. Sono composti da un antigene saccaridico scarsamente immunogenico, che viene covalentemente legato ad una proteina carrier non solo per aumentarne l'immunogenicità, ma anche per convertirne la risposta immunitaria da T-indipendente a T-dipendente, garantendo memoria immunologica. Tipicamente tali vaccini sono ottenuti come miscele eterogenee e complesse di poli o oligosaccaridi estratti dalle colture batteriche.

La sintesi chimica è un nuovo approccio per sviluppare vaccini glicoconiugati che presenta diversi vantaggi tra cui evitare la contaminazione con impurezze batteriche e introdurre un linker per la coniugazione all'estremità riducente dell'oligomero.

Nuove tecniche come la sintesi automatizzata in fase solida e la sintesi chemo-enzimatica hanno inoltre permesso di ridurre i tempi di sintesi e diminuire l'utilizzo di gruppi protettivi durante i vari step sintetici, permettendo una produzione di oligomeri su scala industriale.

Negli ultimi anni, l'utilizzo di nanoparticelle è stato proposto come delivery systems anche per i vaccini a base saccaridica. Le nanoparticelle d'oro (AuNPs) hanno attratto la loro attenzione in questo campo grazie alle loro caratteristiche, alla loro biocompatibilità e facile produzione. Infatti, negli ultimi anni AuNPs sono state testate come carrier per oligosaccaridi in modelli animali.

Delle nanoparticelle naturali sono le Generalized Modules for Membrane Antigen (GMMA). Le GMMA sono Outer Membrane Vescicles (OMV) che sono rilasciate naturalmente durante la crescita di batteri manipolati geneticamente per aumentare il grado di produzione delle vescicole e ridurre la loro tossicità. Come per altri nano-sistemi, le GMMA possono presentare in maniera multivalente gli antigeni, favorendo l'attivazione delle cellule B, ma hanno anche il vantaggio di presentare un effetto self-adiuvante.

In questo lavoro di tesi, oligosaccaridi corti di Streptococco di Gruppo A vengono sintetizzati e coniugati alla proteina carrier CRM_{197} (Cross-Reacting Material 197) per valutare la loro antigenicità comparandola al coniugato del polisaccaride naturale. Gli stessi oligomeri verranno coniugati alle GMMA e alle AuNPs per confrontare le GMMA come carrier alternativo alla proteina carrier CRM_{197} e verificare se l'effetto multivalente delle AuNPs può aumentare l'affinità di legame tra gli antigeni oligosaccaridici e gli anticorpi

Abstract

Glycoconjugate vaccines are one of the most effective ways of preventing bacterial and fungal infections. They are generally composed of a saccharide antigen covalently linked to a carrier protein to convert the saccharide from a T-independent to a T-dependent antigen, resulting in increased immunogenicity from infancy and memory response.

Currently, most of the conjugate vaccines are produced from polysaccharides extracted and purified from bacterial cultures. However, use of synthetic oligosaccharides constitutes a promising alternative approach. Synthetic saccharides have well-defined structure and can be equipped with a linker at their reducing end for selective conjugation allowing sugar epitopes preservation. Moreover, synthetic conjugates allow to avoid the handling of pathogens and presence of bacterial impurities and are characterized by minimal batch-to-batch variability and higher quality control standards compared to conjugates with native polysaccharides. New techniques such as solid phase automated synthesis and chemo-enzymatic approaches reduce reaction time and use of protective groups during synthetic steps and favor oligosaccharides production at large scale.

In addition, nanoparticles have been recently proposed as potential multivalent delivery systems also for carbohydrate-based vaccines. Gold nanoparticles (AuNPs) have attracted great attention in this field due to their unique characteristics of biocompatibility and easy production. In the last years, AuNPs have been tested as carrier for short synthetic oligosaccharides in animal models.

Natural nanoparticles can be obtained by the methodology called Generalized Modules for Membrane Antigens (GMMA). GMMA are Outer Membrane Vescicles (OMV) naturally released from Gram-negative bacteria genetically manipulated to increase blebbing and reduce toxicity. Similar to other nanoparticle systems, GMMA combine the multivalent display of carbohydrates, favoring B-cell activation and in a conformation that resembles on native bacteria, with optimal size for immune stimulation. GMMA also work as self-adjuvants, due to the presence of structures acting as agonist of Toll-like receptors 2 and 4, two receptors expressed on antigen presenting cells surface playing a crucial role in the innate immune response.

Here the chemical synthesis to obtain oligosaccharide fragments of Group A Carbohydrate (GAC) and the preparation of the corresponding glycoconjugates with CRM_{197} (cross-reacting material 197, a non-toxic mutant of diphtheria toxin) carrier protein have been reported. The main aim was to explore such synthetic structures for the development of a vaccine against Group A *Streptococcus* (GAS) disease for which no vaccine is currently available. The use of well-defined synthetic structures will help to better understand the impact of GAC structural features on the immune response induced. Synthetic oligomers have been conjugated to GMMA and AuNPs, with

the aim to i) compare GMMA and CRM_{197} as carrier systems, and ii) to explore multivalency on AuNPs to increase antibodies binding affinity.

CONTENTS

1 INTRODUCTION

1.1 General principles of vaccination

Immune system is responsible to identify and kill invading agents, known as pathogens, from viruses to microbes (bacteria, parasites, fungi), and distinguish them from the healthy tissue through specific interactions. The immune system can be classified into subsystems, the innate immune system and the adaptive immune system (including humoral immunity and cell-mediated immunity). The innate response is usually triggered when microbes are identified by pattern recognition receptors (PRRs), which recognize components that are conserved among broad groups of microorganisms, the pathogen-associated molecular patterns (PAMPs). Innate immune defense is non-specific, meaning these systems respond to pathogens in a generic way. This system does not confer long-lasting immunity against a pathogen. Innate response is able to activate adaptive immunity when it does not prevail on the intruder. The adaptive immune system allows for a stronger immune response as well as immunological memory, where each pathogen is "remembered" by a signature antigen. The adaptive immune response is antigen-specific and requires the recognition of specific "non-self" antigens during antigen presentation. Antigen specificity allows for the generation of responses that are tailored to specific pathogens which is maintained in the body by memory cells. Should a pathogen infect the body more than once, these specific memory cells are used to quickly eliminate it.

Vaccination takes advantage of this potential of adaptive immunity. Vaccination basically mimics a natural infection without causing disease by inducing in the host an immune response that leads to the production of antibodies (Abs). Abs are produced by B lymphocytes and they are able to recognize and specifically bind pathogen (or portion representative of it)[1] to facilitate uptake and elimination of the pathogen by other immune cells. Other important immune effectors are cytotoxic $CD8^+$ T lymphocytes (CTL) that may limit the spread of infectious agents by recognizing and killing infected cells or by secreting specific antiviral cytokines. The generation and maintenance of both B and $CD8^+$ T cell responses is supported by growth factors and signals provided by $CD4^+$ T helper (Th) lymphocytes, which are historically subdivided into T helper 1 (Th1), T helper 2 (Th2) and T helper 17 (Th17) subtypes. These effector cells are controlled by regulatory T cells (Treg) that are involved in maintaining immune tolerance[2]. Most of the antigens and vaccines trigger both B and T cell responses, and the two responses are interconnected: $CD4^+$ T cells are required for most Abs responses, while Abs confer significant influences on T cell responses to intracellular pathogens[3].

The stimulation of antigen-specific T cell responses requires their activation by specific antigen presenting cells (APCs), basically dendritic cells (DCs) recruited by inflammatory signals to the site of infection. APCs present antigens on Major Histocompatibility Complex (MHC) class II molecules, which is recognized by Th $CD4^+$. The activation of a resting helper T cell induce T cell to release cytokines and other stimulatory signals that stimulate the activity of macrophages, CTL and B cells, the latter producing Abs. The stimulation of B cells and macrophages succeeds a proliferation of T helper cells.

The central role for mature DCs in the activation of vaccine responses reflects their unique ability to provide both antigen-specific and co-stimulation signals to T cells. In fact, T cells require at least two signals to become fully activated: i) a first antigen-specific signal provided through the T cell receptor which interacts with the antigen peptide-loaded MHC class II molecules on the surface of the APCs; ii) a second antigen-unspecific signal, a co-stimulatory incentive, provided by the interaction between co-stimulatory molecules expressed on the membrane of the APCs upon maturation with its counterparts on the T cell.

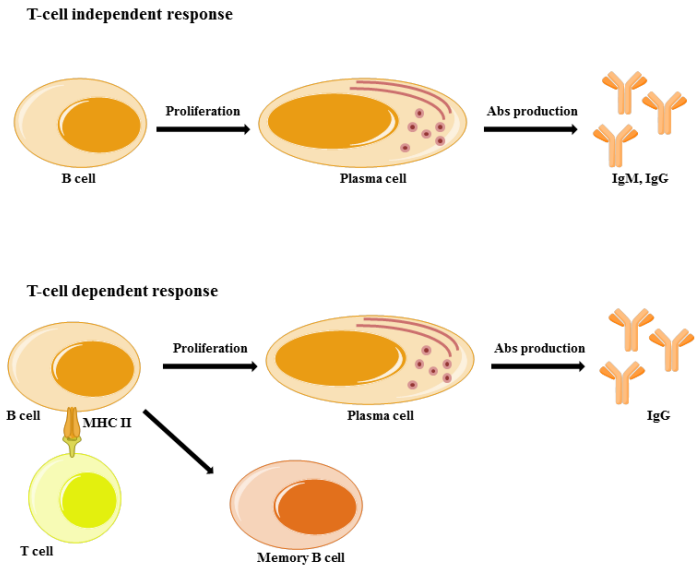

Figure 1: T-cell independent and dependent responses.

The very first requirement to elicit vaccine responses is thus to provide sufficient stimuli through vaccine antigens and eventually adjuvants, to trigger an inflammatory reaction that is mediated by cells of the innate immune system[4]. The protective efficacy of a vaccine is often conferred by microorganism-specific Abs, but just triggering a specific Abs response is not enough. The quality of Abs responses, such as Abs avidity has been identified as a determining factor of efficacy. Although B lymphocytes represent the main driver of Abs production once differentiated in plasma

cells, T cells can largely contribute to effective and long-lasting immune responses. Indeed, these cells are essential to immune memory, and novel vaccine targets have been identified against which T cells are likely to be the prime effectors.

In general, the Abs response to bacterial polysaccharides is poorly affected by adjuvants, IgM represents the major class of antibodies induced and since their immune response does not induce memory, it is not boosted by subsequent immunizations (Figure 1).

Polysaccharides are T-cell independent (TI) antigens as they do not require T-cell activation for the induction of specific B-cell (Abs) responses. Polysaccharides directly activate polysaccharide-specific B cells which differentiate then into plasma cells to produce Abs, but memory B cells are not formed. Moreover a pre-existing memory B-cell pool can be depleted by immunization with unconjugated polysaccharide, with risk of hypo-responsiveness on subsequent immunizations[5].

Differently from polysaccharides, proteins are T-cell dependent (TD) antigens; following interaction with APC (like DCs) macrophages and B-cells, protein antigens are internalized and processed into small peptides which are then re-exposed and presented to T lymphocytes in association with the MHC class II molecules. Interaction with T cells induces B cells to differentiate into plasma cells and memory B cells, thus initiating downstream adaptive immune responses. TD antigens are immunogenic early in infancy and the immune response induced can be boosted, enhanced by adjuvants and it is characterized in the production of antigen-specific IgG.

1.2 Carbohydrate-based vaccines

Polysaccharides are important virulence factor that are present on bacteria surface. They are specific for each bacterium and can be either polymers formed by one monosaccharide unit (homopolymers) or more complex oligosaccharide repeats (heteropolymers), that can be charged or neutral.

Surface polysaccharides have several functions: smooth surface and negative charge limits the ability to enhance phagocytosis. They protect microorganisms from desiccation when they are exposed to the external environment (an example is the hyaluronic capsule of Group A *Streptococcus*, whose adhesive properties help the pathogen to invade the host); mimic molecules produced by human cells so that the pathogen is not recognized as foreign by immune system (serogroup B meningococcal capsular polysaccharide, hyaluronic acid).

In 1945 the first vaccine composed by purified polysaccharides from selected pneumococcal serotypes was tested in humans[6].

Polysaccharide vaccines against meningococcus serogroups ACWY, *Streptococcus pneumoniae* and *Haemophilus influenzae* type b were licensed between the seventies and the eighties,[7,8] but they did not completely solve the problem of bacterial diseases caused by encapsulated microorganisms.

Being T-cell independent antigens, one of their main features which emerged from clinical trials, was their scarce immunogenicity in children under two years of age.[9,10] Consequently, polysaccharide vaccines can be used in adults, but not in infancy and elderly which are the most sensitive target populations.

1.3 Glycoconjugate vaccines

The limitation of carbohydrate-based vaccines can be overcome by covalent linkage of the carbohydrate moiety to a carrier protein as source of T-cell epitopes to make a glycoconjugate.

The first application of this concept to a vaccine for human use started in 1980 with the development of the first conjugate vaccine against *Haemophilus influenzae* type b (Hib) that was later on licensed between 1987 and 1990.[11,12] Glycoconjugate vaccines are among the safest and most efficacious vaccines developed during the last 30 years. They are a potent tool for prevention of life-threatening bacterial infectious disease; in fact, many other glycoconjugate vaccines have been licensed against bacterial pathogens such as *Neisseria meningitidis*, *Streptococcus pneumoniae*.

Many parameters of glycoconjugate vaccine can influence the immune response: the nature of the carrier protein, the site used for conjugation (random approach *vs* site specific approach), the glycan/protein ratio, the length of glycan, the chemistry used for conjugation[13].

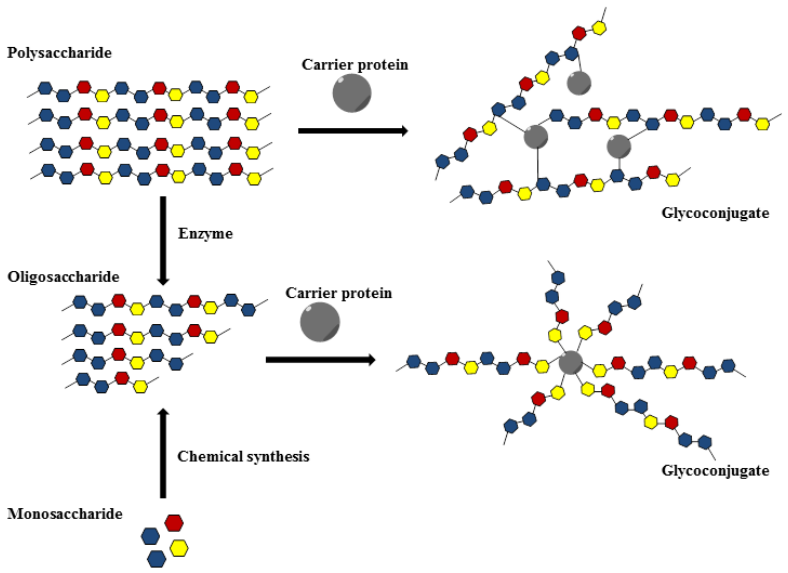

Figure 2: different approach for glycoconjugate synthesis.

Two main approaches are employed to prepare glycoconjugate vaccine (Figure 2). One is based on the random chemical activation of the glycan followed by covalent binding with the protein

obtaining a cross-linked structure between the polysaccharide and the protein. A second approach is based on the generation, by controlled fragmentation of the native polysaccharide, of appropriately sized oligosaccharides which are then activated at their terminal groups, usually with a linker molecule, and subsequently conjugated to the carrier protein obtaining a radial structure. Depending on the conjugation chemistry employed, a linker molecule can be used in order to facilitate the coupling between the protein and the saccharide chains and, in some cases, preliminary derivatization of the protein carriers is also required.

Bioconjugation is the new approach to prepare glycoconjugates, based on glyco-engineering of the bacterial N-glycosylation pathway in bacteria such as *Escherichia coli*. The polysaccharide, encoded by the inserted genes, is produced on a polyisoprenoid carrier then transferred to an asparagine residue of the carrier protein which has to contain at least one (native or engineered) N-glycosylation site.[14,15]

Different clinical trials have been conducted to compare the immunogenicity of different conjugate vaccines with different carrier proteins.[16–20] It is very difficult to make a direct comparison of the effect of different protein carriers, due to the coexistence of other variables as conjugation chemistry, saccharide chain length, adjuvant, formulation technology, and previous or concomitant vaccination with other antigens.

In the last years, studies about the role of saccharide/protein conjugation site on influencing immunogenicity were reported.[21] Two studies were conducted on CRM_{197} (cross-reacting material 197, a non-toxic mutant of diphtheria toxin) to understand if there are predominant attachment sites when random conjugation at lysines occur.[22,23] 6 out of the 40 lysine residues came out as the most exposed ones, but a complete control of conjugations to lysines is not possible. To overcome this problem, a novel conjugations strategy allowed selective introduction of synthetic oligosaccharide or polysaccharide on other residues such as tyrosines or disulfide bond.[24,25]

1.4 Advantages of synthetic oligosaccharides in vaccine development

Currently, most of the conjugate vaccines are produced from poly- or oligosaccharides extracted and purified from microbial cultures[5]. However microbial contamination (such as endotoxins) and heterogenicity (capsular polysaccharide fragments of different size) are inevitable drawbacks.

Synthetic approach provide well-defined, homogeneous and characterized oligosaccharides useful to support structural analyses to reveal protective epitopes, especially when carbohydrates are composed by complex structure.[26]

The use of synthetic oligosaccharides for vaccine development has many advantages: i) in theory, a well-established and optimized synthetic route can provide a much higher amount of carbohydrate

antigens than the natural source; ii) the fermentation of pathogenic bacteria is avoided; iii) possibility to evaluate the influence of antigen chain length, density and structure on immunogenicity; iv) introduction of a single reactive group per molecule for covalent conjugation, consistency and easiness of characterization; v) reproduciblity of biological process and high safety profile; vi) the use of automated system for the synthesis of oligosaccharides can facilitate the implementation of a synthetic vaccine approach at industrial scale.

There are a lot of examples of glycoconjugate vaccines exploiting synthetic glycan antigens[27] to combat bacterial and fungal infections at preclinical and clinical level. The feasibility of this approach has been shown by the licensing of QuimiHib®,[28] a glycoconjugate vaccine against *Haemophilus influenzae* type b, which is a second generation vaccine of synthetic glycan conjugated to TT carrier protein.[27,28]

In the last years, also the enzymatic synthesis of oligosaccharides was developed and generally it gives high yields, with complete regio- and stereospecificity without the need of installation and removal of a large number of protecting and activating groups. When combined, chemical and enzymatic approaches can lead to the production of well-defined synthetic oligosaccharides, avoiding huge synthesis timelines above all when challenging structures motifs and/or oligosaccharides with several repeating units are needed.[29]

1.5 Alternative carrier system to develop glycoconjugate vaccines

1.5.1 Glyco Gold-Nanoparticles (AuNPs): an inorganic core for oligosaccharide

The growing interest in nanoscience, the discipline aimed at the preparation and manipulation of materials at a nanometric scale, has led to in-depth study of the properties of organic-inorganic hybrid materials.[30] These materials present new collective chemical-physical properties due to the interaction between organic and inorganic units and they find numerous applications in different fields such as electronics, catalysis, and biomedical.

Among the large number of nanomaterials, gold nanoparticles (AuNPs) offer great potential for many applications due to their biocompatibility, low toxicity, chemical stability, and plasmonic features. Thanks to the high surface/volume ratio and to the easy surface functionalization which exploits the strong Au-S bond (~50 Kcal/mol), AuNPs are suitable polyfunctional scaffolds to explore the multivalent presentation of antigens (Figure 3).[31] Moreover, some examples of carbohydrate antigens conjugated to AuNPs showing high *in vivo* immunogenicity have been already reported.[32]

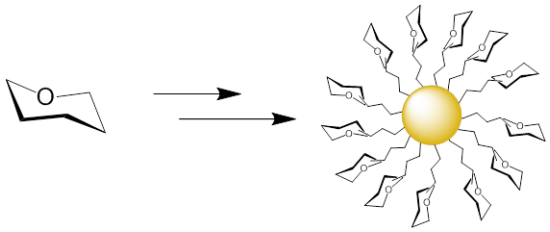

Figure 3: AuNPs coated with carbohydrates.

The AuNP-based multivalent systems have been explored in the field of carbohydrate-based vaccine and AuNPs coated with synthetic glycan can be used as nanocarriers to improve the enhancement of immune response. The introduction of a T-cell helper on AuNP surface can trigger a T-dependent response and glyco-AuNPs can be considered as novel platform for vaccine development.[31–33] The examples in the use of AuNPs as nanocarriers for vaccine development has been reported for *Streptococcus Pneumoniae* type 14 and type 19F and by *Neisseria Meningitidis* serogroup A.[31] In each case, AuNPs were coated with the glycan antigens and the ovalbumin (OVA 323-339) T-cell helper peptide. The nanosystems were able to induce high Abs titers and the size of AuNPs has an impact on the immune response. Indeed, it is known that multivalency depends on the size and morphology of AuNPs and, as consequence, can influence the immune response induced.

1.5.2 Generalized Modules for Membrane Antigens (GMMA)

Gram-negative bacteria naturally release outer membrane vesicles (OMV) during the growth.[34,35] The genetic modification of bacteria induce over blebbing of OMV, known as Generalized Modules for Membrane Antigen, GMMA (Figure 4).[36]

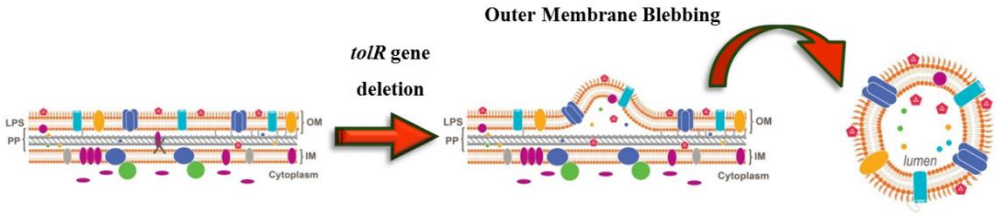

Figure 4: Generalized Modules for Membrane Antigens (GMMA) blebbing.

GMMA contain the membrane antigens, like proteins, lipids, and the lipopolysaccharide (LPS), the main virulence factor of Gram-negative bacteria. Different genetic modification of bacteria can be introduced in order to detoxify LPS of resulting GMMA, modulating the degree of acyl chains of Lipid A.[37] GMMA can be obtained in high yield and with low production and manufacturing costs compared to classical vaccines. OMV-based vaccines have been successfully developed and used,

i.e. BexSero®, MenBvac®, MeNZB, and other promising vaccine against *Bordetella pertussis*,[38] *Burkholderia pseudomallei*[39,40] and *Vibrio cholerae*[41,42] were tested. The main problem of OMV vaccines is the manipulations of large volume of bacteria for the manufacturing and the safety due to LPS for administration in humans. GMMA based vaccine can overcome these limits.

The advantages in the use of GMMA for vaccine development are many: they present optimal size for immune-stimulation (~100 nm), adjuvant effect, ability to be uptaken from mammalian cells and can result in a multivalent vaccine. Indeed, it is possible to delete the undesired antigens or overexpress the desired antigens using a combination of different and subsequent genetic modification.[43,44] Because of their composition which combines proteins and components activating the immune system (TLR2 and TLR agonists), GMMA hold the potential to be used as carrier alternative to more traditional proteins (TT, CRM_{197}).[45]

1.6 Group A Streptococcus*:* a pathogen in need of a vaccine

Streptococcus pyogenes (Group A streptococcus, GAS) is a Gram-positive bacterium with a diameter of 0.5-1.0 μm that grows in long chain, 1-2 mm colonies, with β-hemolytic activities after 24 hours. GAS is an optional anaerobic bacterium, capsulated, asporigen, with homolactic metabolism and catalase negative. GAS cell wall consists of several proteins: R and T proteins are epidemiologic markers; the M protein (encoded by *emm* gene) is the most virulence factor and responsible of more than 200 *emm* serotypes. GAS is surrounded by a peptidoglycan layer consisting in N-acetylglucosamine and N-acetylmuramic acid repeating units, while the capsule is composed of hyaluronic acid[46] (Figure 5). The cell surface exposes also a carbohydrate, the Lancefield Group A Carbohydrate (GAC), consisting of α-L-Rha*p*(1→3)-α-L-Rha*p*(1→2)-[β-D-Glc*p*NAc-(1→3)] repeating units.[47,48]

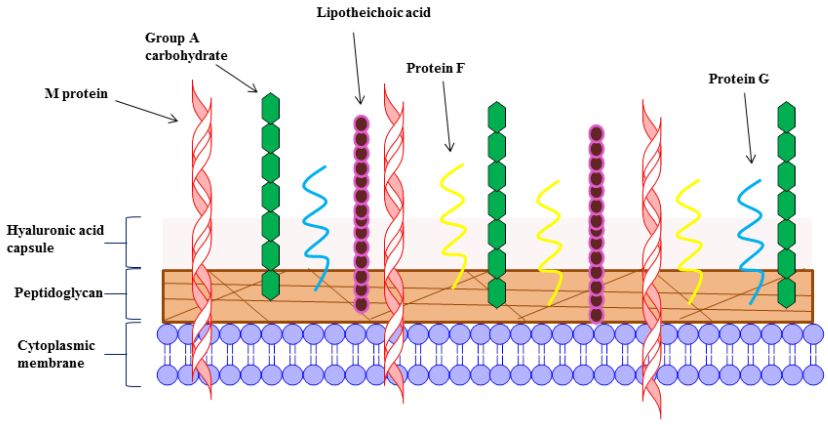

Figure 5: Group A Streptococcus.

Distribution of GAS *emm* types varies according to geographic and socio-economic factors. In industrialized countries (Europe, United States, New Zealand) a significant percentage of GAS isolates belongs to *emm* types 1, 3, 12 and 28 and are responsible for 40% of disease in these countries, while in developing countries (Africa, Asia) they are less common.[49,50,51]

GAS cause a large range of superficial infections, like pharyngitis, scarlet fever and impetigo, and post-infection sequelae, like acute rheumatic fever, rheumatic hearth disease and acute poststreptococcal glomerulonephritis which are predominant in impoverished communities. Acute rheumatic fever and rheumatic hearth disease are the major cause of heart disease in children, adolescents and young adults responsible of more than 350,000 deaths per year among children aged 5-14 years. The cases of pharyngitis and scarlet fever are greater than those of more severe disease; although, these diseases seem relatively unimportant they cause significant healthcare-related social costs, in particular because of the use of antibiotics[50].

GAS is resistant to immune defense system of the host thanks to the presence of surface-bound and secreted virulence factors. Moreover, it is resistant to opsonophagocytosis due to the presence of complement inhibitors, like M protein, leukocidal toxins and immunoglobulin (Ig) binding proteins.[51]

1.7 The M protein and vaccine currently in use

There are no safe and efficacious licensed vaccine against GAS due to the diversity of GAS *emm* strains, antigenic variation and differences in the geographical distribution of serotypes. Moreover, the autoimmune reaction raised by GAS antigen represent an additional critical issue.[50,52]

The main driver of autoimmunity is the M protein which is formed by 3 domains: the N-terminal domain, highly variable and responsible of *emm* types differentiation; the B-repeat domain, inducing not-opsonic Abs; the C-repeat domain, that is highly conserved.[53] Several studies involved M protein formulation administered to human volunteers followed by challenge with GAS bacteria, resulting in decreased GAS colonization but increased incidence of acute rheumatic fever in immunized subjects.[50,53] Several M protein-based vaccines have been investigated using the N-terminal region of the protein that maybe is not involved in autoimmunity.[54] There are three formulations of M protein-based vaccine: a hexavalent preparation[54], a 26-valent preparation[55] and a 30-valent formulation, currently, the only one in clinical Phase I[56] which is well tolerated by adult volunteers. The main problem of these vaccines is that they are protective only against the serotypes included in the formulation. To overcome this problem, other M protein-based vaccines have been designed using the highly conserved C-region of the M protein, since this can eliminate concerns about autoimmunity[57]. These vaccines, J8 and J14, contain shorter B cell epitopes from C-region of M protein and induced protective and bactericidal Abs.[58–60]

1.8 Group A Carbohydrate (GAC) as universal GAS antigen

The group A carbohydrate (GAC), composed of α-L-Rha*p*(1→3)-α-L-Rha*p*(1→2)-[β-D-Glc*p*NAc-(1→3)] repeats[3] (Figure 6), is a polysaccharide exposed on the cell wall of GAS. Since this polysaccharide is preserved and expressed by all GAS serotypes and, therefore, it has been considered a common antigen to develop a GAS vaccine. Indeed, GAC conjugated to tetanus toxoid (TT) induces high Abs titers in rabbits.[61]

In 2005, Sabharwal et al. reported that GAC-TT conjugate is able to induce Abs titers in animal model and humans and the titers of these Abs increase with increasing age. The raised Abs were opsonic and induced protection after active and passive challenge in mice.[61,62]

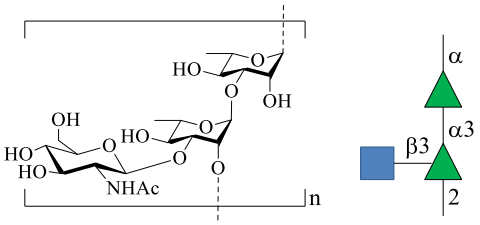

Figure 6: Group A Carbohydrate (GAC) repeating unit.

Several studies have been published about the use of GAC oligosaccharides in order to identify the minimal epitope recognized from Abs. The synthetic strategy used to prepare GAC trisaccharide and GAC hexasaccharide (GAC dimer) was reported by M. Pinto and coworkers. An efficient and convergent synthesis of GAC oligosaccharides was achieved in 1996 by the same group, following a strategy that limit the number of protections and deprotections to prepare an allyl glycoside for conjugation to a carrier protein. The oligomers were conjugated to BSA (bovine serum albumin) and Ovalbumin carrier proteins using N-acryloylated or diethyl squarate linkers.[63–65]

Epitope mapping studies were conducted to understand the minimal epitope recognized by monoclonal Abs (mAbs) using STD-NMR and other bidimensional NMR experiments. STD-NMR spectra of the trisaccharide were acquired in the presence of mAbs resulting in a strong enhancement of GlcNAc signal, especially the acetyl group. The STD-NMR spectra of GAC dimer showed an extended pattern of signals: the strongest binding is with GlcNAc, while the weak interaction was observed between the mAbs and the methyl group of Rha units, suggesting that the GlcNAc is the immunodominant epitope recognized, while the Rha residues are an extended surface of binding.[66,67] In 2011, Kabanova et al reported the conjugation to CRM_{197} of GAC dimers and tetramers bearing an amino linker at the reducing end and presenting the GlcNAc residue at the upstream end or within the backbone protein[68] (Figure 7). These conjugates were fully characterized and used for mice immunization with the GAC-CRM_{197} conjugate as positive control.

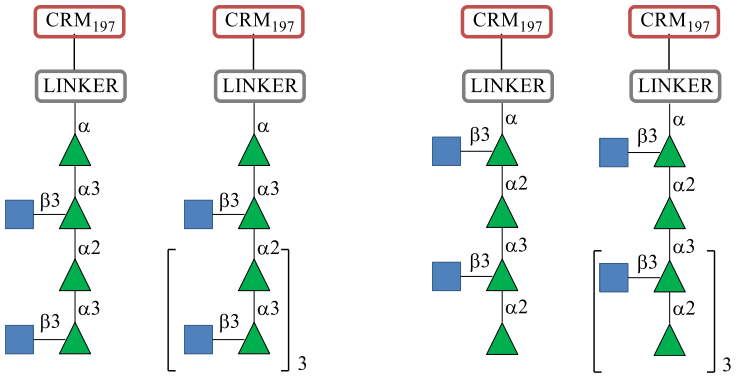

Figure 7: GAC oligosaccharides used for study in mice in reference [67]

The conjugated oligosaccharides showed Abs titers comparable to the native GAC. Furthermore, they induced protection against two GAS isolates of M1 and M23 serotypes after challenge. Of note, the GAC dimer and tetramer conjugated to CRM_{197} induced similar Abs titers, regardless of the GlcNAc position, however the loading on protein was higher for the shorter oligomers. Therefore, higher levels of glycan incorporation onto the protein could compensate the shorter length. Recently, M. Pinto et al. reported the mice immunization with conjugates of synthetic GAC dimer to TT carrier protein.[69] They confirmed the immunogenicity of the GAC dimer-TT conjugate by primary and secondary Abs response (IgM and IgG response). The Abs titers were similar to GAC-TT conjugate, according to the data reported by Kabanova. Collectively these data indicate that the GAC dimer has a sufficient chain length to be used as a potential synthetic structure to develop an anti-GAS glycoconjugate vaccine.

1.9 Polyrhamnose: an alternative antigen to develop a GAS vaccine

GAS causes an autoimmune response that leads to rheumatic disease and the main driver of autoimmunity is the M protein. During the last years, it was hypothesized that GlcNAc side chain of GAC can induce cross-reactive Abs relevant to immunopathogenesis of rheumatic diseases.[70] Monoclonal Abs against the GlcNAc epitope of GAC were proved able to recognize myosin, a protein associated with myocarditis and rheumatic disease.

Glycoproteins from human heart valves, when used to immunize rabbits, produce antibodies that bind GAC in a manner inhibited by GlcNAc (but not by rhamnose and other sugars), and persistence of anti-GlcNAc/GAC antibodies (from 1 to 20 years) are a marker of poor prognosis of heart valve problems in rheumatic heart disease, whereas antibodies against streptolysin O and the polyrhamnose core of GAC decline independently of valve complications. The specificity and persistence of elevated anti-GAC (GlcNAc) antibody titers for rheumatic mitral valve heart disease was also suggested in a study of 30 patients versus equal-sized control groups of individuals, patients with congenital heart disease, and patients with nonrheumatic mitral valve prolapse. Finally, anti-GlcNAc monoclonal antibodies (mAbs), cross-reactive for heart or brain tissue, have been derived from patients with rheumatic fever and related cardiac or neurological complications.[71]

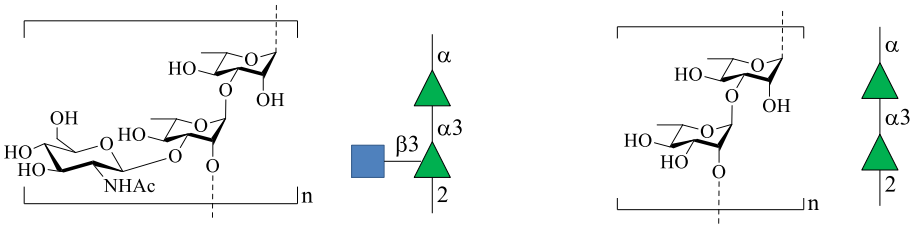

Figure 8: GAC repeating unit and polyRha repeating unit.

Moreover, it has been reported that Abs to GAC lacking the GlcNAc side chain and containing only the polyrhamnose (polyRha) backbone (Figure 8) promoted opsonophagocytic killing of multiple GAS strains and protected against systemic GAS challenge after passive immunization.[71] Henningham et al proposed that GlcNAc side chain is a virulence factor in the context of other antigens.[72] The GlcNAc side chain contributes to innate immune resistance of serotype M1 of GAS but the relative contribution is different among individual strains and, consequently, the GlcNAc could not be a universal prerequisite for GAS virulence in animal model that depends on the relative contribution of other virulence factors that each strain possesses.

Based on these findings, polyRha has been proposed as alternative antigen to develop an anti-GAS glycoconjugate vaccine.

2 AIM OF THE PROJECT

2.1 Synthetic approach to develop an anti-GAS glycoconjugate vaccine

GAS causes a range of diseases, from simple superficial skin infections and pharyngitis to severe invasive infections.[49] As reported in the introduction, GAC, a conserved surface polysaccharide comprising α-L-Rha*p*(1→3)-α-L-Rha*p*(1→2)-[β-D-Glc*p*NAc-(1→3)] repeats, has been proposed for the design of an efficacious anti-GAS glycoconjugate vaccine.[62]

Although the main driver of GAS autoimmune responses is the so-called M protein,[50] some studies have linked GlcNAc side chain of GAC with cross-reactive epitopes that might also be responsible for rheumatic diseases.[71] On the other hand, it has been shown that Abs induced by the polyRha backbone alone promote opsonophagocytic killing of multiple GAS strains and, therefore, polyRha could be an alternative to GAC for a broadly conserved vaccine candidate against GAS infections.

Synthetic GAC oligosaccharides (hexasaccharides and dodecasaccharides, Figure 7), conjugated to CRM_{197} carrier protein, have been tested as vaccine antigens in a mouse challenge model showing similar immunoprotection to conjugates of native GAC.[68] Two repeating units (GAC-dimer) have been reported as the minimal GAC epitope that could secure efficient opsonophagocytosis and protection.[73]

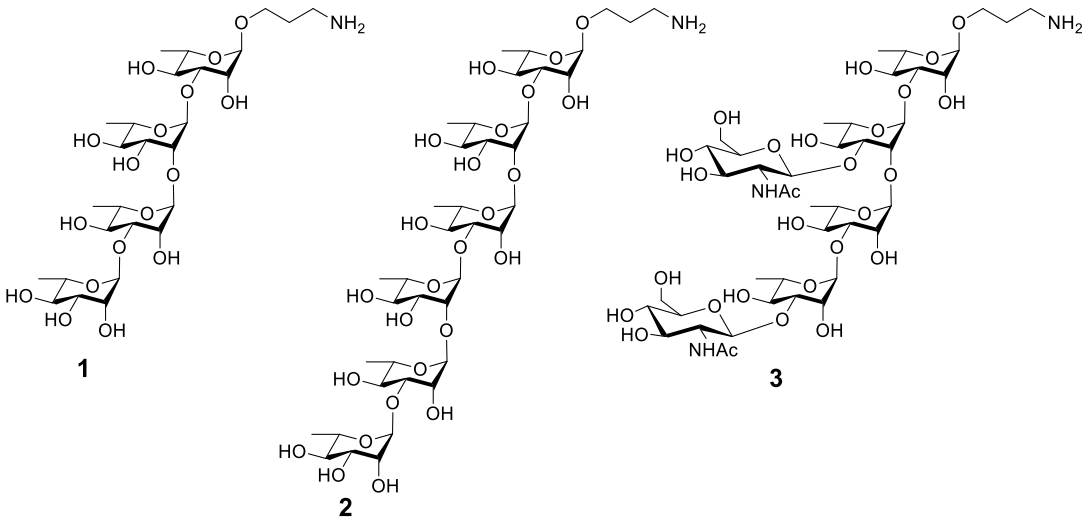

Figure 9: Synthetic target: tetraRha **1**, hexaRha **2**, GAC-dimer **3**.

In this context the major aim of my PhD project was the synthesis of oligorhamnose (oligoRha) structures with two different chain length, tetraRha **1** and hexaRha **2**, and the dimer structure of two repeating units of GAC (GAC-dimer **3**) (Figure 9). Such oligomers have been conjugated to CRM_{197} carrier protein. Immunological evaluation in mice of these well-defined constructs, in comparison to native GAC, helps to clarify the role of GlcNAc residues and polyrhamnose

backbone in the immune response induced by GAC glycoconjugate. In particular, the first objective was to clarify if oligoRha can be an antigen to develop a GAS vaccine. It is reported that polyrhamnose extracted from modified GAS bacteria was recognized by an autoreactive human mAb derived from a patient with rheumatic carditis.[71] However the use of synthetic well-defined and purified structures conjugated to a carrier protein helps clarify the role of polyRha core of GAC during the immune response. Two different length of oligorhamnoses were chosen: tetraRha **1** has the same number of rhamnose units of GAC-dimer **3**, which is known to raise high Abs titers comparable to the native GAC polysaccharide.[68] HexaRha **2** is one unit longer than tetraRha **1** to understand if the chain length can have an impact during the immune response induced.

Different conjugation chemistries have been explored to find the best conditions for preparing glycoconjugates with synthetic oligomers. The use of well-defined and purified oligosaccharides to make a conjugate can allow to use a site-selective conjugation approach instead of the random approach resulting in higher synthetic reproducibility compared to the conjugate of the native GAC. Moreover, shorter oligosaccharide can allow to evaluate the influence of antigen chain length and density on the immunogenicity.

2.2 Investigation of multivalent nanosystem for vaccine development

Recently, different kinds of nanosized systems have been used as alternative carriers to more traditional proteins.[74] In this context, the GSK Vaccines for Global Health (GVGH) Institute is using GMMA as carriers for protein and polysaccharide antigens. GMMA are OMV naturally released from Gram-negative bacteria that are genetically modified to enhance the level of particles produced and reduce reactogenicity.[37,43] Here, *Salmonella Typhimurium* GMMA will be used as carrier for native GAC and GAC oligomers (tetraRha **1**, hexaRha **2** and GAC-dimer **3** showed in Figure 9), with the potential to result in a vaccine covering both nontyphoidal *Salmonella*[44] and GAS diseases. Different conjugation chemistries will be explored – targeting LPS or proteins on GMMA surface (Figure 10) to evaluate possible impact on glycan loading and immune response induced.

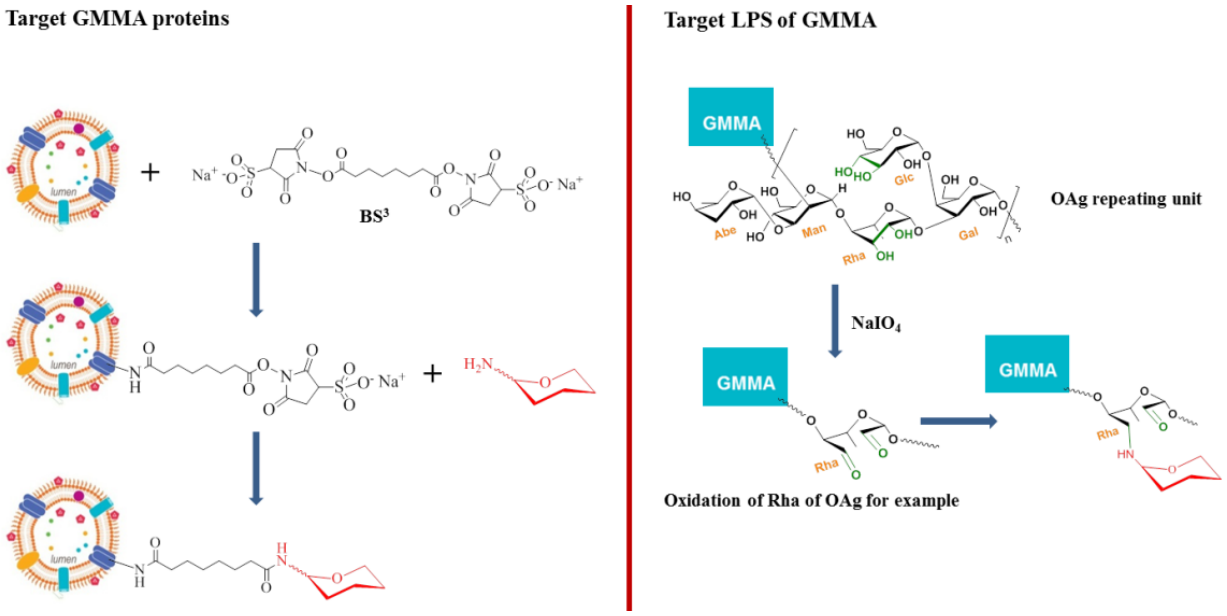

Figure 10: Strategy of GMMA conjugates synthesis: targeting the GMMA protein with a linker and targeting the LPS of GMMA with reductive amination reaction after oxidation of LPS sugar units.

Alternatively, AuNPs are suitable polyfunctional scaffolds to explore the multivalent presentation of antigens.

To explore the multivalency of AuNPs, two different types of AuNPs will be prepared, sphere and star, and will be coated with oligoRha **1** and **2**. AuNPs will be tested as nanoscaffolds to increase antibodies (Abs) binding affinity.

3 RESULT AND DISCUSSION

3.1 Synthesis of oligorhamnoses: tetraRha and hexaRha

The synthesis of tetraRha and hexaRha has been performed starting from building blocks **4** and **5**, already available in GSK Vaccines Lab (Adamo R.'s group). The synthetic approach followed had been already reported[22] and it is summarized in Figure 11.

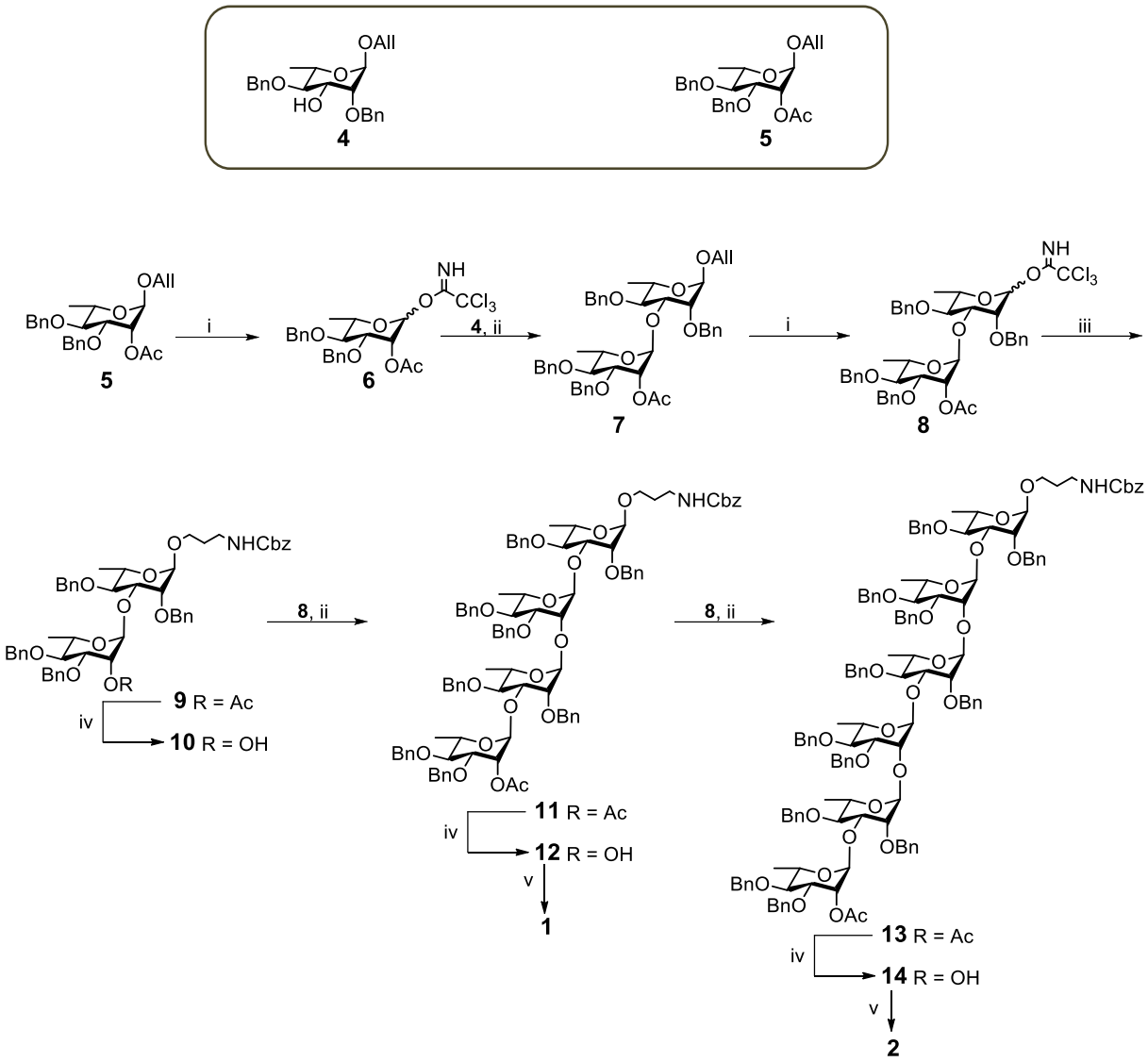

Figure 11: Synthesis of tetraRha **1** and hexaRha **2**. Reagents and conditions: i) a) Ir cat, THF, H_2; I_2, H_2O; b) CCl_3CN, DBU, DCM, 95% yield; ii) TMSOTf, DCM, 0°C, 75%-86% yield; iii) $HO(CH_2)_3NHCbz$, TMSOTf, DCM, 0°C, 60% yield; iv) NaOMe/MeOH, quantitative yield; v) H_2O/EtOH 1:1 + 5% HCl, H_2(20 bar), Pd/C, 90% yield.

The allyl glycoside **7** was prepared from monosaccharides **4** and **5**. Compound **5** was deallylated and activated as trichloroacetimidate, which is a good leaving group in the glycosylation step. The deallylation involves the use of Iridium catalyst and hydrogen to isomerize the allyl group; addition of iodine and water gives the hydrolysis. Then donor **6,** needed to install the *α*-L-Rha*p*(1→3)-α-L-

Rha*p*(1→OAllyl) moiety, was prepared from the hemiacetal by reaction with trichloracetonitrile and DBU in 95% yield. Donor **6** reacted with acceptor **4** (0°C and trimethylsilyl triflate as promoter) to give disaccharide **7** in 75% yield, which is a key intermediate for both the donor and the acceptor leading to longer structures. Compound **7** was deallylated and activated as trichloroacetimidate. Benzyl N-(3-hydroxypropyl)-carbamate was reacted with donor **8** under the a before mentioned conditions leading to **9** in 60% yield. Deacetylation of **9** with sodium methoxide in methanol provided the disaccharide acceptor **10**. This was reacted with the disaccharide donor **8** to obtain tetrarhamnose **11**, in 86% yield. Next, **11** was deacetylated and compound **12** was glycosylated with donor **8** to obtain hexasaccharide **13**, in 86% yield.

Finally, target compounds **1** and **2** were obtained with two deprotection steps: deacetylation of the downstream rhamnose residue, followed by hydrogenolysis. The latter reaction was conducted at high pressure of hydrogen (20 bar) in the presence of Pd/C catalyst in EtOH/H_2O 1:1 + 5% aq. HCl. Final products were obtained both in 90% yield.

3.2 Synthesis of GAC dimer

The synthesis of oligoRha described in Figure 11 cannot be used to prepare the GAC-dimer because the introduction of the GlcNAc residues requires an orthogonal protective group at 3-OH of the two rhamnose units to be glycosylated. The naphtyl group was chosen as additional and orthogonal protecting group and three new monosaccharide building blocks were prepared: the acceptor **22** (bearing the linker moiety), the donor precursor **28** and the allyl glycoside acceptor **30** (Figure 12).

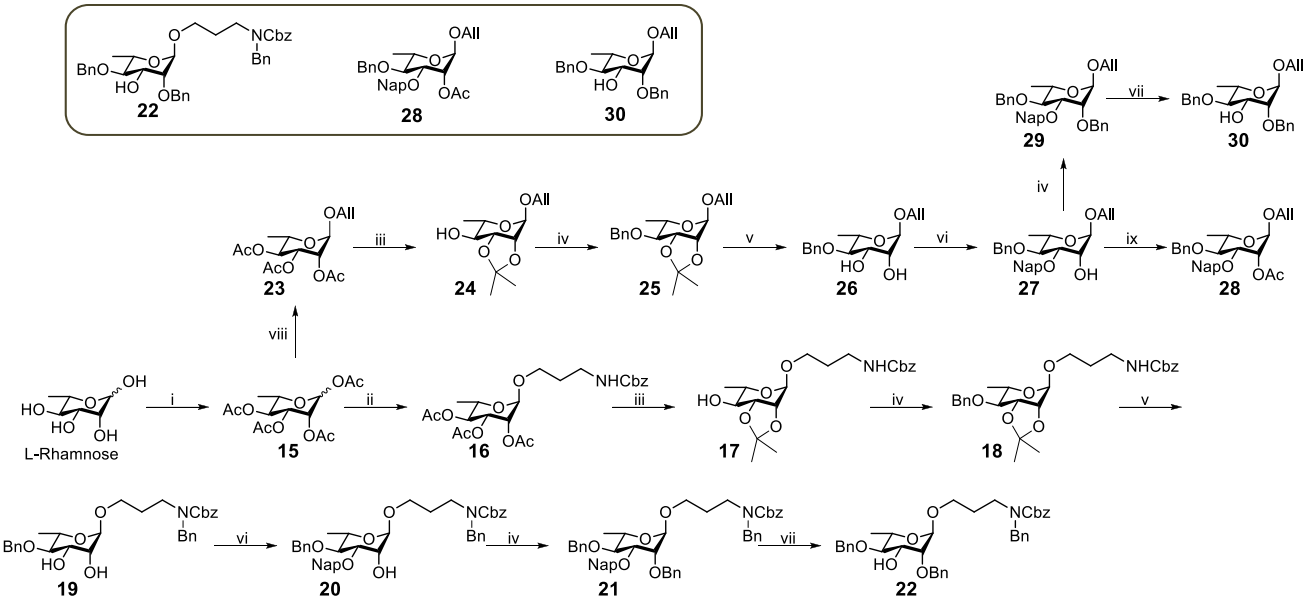

Figure 12: Synthesis of building blocks **22**, **28** and **30**. Reagents and conditions: i) I_2, Ac_2O, quantitative yield; ii) $HO(CH_2)_3NHCbz$, BF_3Et_2O, DCM, 0°C→rt, 62% yield; iii) a) MeONa/MeOH; b) $(CH_3O)_2C(CH_3)_2$/DCM 4:1, p-TsOH, 85% yield; iv) NaH, BnBr, DMF, 72%-95% yield; v) TFA 50%, DCM, quantitative yield; vi) Bu_2SnO, toluene; NapBr, TBAI, 45°C, 54%-58% yield; vii) DDQ, DCM/MeOH 4:1, 82% yield; viii) CH_2CHCH_2OH, BF_3Et_2O, DCM, 0°C→rt, 60% yield; ix) Py, Ac_2O, 98% yield.

The treatment of Rha peracetate **15** with benzyl N-(3-hydroxypropyl)-carbamate or allyl alcohol in the presence of BF_3Et_2O in dichlorometane gave α-glycosides **16** and **23** in 62% and 60% yield, respectively. Compound **16** was deacetylated with MeONa/MeOH and the isopropylidene acetal was introduced at 2- and 3-positions to give **17** in 87% yield, which was benzylated at 4-OH using benzyl bromide and sodium hydride and converted into compound **19** by removal of the isopropylidene acetal.

The naphtylmethyl group was regioselectively installed in the equatorial 3-OH of diol **19** by reaction with dibutyltin oxide and subsequent treatment with 2-(bromomethyl) naphtalene and tetrabutylammonium iodide for in situ formation of the more reactive NapI intermediate in 54% yield. Compound **20** was benzylated at 2-OH; using a large excess of NaH and BnBr, N-benzylation also occurred, providing rhamnoside **21** in 78% yield. Compound **21** was treated with dichloro dicyano benzoquinone in DCM/MeOH 4:1 to remove the Nap group obtaining the monosaccharide acceptor **22** in 82% yield.

Likewise, the same manipulations of protective groups were applied to monosaccharide **23** to synthesize the alcohol intermediate **27** (yield 58%). Subsequent 2-O-acetylation of **27** provided allyl glycoside **28**, whereas 2-O-benzylation followed by removal of the Nap group with DDQ led to the formation of acceptor **30** in 82% yield (Figure 12).

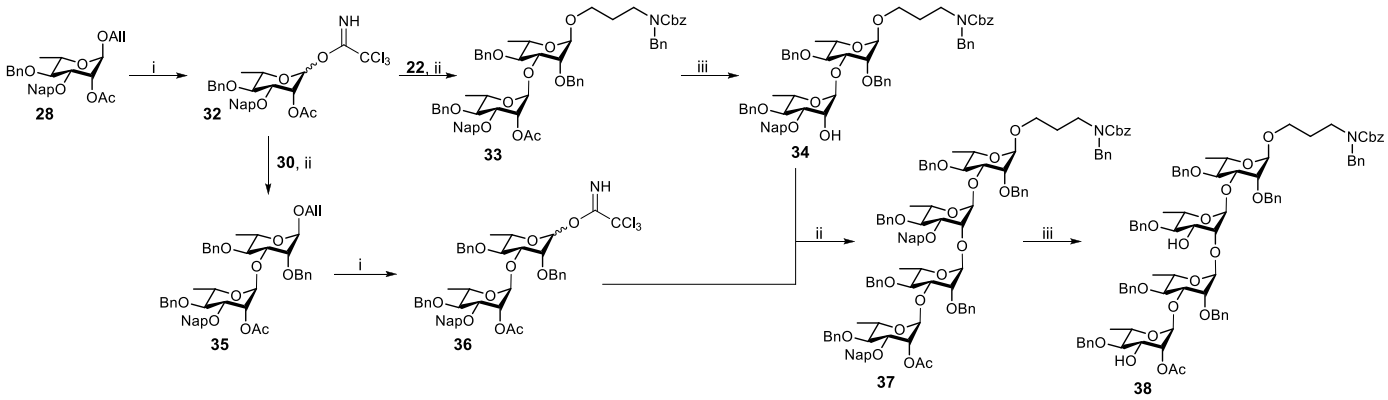

Figura 13: Synthesis of tetrasaccharide **38**. Reagents and conditions: i) Ir cat, THF, H_2; I_2, H_2O; CCl_3CN, DBU, DCM, 85% yield; ii) TMSOTf, DCM, 0°C, 72%-87% yield; iii) NaOMe/MeOH, quantitative yield; iv) DDQ, DCM/MeOH 4:1, 78% yield.

As illustrated in Figure 13, compound **28** was deallylated and activated as trichloroacetimidate **32** (85% yield), which reacted with acceptor **22** in the presence of TMSOTf to give disaccharide **33** containing the linker for future conjugation in 85% yield. Disaccharide **33** was treated with MeONa in MeOH to remove the acetate leading to the formation of disaccharide acceptor **34**. In parallel, donor **32** and acceptor **30** were coupled to obtain disaccharide **35** in 72% yield. This intermediate is a key building block in our synthesis because it is the common precursor of both the acceptor and the donor required for chain elongation Disaccharide **35** was deallylated and activated as trichloroacetimidate **36** to react with disaccharide **34** and obtain tetrasaccharide **37** in 87% yield.
The simultaneous cleavage of the two Nap groups provided compound **38** in 78% yield (Figure 13).
A number of glucosamine donors to perform a double glycosylation were tested by using different conditions, as reported in Table 1. Donors **39**, **40** and **41** (Figure 14) were already available in L. Lay's group (University of Milan) and R. Adamo's group (GSK Vaccines). With thioglycosides **39** and **40** the product of double glycosylation was never isolated due to the formation of many byproducts that made the reaction mixture difficult to purify. On the contrary, using trichloroacetimidate **41** as the donor the product of double glycosylation was successfully obtained (Figure 14).

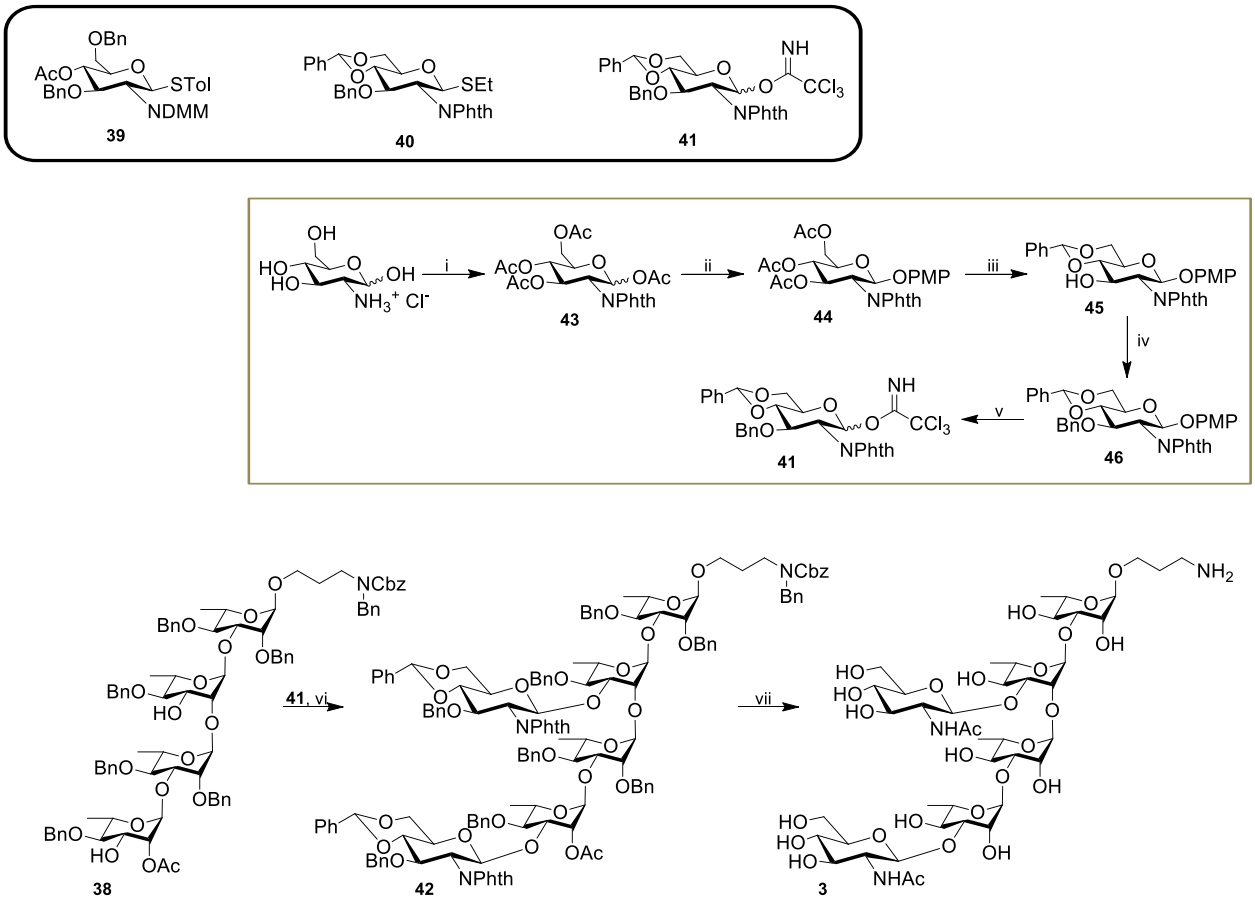

Figure 14: Synthesis of GAC-dimer **3**. Reagents and conditions: i) NaOMe/MeOH, phthalic anhydride, TEA; Ac_2O, Py, 47% yield; ii) p-methoxyphenol, BF_3 Et_2O, DCM, 0°C, 89% yield; iii) NaOMe/MeOH; benzaldehyde dimethyl acetal, PTSA, CH_3CN, 84% yield; iv) BnBr, NaH, DMF, 82% yield; v) CAN, CH_3CN; CCl_3CN, DBU, DCM, 70% yield; vi) TMSOTf, DCM, 0°C, 47% yield; vii) ethylenediamine, EtOH; Py, Ac_2O; NaOMe/MeOH; H_2O/EtOH 1:1, Pd/C, H_2(3 bar), 40% yield.

Table 1: reaction conditions of double glycosilation reactions	
Reagents	**Conditions**
Donor **39** Acceptor **38**	Triflic acid 0.2 eq, N-iodosuccinimide 2.5 eq, DCM, -40°C→0°C [acceptor **38**] = 50 mM, mol/mol donor/acceptor = 5
Donor **39** Acceptor **38**	Ag Triflate 0.2 eq, N-iodosuccinimide 5 eq, DCM, -40°C→0°C [acceptor **38**] = 50 mM, mol/mol donor/acceptor = 5
Donor **40** Acceptor **38**	Ag Triflate 0.2 eq, N-iodosuccinimide 5 eq, DCM, -40°C→0°C [acceptor **38**] = 50 mM, mol/mol donor/acceptor = 5
Donor **41** Acceptor **38**	Trimethylsilyl triflate 0.2 eq DCM, 0°C [acceptor **38**] = 100 mM, mol/mol donor/acceptor = 5

A double glycosylation of tetrasaccharide acceptor **38** was performed with the donor **41** and TMSOTf as a promoter to give the fully protected GAC-dimer **42** in 47% yield**.** Donor **41** was

prepared starting from the commercially available D-glucosamine chloroidrate. Compound **43** was synthesized introducing the phthalimido group at 2-posistion followed by O-acetylation. The *p*-methoxyphenyl (PMP) group was introduced at the anomeric position by the treatment of **43** with *p*-methoxyphenol using BF_3Et_2O as a promoter to give compound **44** in 89% yield. After deacetylation, the benzylidene acetal was introduced at 4- and 6-OH to achieve compound **45** in 84% yield. Final 3-O-benzylation, deprotection of the anomeric position and conversion of the hemiacetal into trichloroacetimidate provided **41** (70% yield).

Hexasaccharide **42** was fully characterized and subjected to global deprotection. The cleavege of the two phtalimido groups followed by N-acetylation, treatment with NaOMe in MeOH, and hydrogenolysis of the remaining protecting groups allowed to obtain the target compound GAC-dimer **3** in 40% yield (Figure 14).

3.3 Synthesis and characterization of CRM_{197} conjugates

The synthesized oligomers were conjugated to CRM_{197} carrier protein. Different chemistries were tested in order to obtain good conjugation efficiency. In the following paragraphs the synthesis of glycoconjugates by using SIDEA [adipic acid bis-(N-hydroxysuccinimide) ester], EMCS (N-malemidocaproyl-oxysuccinimide ester) and SBAP [succinimidyl 3-(bromoacetamido)propionate] linkers will be illustrated.

3.3.1 Conjugation of oligosaccharides to CRM_{197} by SIDEA chemistry

OligoRha **1** and **2** were conjugated to CRM_{197} carrier protein, through adipic acid bis-(N-hydroxysuccinimide) ester (SIDEA) chemistry (Figure 15a).

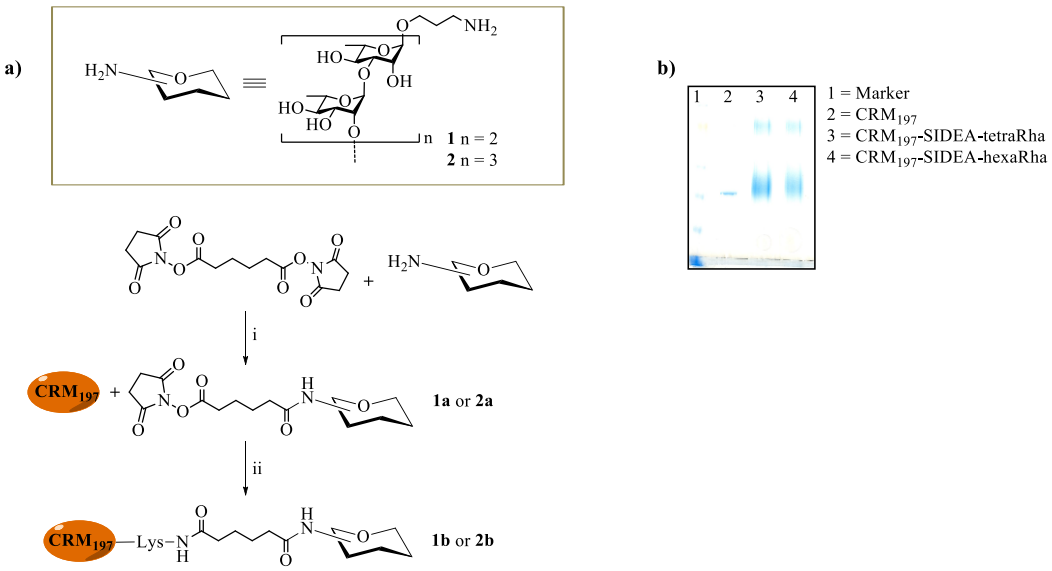

Figure 15: a) synthesis of tetraRha-SIDEA-CRM_{197} **1b** and hexaRha-SIDEA-CRM_{197} **2b** conjugates. Reagents and conditions: i) SIDEA, TEA, DMSO/H_2O 9:1; ii) NaPi 100mM pH 7.5, [CRM_{197}] = 5mg/mL, w/w glycan/CRM_{197} 1:1; **b)** SDS-PAGE of oligoRha conjugates **1b** and **2b** in comparison to unreacted CRM_{197}.

The derivatization reactions of **1** and **2** with SIDEA linker were performed using a large excess of SIDEA to favor the formation of monofunctionalized derivatives OS-SIDEA **1a** and **2a**. Use of triethylamine (TEA) facilitates the reaction, and the use of DMSO/H_2O = 9:1 prevents the hydrolysis of the active ester. The classical purification procedure of the activated OS through precipitation with ethyl acetate[68] (AcOEt) did not work, probably due to the short chain length of the oligomers. For this reason, a different purification procedure was tested: excess of unreacted SIDEA was precipitated by addition of HCl (55 ppm) and OS-SIDEA collected in the supernatant was lyophilized. The derivatized oligoRha, **1a** and **2a**, were characterized by High Performance

Anion Exchange Chromatography with Pulsed Amperometric Detection (HPAEC-PAD) to quantify the glycan recovered and by trinitrobenzenesulphonic acid (TNBS) colorimetric assay to detect the unreacted amino groups and calculate the percentage of $–NH_2$ groups derivatized with SIDEA. We obtained a good recovery of oligoRha, 73% for tetraRha-SIDEA **1a** and 71% for hexaRha-SIDEA **2a**, with a derivatization of $-NH_2$ groups of 95% and 91%, respectively. Conjugation to CRM_{197} was performed in sodium phosphate buffer (NaPi 100mM pH 7.5) working with a weight ratio of oligoRha-SIDEA to CRM_{197} of 1:1 (Figure 15a) and protein concentration of 5 mg/mL. The conjugates, **1b** and **2b**, were purified by size exclusion chromatography (SEC) and the fractions corresponding to the purified conjugates, separated from the unconjugated OS, were pooled and concentrated by Vivaspin 10k. Resulting products were characterized by HPAEC-PAD, Bicinchonic Acid Assay (microBCA) and Sodium Dodecyl Sulfate–Polyacrylamide Gel Electrophoresis (SDS-PAGE). The protein recovery was about 60% for both the conjugates and the average molar ratio of tetraRha to CRM_{197} and hexaRha to CRM_{197} resulted 4 and 5, respectively. The SDS-PAGE analysis confirmed conjugate formation, with typical smears for the conjugates at higher molecular weight compared to the protein alone (Figure 15b). The SDS-PAGE analysis also showed weak bands at higher molecular weight, suggesting that CRM_{197} crosslinking took also place. The chemistry used is in fact a selective approach that can induce the formation of a conjugate with "sun" structure, where different glycan chains are terminally linked to the protein. However, the step of purification of OS-SIDEA derivatives is critical and if not all the excess of SIDEA linker is removed, this can lead to crosslinking among CRM_{197} molecules. To overcome this problem, we tried to optimize the purification step using the hexaRha **2** as model.

HexaRha **2** was derivatized with SIDEA linker as previously described to give **2a**. Purification of the activated intermediate was performed this time by desalting on a prepacked G10 SEC column. Sample was loaded in DMSO/H_2O 1:1 and eluted with H_2O. The foregoing HexaRha-SIDEA **2a** was concentrated and immediately added to CRM_{197} to limit active ester groups deactivation. Conjugation with CRM_{197} was performed using a weight ratio of hexaRha to CRM_{197} 2 to 1 in NaPi 100 mM pH 7.2 (assuming a 65% OS recovery post G10 column) and with CRM_{197} concentration of 5 mg/mL. Conjugation occurred overnight at room temperature. SDS-PAGE of the purified conjugate CRM_{197}-SIDEA-hexaRha **2b$_1$** (Figure 16b) showed absence of crosslink among CRM_{197} molecules, indicating more efficient removal of SIDEA in excess by G10 desalting compared to precipitation procedure.

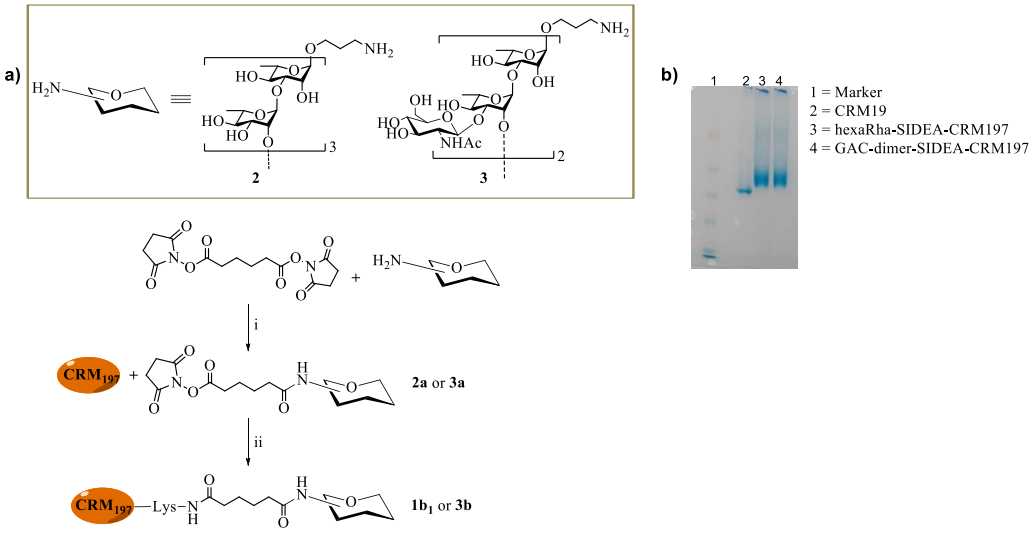

Figura 16: a) synthesis of hexaRha-SIDEA-CRM_{197} **$2b_1$** and GAC-dimer-SIDEA-CRM_{197} **3b** conjugates; *Reactions and conditions*: i) SIDEA, TEA, DMSO; ii) NaPi 100mM pH 7.2, [CRM_{197}] = 5 mg/mL, w/w glycan/CRM_{197} 2:1; **b)** SDS-PAGE of conjugates **$2b_1$** and **3b**.

Resulting conjugate had a molar ratio hexaRha/CRM_{197} of 3.7, as also confirmed by MALDI-MS analysis. Same derivatization and conjugation conditions were applied to produce GAC-dimer-SIDEA-CRM_{197} conjugate **3b** (Figure 16a). Purified conjugate showed a GAC-dimer to CRM_{197} molar ratio of 5, as determined by microBCA and HPAEC-PAD analysis. Also in this case no crosslinking among CRM_{197} molecules was observed in SDS-PAGE (Figure 16b).

3.3.2 Conjugation of tetraRha and hexaRha to CRM_{197} by maleimido chemistry

TetraRha **1** and hexaRha **2** were used to explore the efficiency of maleimido chemistry for conjugation.

The idea was to derivatize oligoRha with N-ε-maleimidocaproyl-oxysuccinimidoyl ester (EMCS) and CRM_{197} with N-acetyl homocysteine as a thiol linker or, other way around, to insert EMCS on the protein and N-acetyl homocysteine on oligoRha before performing conjugation (Figure 17).

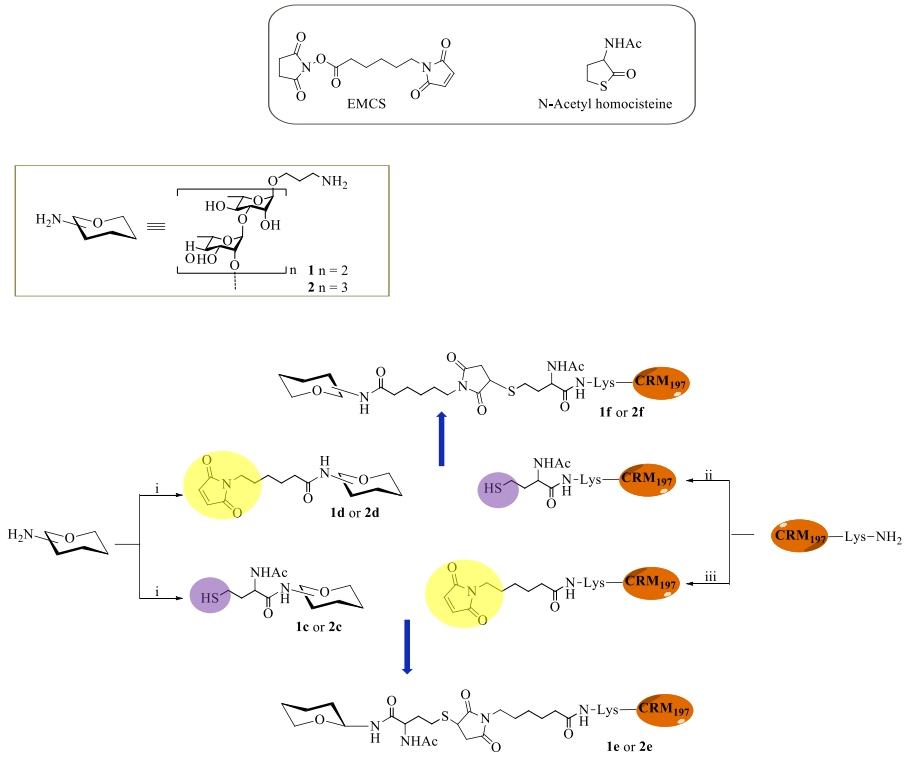

Figure 17: Synthesis of derivatized oligoRha with thiol or EMCS linkers before conjugation to CRM_{197}-EMCS or CRM_{197}-SH respectively. *Reagents and conditions*: i) EMCS (or N-Acetyl homocysteine), TEA, DMSO/H_2O 9:1; ii) N-Acetyl homocysteine, Borate 100mM pH 11 + 45 mM EDTA + 16mM DTT; iii) EMCS in DMSO, NaPi 100mM pH 8 + 1 mM EDTA. Conjugation conditions are reported in Table 2.

TetraRha **1** and hexaRha **2** were derivatized with N-acetyl homocysteine in the presence of TEA and in DMSO/H_2O 9:1 to give oligoRha-SH **1c** and **2c**, respectively (Figure 17). After purification by desalting on a G10 prepacked column, products formation was confirmed by ESI-MS, but also the presence of residual unreacted tetraRha **1** and hexaRha **2**.

Similar reaction conditions were used to prepare oligoRha derivatized with EMCS leading to tetraRha-EMCS **1d** and hexaRha-EMCS **2d**. ESI-MS spectra of derivatized tetraRha-EMCS **1d** and hexaRha-EMCS **2d** showed product formation. CRM_{197} was derivatized with both linkers, EMCS and N-Acetyl homocysteine (Figure 17). EMCS linker is not soluble in water and was dissolved in

DMSO before addition to CRM_{197} in NaPi 100 mM pH 8 + 1mM EDTA, while the thiol linker was introduced using N-Acetyl homocysteine in buffer at pH 11 containing ethylendiamine tetraacetic acid (EDTA) and dithiotreitol (DTT). The presence of EDTA and DTT is necessary to preserve the –SH groups from oxidation to S-S. The average number of linker molecules introduced per CRM_{197} was calculated by MALDI-MS and resulted to be of 10 for EMCS and of 7 for N-Acetyl homocysteine. Analysis by HPLC-SEC showed in both cases only one peak maintaining elution time of underivatized CRM_{197}.

The derivatized CRM_{197}-EMCS reacted with tetraRha-SH **1c** and hexaRha-SH **2c** to give the corresponding conjugates **1e** and **2e**, while CRM_{197}-SH reacted with tetraRha-EMCS **1d** and hexaRha-EMCS **2d** to obtain the corresponding conjugates **1f** and **2f** (Figure 17). Conjugations were performed using the conditions summarized in Table 2. Conjugation performed between CRM_{197}-EMCS and hexaRha-SH **2c** with high concentration of CRM_{197}-EMCS, 45 mg/mL, resulted in high % of unconjugated protein, with conjugate recovery of only 10% by microBCA. Purified conjugate was characterized by a molar ratio of hexaRha to CRM_{197} of 0.7. Conjugation was repeated with lower concentration of CRM_{197}-EMCS, 10 mg/mL, but also in this case there was free CRM_{197}-EMCS and the recovery of conjugate was 11% in terms of protein. No conjugate formation was observed using tetraRha-SH **1c**.

Table 2: conjugation reactions conditions

Reagents	Conjugation conditions	Note
CRM_{197}-EMCS + **2c**	[CRM_{197}]= 45 mg/mL, NaPi 100 mM pH 7.2 + 1 mM EDTA w/w glycan/CRM_{197} 1:1, 4h, rt	Presence of unconjugated CRM_{197} in reaction mixture*
CRM_{197}-EMCS + **2c**	[CRM_{197}]= 10 mg/mL, NaPi 100 mM pH 7.2 + 1 mM EDTA w/w glycan/CRM_{197} 1:1, overnight, rt	Presence of unconjugated CRM_{197} in reaction mixture*
CRM_{197}-EMCS + **1c**	[CRM_{197}]= 10 mg/mL, NaPi 100 mM pH 7.2 + 1 mM EDTA w/w glycan/CRM_{197} 1:1, overnight, rt	No conjugate formation was observed*
CRM_{197}-SH + **2d**	[CRM_{197}]= 4.6 mg/mL, MES 100mM pH 6.2 + 1 mM EDTA w/w glycan/CRM_{197} 1:1, overnight, rt	Precipitation of CRM_{197}
CRM_{197}-SH + **1d**	[CRM_{197}]= 10 mg/mL, NaPi 50 mM pH 7.2 + 1 mM EDTA w/w glycan/CRM_{197} 1:1, overnight, rt	Precipitation of CRM_{197}

*as shown by HPLC-SEC analysis of the reaction mixture

HexaRha-EMCS **2d** was conjugated to CRM_{197}-SH in MES (4-morpholine ethane sulfonic acid) 100 mM pH 6.2 + 1mM EDTA, but protein precipitation occurred due to the low pH of reaction. When the tetraRha-EMCS **1d** was conjugated to CRM_{197}-SH in NaPi buffer at pH 7.2 protein

precipitation was observed again. We concluded that in the absence of fast conjugation to OS, CRM_{197}-SH tends to aggregate and precipitate.

As by using N-acetyl homocysteine not all the OS molecules resulted derivatized, we decided to introduce the -SH function through the linker N-succinimidoyl S-acetylthioacetate (SATA) and to test again the conjugation with CRM_{197}-EMCS (Figure 18). The tetraRha **1** was derivatized with SATA in the conditions previously described for the other linkers. The acetate group was then cleaved with hydroxylamine 500 mM in the presence of EDTA to preserve –SH groups from oxidation (S-S formation). Conjugation was performed between tetraRha-(SATA)SH **1h** and CRM_{197}-EMCS in NaPi 100 mM pH 7.2 + 20 mM EDTA, but also in this case no conjugate formation was verified by HPLC-SEC.

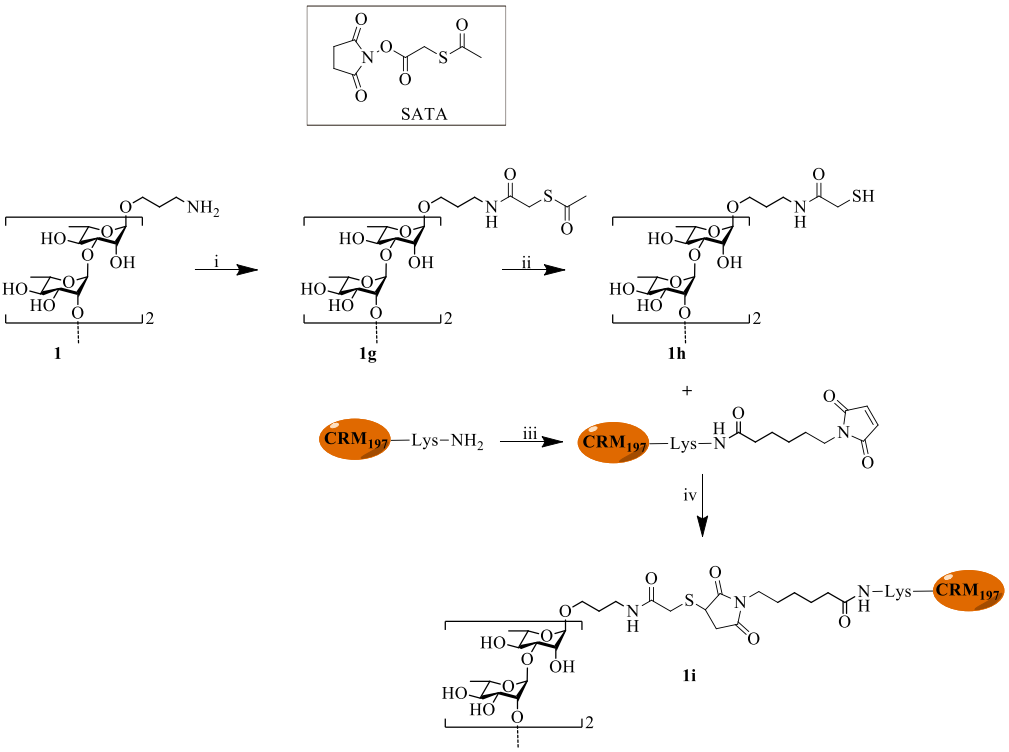

Figura 18: Synthesis of tetraRha-SATA and deprotection. Reactions and conditions: i) SATA, TEA, DMSO/H_2O 9:1; ii) hydroxylamine 500mM + EDTA 25mM; iii) EMCS in DMSO, NaPi 100mM pH 8 + 1mM EDTA; iv) NaPi 100mM pH 7.2 + 20mM EDTA.

To understand the reason why the CRM-EMCS did not react with OS-SH, we decided to characterize one freshly prepared CRM_{197}-EMCS by Ellman colorimetric method.[75] The synthesis of CRM_{197}-EMCS resulted reproducible, indeed 9 chains of EMCS per CRM_{197} were introduced according to MALDI-MS, but just 20% of the introduced linkers were able to react with cysteamine in the Ellman assay. This means that even if EMCS linkers are introduced on CRM_{197}, they are

subjected to rapid degradation at some extent that prevents their reaction with -SH functionalized molecules.

3.3.3 Conjugation of tetraRha and hexaRha to CRM_{197}-SH by using the SBAP linker

CRM_{197}-SH was also reacted with oligoRha derivatized with SBAP linker (Figure 19).

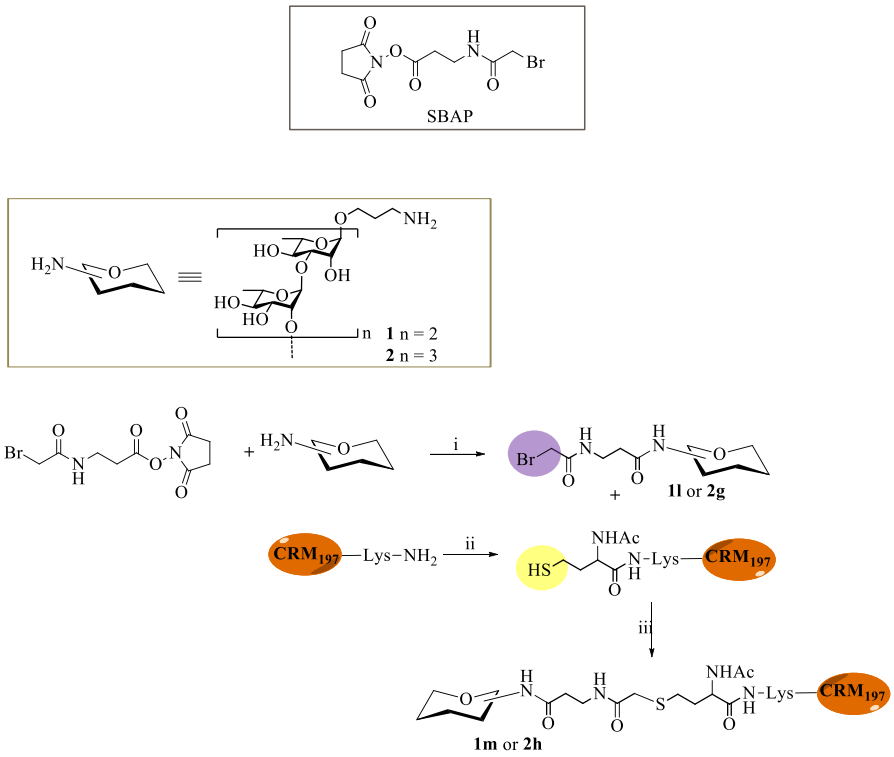

Figura 19: Synthesis of CRM_{197}-SH-oligoRha by means of oligoRha derivatized with SBAP linker. Reactions and conditions: i) SBAP, TEA, DMSO/H_2O 9:1; ii) N-Acetyl homocysteine, Borato 100 mM pH 11 + 45mM EDTA + 16mM DTT iii) NaPi 100mM pH 7.2 + 1 mM EDTA, [CRM_{197}] = mg/mL, w/w glycan/CRM_{197} 1:1.

The oligoRha **1** and **2** were derivatized with SBAP in the presence of TEA in DMSO/H_2O 9:1, to obtain tetraRha **1l** and hexaRha **2g**. CRM_{197} was derivatized with N-acetyl homocysteine introducing an average of 7 chains of linkers per CRM_{197}, as verified by MALDI-MS (paragraph 3.3.2, Figure 17). Conjugation reactions were performed in a buffer at pH 7.2 in the presence of EDTA (Figure 19). Differently from reaction with oligoRha-EMCS **1d** and **2d** (Figure 17) this time no precipitation of CRM_{197} was observed. Recovery in terms of CRM_{197} was around 50% for both conjugates, **1m** and **2h**. Molar ratio oligoRha to CRM_{197} was of 1.5 for **1m** conjugate and 1 for **2h** conjugate.

Using a more reactive linker (SBAP instead of EMCS) the precipitation of CRM_{197}-SH is avoided, but the loading of oligoRha on protein was very low compared to the loading obtained with SIDEA chemistry (paragraph 3.3.1). Among all the chemistries tested, SIDEA chemistry provided the best result, with an average of 5 oligosaccharide chains introduced per CRM_{197} molecule.

3.4 Immunogenicity study in mice: oligo-SIDEA-CRM$_{197}$ conjugates compared to GAC-CRM$_{197}$

A first study in mice was performed by testing hexaRha-SIDEA-CRM$_{197}$ conjugate **2b** (paragraph 3.3.1, Figure 15) and native the GAC-CRM$_{197}$ conjugate, already available in GVGH laboratory.

CD1 female mice, 5 weeks old (8 per group) were immunized intraperitoneally (IP) with 200 µL of formulated vaccines at day 0 and day 28. Sera were collected at days -1, 14, 27 and 42, when mice were sacrificed. The immunization scheme is summarized in Table 3. Conjugates were formulated with Alhydrogel (2 mg/mL as Al^{3+} content in the final formulation) and the glycan dose was normalized at 2 µg of Rha per dose. Consequently, the CRM$_{197}$ dose resulted different for the two groups, depending on the glycan loading in the two conjugates: 2 chains of GAC per CRM$_{197}$ and 5 chains of hexaRha per CRM$_{197}$.

Table 3: immunization scheme

Antigen	Rha (saccharide) dose per mouse per injection	CRM$_{197}$ (protein) dose per mouse per injection	mol/mol Glycan/CRM$_{197}$
GAC-CRM$_{197}$ + Alhydrogel (2 mg/mL)	2 µg	12.1 µg	2
hexaRha-SIDEA-CRM$_{197}$ **2b** + Alhydrogel (2 mg/mL)	2 µg	24.0 µg	5

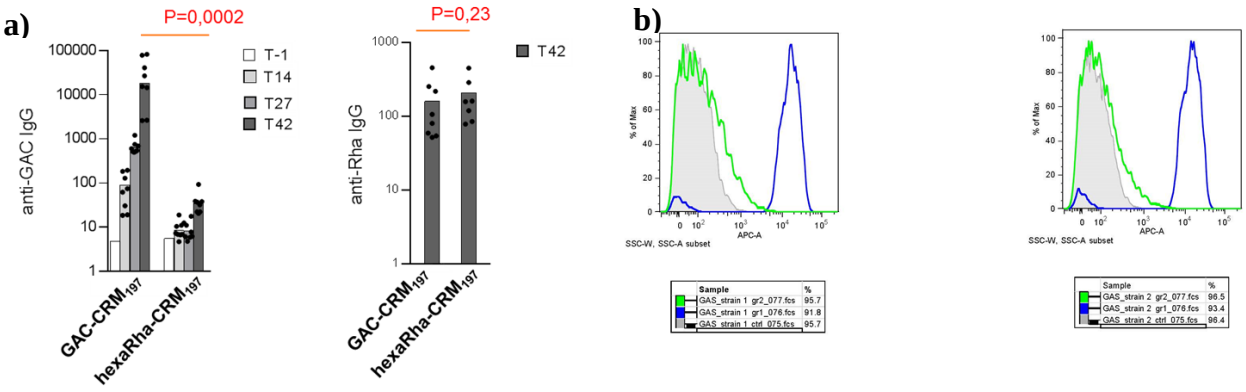

Figure 20: a) Anti-GAC and anti-Rha IgG titers (bars) induced in mice (dots) by hexaRha-SIDEA-CRM$_{197}$ **2b** compared to GAC-CRM$_{197}$; **b)** Fluorescent Activated Cell Sorting (FACS) of anti-Rha Abs induced by hexaRha-SIDEA-CRM$_{197}$ **2b** with two GAS strains (strain 1 = GAS 443; strain2 = GAS 51 emm1)

The sera were analysed to estimate the anti-GAC IgG and anti-Rha IgG titer by ELISA assay (Figure 20). HexaRha conjugated to CRM_{197} was able to induce anti-Rha IgG titer comparable to the conjugate of native GAC, but anti-GAC IgG titers induced were significantly lower compared to GAC conjugate (Figure 20a). Based on these results, the ability of anti-Rha Abs to bind the GAS bacterial surface was explored by FACS analysis and using. two GAS strains, GAS 443, which is a wild type strain, and GAS 51 *emm*1 that does not produce M protein. Anti-Rha sera were not able to recognize either of GAS strains (in green, Figure 20b), while anti-GAC sera did (in blue, Figure 20b)

A second study in mice is currently ongoing comparing tetraRha-SIDEA-CRM_{197} **1b**, hexaRha-SIDEA-CRM_{197} **2b₁** and GAC-dimer-SIDEA-CRM_{197} **3b** (paragraph 3.3.1) to verify the ability of GAC-dimer to induce an anti-GAC IgG response comparable to native GAC conjugate and to further elucidate the role of GlcNAc on the immune response induced.

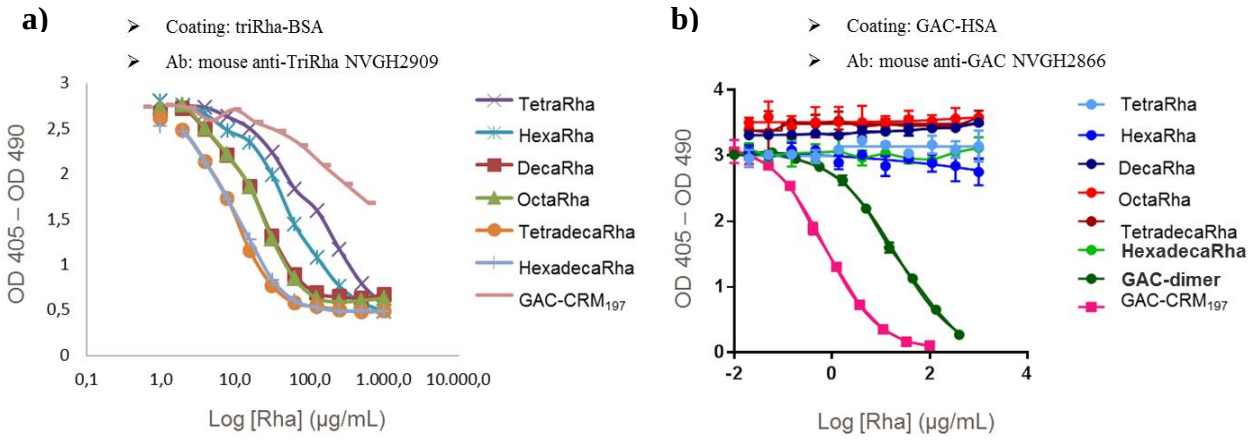

Figura 21: a) Competitive ELISA of GAC-CRM_{197} conjugate and oligoRha (tetraRha **1**, hexaRha **2**, octaRha, decaRha, tetradecaRha, hexadecaRha) using triRha-BSA conjugate as coating antigen and mouse anti-triRha Abs; **b)** Competitive ELISA of GAC-CRM_{197} conjugate, GAC-dimer **3** and oligoRha (tetraRha **1**, hexaRha **2**, octaRha, decaRha, tetradecaRha, hexadecaRha) using GAC-HSA conjugate as coating antigen and mouse anti-GAC Abs.

To confirm the previous data and verify if oligoRha length can have an impact on the immune response induced by oligoRha, a competitive ELISA experiment was performed with tetraRha **1**, hexaRha **2** and longer oligoRha (octaRha, decaRha, tetradecaRha, hexadecaRha) prepared in Leiden by automated synthesis.[76] A first experiment was performed by using triRha-BSA conjugate as coating antigen and sera generated by mice immunized with a triRha-CRM_{197} conjugate (Figure 21a). Data show that Abs generated against oligoRha recognise oligoRha of different chain length: longer chains induce stronger binding affinity. Abs generated against triRha, however, poorly recognize the GAC-CRM_{197} conjugate, suggesting that GlcNAc can mask the polyRha structure to Rha-specific Abs. A second experiment was performed by using GAC-HSA conjugate as coating

antigen and anti-GAC sera (Figure 21b): Abs generated against GAC do not recognize oligoRha structures, independently of their size, while they recognize GAC-CRM_{197} and GAC dimer **3**, suggesting that GlcNAc could be a dominant epitope. These results are in agreement with those reported in literature by Michon F. and coworkers.[73]

3.5 STD-NMR of GAC-dimer, tetraRha and GlcNAc: is the GlcNAc an immunodominant epitope of GAC?

The Saturation Transfer Difference (STD)-NMR methodology was used to clarify the role of GlcNAc side chain in GAC polysaccharide. A commercial anti-GAC polysaccharide mAb from AbNova was used to perform the experiments. The assignment of NMR proton signals of oligosaccharides was obtained by combining mono- and bi-dimensional homo- and hetero-nuclear experiments. GAC-dimer was tested (Figure 22) using a molar ratio mAb/GAC-dimer 100:1 in Tris d-11 50 mM in D_2O at pH 7.2 +/- 0.1. Qualitative analysis showed that GAC-dimer binds the mAb, and the two acetamides of GlcNAc side chains are the groups primarily involved in the interaction, with 100% (defined as reference at 100% because the highest intense peak) and 80% binding. Of note, Rha backbone is involved in the binding through positions H-2 and H-4 of the second and third Rha with a percentage between 40-60% and weakly with proton H-6 (~12%). These data are in agreement with those reported by Pinto M. and coworkers[66,67], confirming that the minimal motif recognized is the motif α-L-Rha*p*-(1-2)-[β-D-Glc*p*NAc-(1-3)]-α-L-Rha*p*: both GlcNAc residues of the GAC-dimer **3** are involved in the interaction with the mAb with a major interaction for the inner trisaccharide.

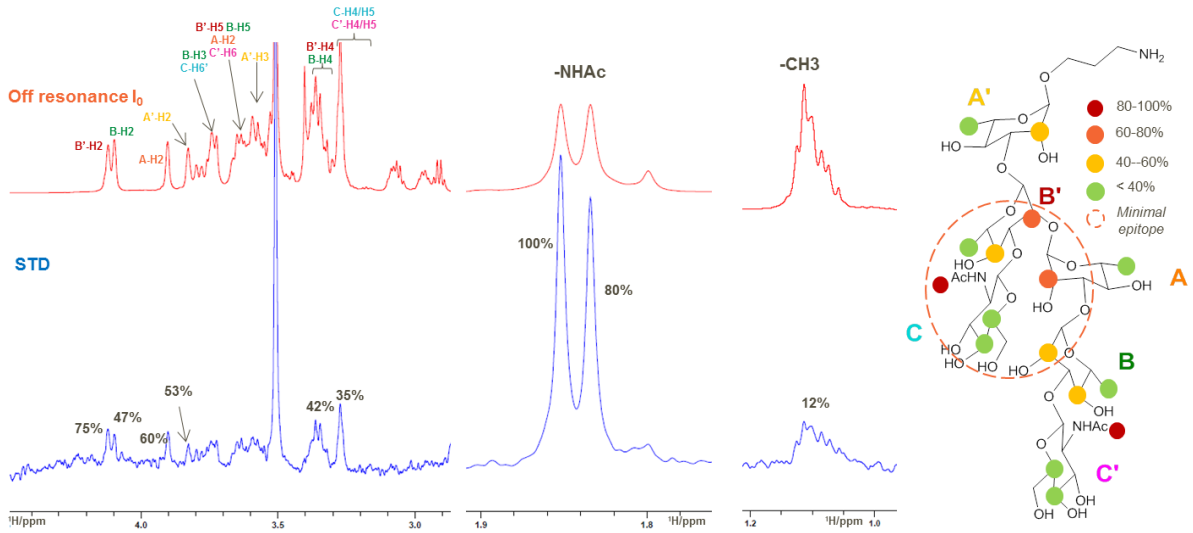

Figure 22: STD-NMR of GAC-dimer with anti-GAC mAb. Top spectra: ^{1}H NMR of GAC-dimer. Bottom spectra: ^{1}H STD-NMR.

To elucidate the role of the tetraRha in the binding with mAb, STD-NMR of its complex was compared with GAC-dimer. The tetraRha amount in the tube was normalized to the same amount of Rha contained in GAC-dimer sample tube. Figure 23 shows that, despite the absence of the GlcNAc residues, the anti GAC mAb binds to tetraRha. The protons H-2 of α-L-Rha*p*-(1-2)-α-L-Rha*p* motif

are preferentially involved in a binding between 60-100% while the binding with protons H-4 and H-6 is weaker (~ 27%).

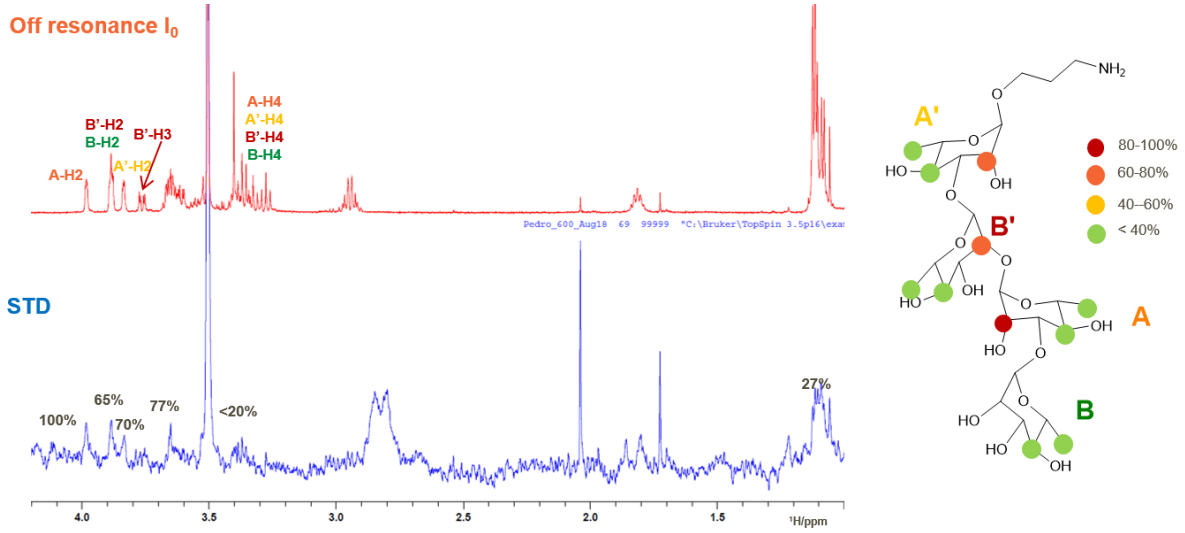

Figure 23: STD-NMR of tetraRha. Top spectra: ^{1}H NMR of tetraRha. Bottom spectra: ^{1}H STD-NMR.

To understand which of the two structures, the GAC-dimer and the tetraRha, preferentially binds mAb, an additional STD-NMR experiment was performed using the two glycans in a sort of competition experiment with mAb (Figure 24).

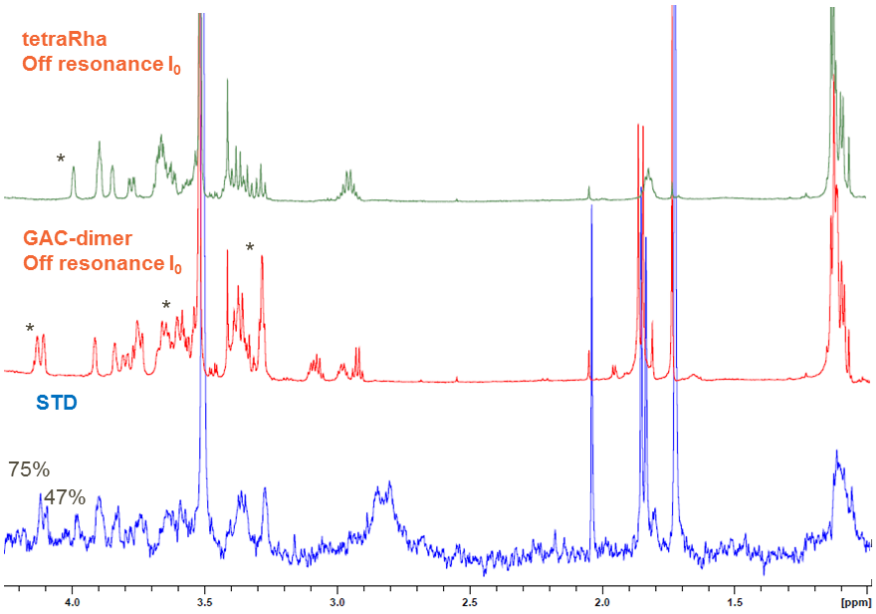

Figure 24: ^{1}H STD-NMR of competition between GAC-dimer and tetraRha. Top spectra: ^{1}HNMR of tetraRha. Middle spectra: ^{1}H NMR of GAC-dimer. Bottom spectra: ^{1}H STD-NMR.

The mAb showed preferential binding for GAC-dimer and compared to the tetraRha, as demonstrated by the high intensity of the two acetamides peaks and the depletion of 100% proton H-2 signal of tetraRha (Figure 23) to 47% (Figure 24). These results, together with the immunogenicity study in mice FACS analysis of anti-Rha sera and the competitive ELISA reported in the previous paragraphs, suggest that the GlcNAc side chain is an immunodominant epitope of GAC polysaccharide and that GlcNAc masks the rhamnose backbone. Our results are in agreement with published data showing that GAC polysaccharide adopts a helical conformation, where the polyRha backbone is the core of the helix and GlcNAc residues are exposed on the periphery.[73]

Finally, ^{1}H STD-NMR of GlcNAc alone with mAb was performed in order to verify the hypothesis that GlcNAc binds the mAb only in the context of polyRha backbone. A GlcNAc structure blocked in the anomeric position in β-configuration with an amino linker was prepared in Milan in Lay L.'s laboratory. The NMR tube was prepared as previously described, using the same molar amount of GlcNAc that was contained in the GAC-dimer sample. The STD-NMR of GlcNAc did not show any relevant interaction (Figure 25), indicating that the mAb doesn't bind to GlcNAc alone, while it strongly binds GlcNAc side chain of GAC-dimer.

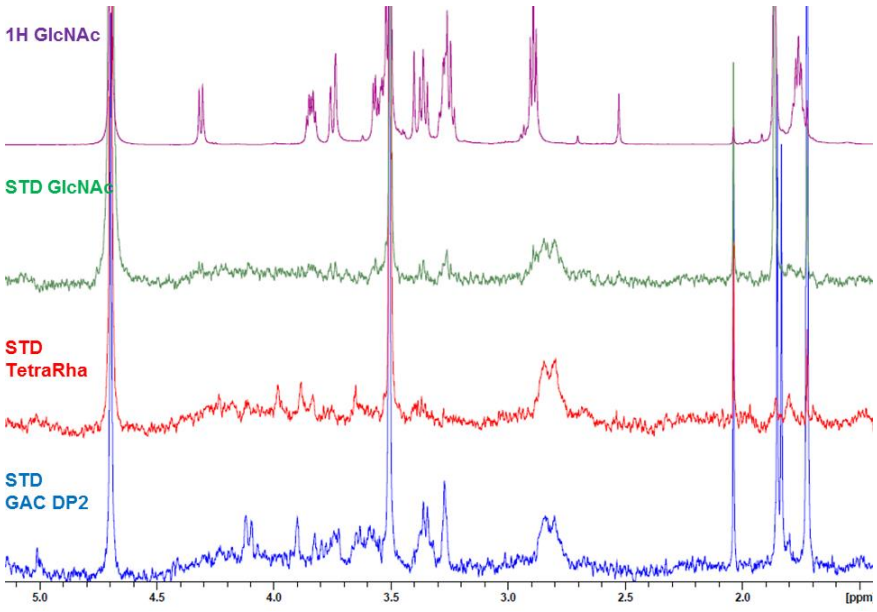

Figura 25: ^{1}H STD-NMR of GlcNAc, tetraRha and GlcNAc-linker.

To conclude, all these experiments support the hypothesis that the GlcNAc side chain is a dominant epitope in the GAC polysaccharide and it is recognized by GAC specific Abs in the context of the polyRha backbone. To further support this finding, a competitive ELISA has been performed to compare the GAC-dimer, tetraRha, GlcNAc alone and one synthetic fragment of GBSIII polysaccharide (Group B *Streptococcus* type III), which contains the GlcNAc residue, in order to

understand if anti-GAC sera can recognize the GlcNAc alone or in a context different from GAC structure (as it is the case of GBSIII). Anti-GAC Abs were not able to recognize either GlcNAc, GlcNAc-HSA or GBSIII oligomer, confirming that antibodies generated by GAC polysaccharide are able to recognize GlcNAc in the context of the polyRha backbone only.

3.6 Investigating multivalent antigen presentation

3.6.1 GMMA as carrier for GAC and synthetic oligosaccharides

In order to evaluate GMMA as alternative carrier to the more traditional protein CRM_{197}, GAC and the synthetic oligomers were conjugated to GMMA (a strain modified for overblebbing and to reduce LPS toxicity, modulating the degree of lipid A acyl chains[37]).

GAC, tetraRha **1** and hexaRha **2** were conjugated to GMMA by using two different chemistries, i.e. targeting proteins on GMMA surface through a bifunctional linker and targeting LPS molecules on GMMA by performing oxidation of *cis* diols followed by reductive amination reaction (paragraph 2.2).

To prepare the GMMA-GAC conjugate, the adipic acid dihydrazide (ADH) linker was introduced at the reducing end of GAC by reductive amination reaction in a buffer at pH 4.5 (Figure 26).

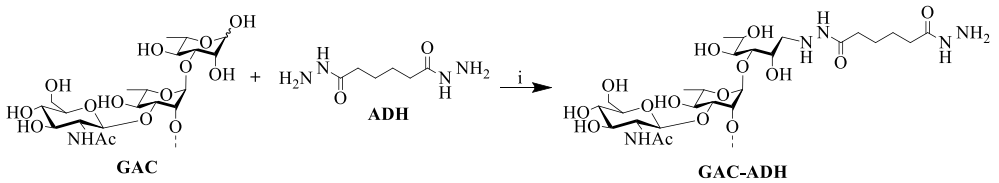

Figura 26: synthesis of GAC-ADH. Reaction and contidions: i) $NaCNBH_3$, NaOAc 20mM pH 4.5, 30°C, 5 days, [GAC] = 30 mg/mL, w/w/w GAC/ADH/$NaCNBH_3$ 1:1:1

GAC-ADH was recovered in 90% yield as estimated by HPAEC-PAD. TNBS colorimetric assay indicated 56% saccharide chains were activated (assuming an average size of 7.5 kDa for GAC), and analysis by Ultra High Performance Liquid Chromatography (UHPLC) was performed to quantify free ADH %, that resulted to be 5% (reported as free /total NH_2 groups).

To prepare the conjugates by targeting proteins on GMMA, the bifunctional linker bis(sulfosuccinimidyl)suberate (BS^3) was used (Figure 27). GMMA were derivatized with BS^3 linker at pH 6 with GMMA concentration of 4 mg/mL and using large excess of BS^3 ([BS^3] = 50 mg/mL) to avoid crosslinking among GMMA. Resulting GMMA-BS^3 were purified by ultracentrifuge (UC), and the solutions of GAC-ADH, tetraRha **1** or hexaRha **2** in PBS were added to GMMA pellet ([GMMA] = 10 mg/mL, w/w glycan/GMMA 3:1). Reaction mixtures were stirred overnight at room temperature. The resulting conjugates, GMMA-GAC, GMMA-tetraRha and GMMA-hexaRha, were purified by two UC steps and re-suspended in PBS.

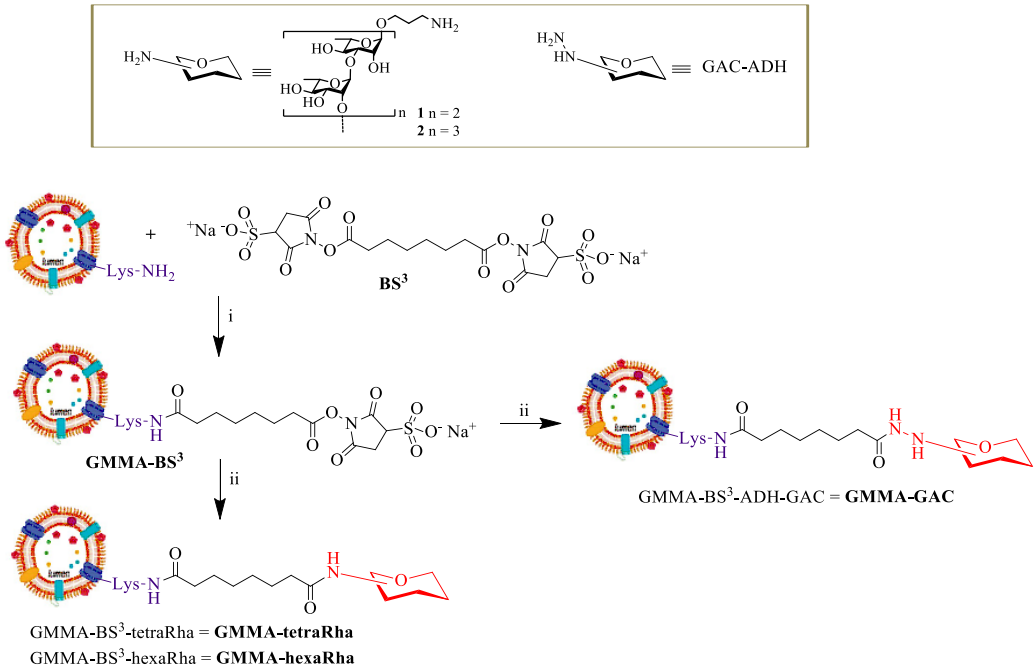

Figura 27: Synthesis of GMMA conjugates, GMMA-GAC, GMMA-tetraRha and GMMA-hexaRha, with BS^3 chemistry. Reactions and conditions: i) MES 100mM pH 6, 25°C, 30 min [GMMA] = 4 mg/mL, [BS^3] = 50 mg/mL; ii) GAC-ADH or tetraRha **1** or hexaRha **2,** PBS, rt, overnight, [GMMA] = 10 mg/mL, w/w glycan/GMMA 3:1.

Table 4: Characterization of GMMA-BS^3 and GMMA conjugates			
	Protein recovery	**Activated NH_2**	**Activated esters**
GMMA-BS^3	100%	61%	32%
	Protein recovery	**Z-average d (nm)**	**Glycan chain numbers/ GMMA particle**
GMMA-GAC	66%	90.26	159
GMMA-tetraRha	67%	91.86	1392
GMMA-hexaRha	65%	62.74	959

The full characterization of GMMA-$BS^3$and GMMA conjugates is summarized in Table 4.

61% of Lys residues on GMMA were derivatized with BS^3 linker (by TNBS) and 32% of BS^3 linkers was as active esters at the time of conjugation. Conjugates recovery in terms of GMMA proteins was about 65% for all the conjugates and glycan loading decreased with the length of the saccharide chain: GMMA-GAC loading < GMMA-hexaRha loading < GMMA-tetraRha loading, probably due to the steric hindrance. For the conjugate GMMA-GAC, a higher weight ratio GAC/GMMA during the conjugation was used (GAC/GMMA 10:1 instead of 3:1) in order to increase the number of saccharide chains per GMMA particles, but this only resulted in 259 instead of 159 chains of GAC per GMMA particle.

A second conjugation strategy was also tested: LPS molecules of GMMA were oxidized to generate aldehyde groups which then reacted under reductive amination conditions with GAC-ADH, tetraRha **1** and hexaRha **2** (Figure 28). The oxidation mainly occurs on Rha residues of O-antigen repeats, probably because the O-antigen is the most exposed portion of LPS of GMMA.

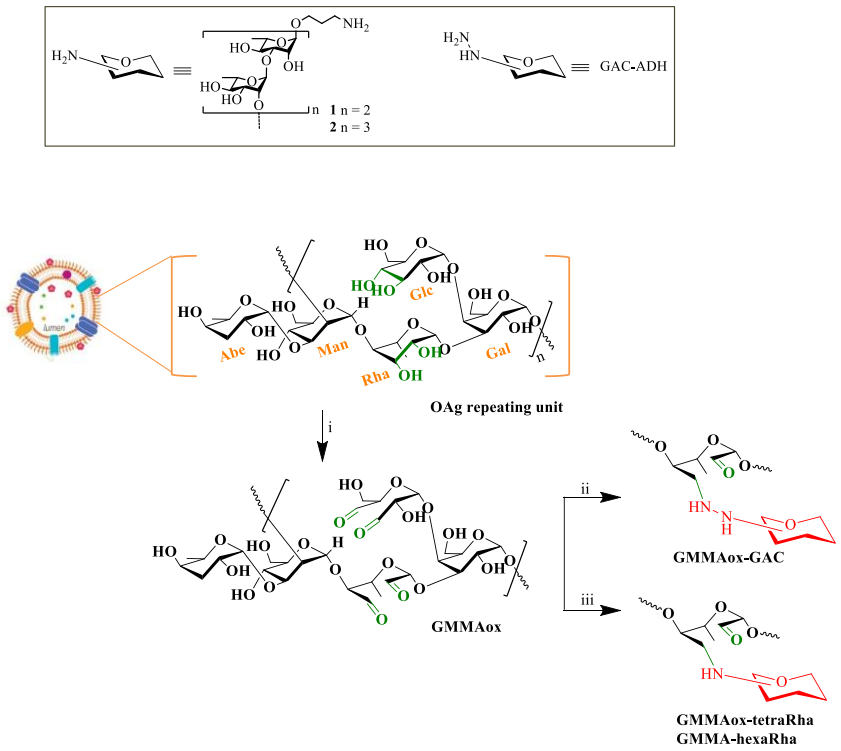

Figura 28: Synthesis of GMMA conjugates by reductive amination chemistry. Reactions and conditions: i) $NaIO_4$ 10 mM, NaOAc 100mM pH 5, 2h, rt [GMMA] = 2.38 mg/mL; ii) GAC-ADH, $NaCNBH_3$ NaOAc 100 mM pH 4.5rt, overnight [GMMA] = 5 mg/mL, w/w/w GAC-ADH/GMMA/$NACNBH_3$ 1:1:1; iii) tetraRha **1** or hexaRha **2**, $NaCNBH_3$, NaPi 100 mM pH 7.2, rt, overnight, [GMMA] = 5 mg/mL, w/w/w GAC-ADH/GMMA/$NACNBH_3$ 1:1:1.

Table 5: Characterization of GMMAox and GMMAox conjugates			
	Protein recovery	**% oxidation***	
GMMAox	100%	73%	
	Protein recovery	**Z-average d (nm)**	**glycan chain numbers/ GMMA particle**
GMMAox-GAC	59%	94.39	1198
GMMAox-tetraRha	51%	81.01	2186
GMMAox-hexaRha	53%	82.74	1079

*Rhamnose units oxidized

GMMA were oxidized with $NaIO_4$ (10 mM in the final reaction mixture) in a buffer at pH 5 for 2 hours with GMMA concentration of 2.38 mg/mL, then purified by UC. The reductive amination

reaction was then carried out with $NaCNBH_3$ as reducing agent. Reaction was performed at pH 4.5 for GAC-ADH (having a hydrazide linker) and at pH 7.2 for oligoRha (having an amino linker) working with a weight ratio glycan/GMMA/$NaCNBH_3$ 1:1:1 ([GMMA] = 5 mg/mL). The resulting conjugates, GMMAox-GAC, GMMAox-tetraRha and GMMAox-hexaRha, were purified by two UC steps. Characterisation of GMMAox conjugates is reported in Table 5.

73% of Rha units of LPS on GMMA were oxidized (% oxidation was calculated by comparing starting GMMA with GMMAox) and the number of glycan chains per GMMA particle was higher compared to the corresponding GMMA-BS[3] conjugates (Table 4). Conjugation chemistry has an impact on glycan loading on GMMA. The high difference in the number of saccharide chains per GMMA linked with the two methodologies could be due to the different exposition of proteins compared to LPS molecules on GMMA surface. LPS and in particular their OAg portion are more exposed than proteins, therefore more accessible to glycans. It is also important to consider the high percentage of LPS oxidation (about 70%, Table 5) that allows to have many reactive groups.

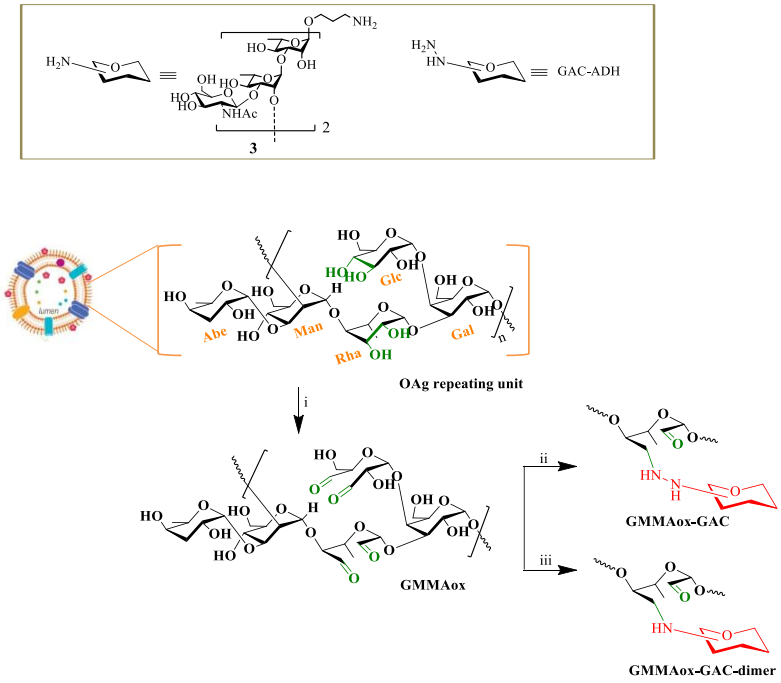

Figure 29: Synthesis of GMMAox-GAC and GMMAox-GAC-dimer conjugates. Reactions and conditions: i) $NaIO_4$ 5mM, NaPi 100 mM pH 6.5, 25°C, 30min, [GMMA] = 2 mg/mL; ii) GAC-ADH, NaOAc 100 mM pH 4.5, rt, overnight, [GMMA] = 5 mg/mL, w/w/w GAC.ADH/GMMA/$NaCNBH_3$ 3:1:3; iii) GAC-dimer **3**, NaPi 100 mM pH 7.2, rt, overnight, [GMMA] = 5 mg/mL, w/w/w GAC.ADH/GMMA/$NaCNBH_3$ 3:1:3.

GMMAox conjugate with GAC was prepared in different oxidation conditions (Figure 29, Table 6) to preserve the LPS structural integrity. Same procedure was used to prepare a GMMAox-GAC-dimer conjugate (Figure 29). GMMA were oxidized with $NaIO_4$ (5 mM in the final reaction

mixture) in a buffer at pH 6.5 for 30 min, working with a GMMA concentration of 2 mg/mL, then purified by UC. The reductive amination reactions were performed with $NaCNBH_3$ as reducing agent at pH 4.5 for GAC-ADH and 7.2 for GAC-dimer **3** using a weight ratio GMMA/glycan/$NaCNBH_3$ 1:3:3 and with GMMA concentration of 5 mg/mL.

Table 6: Characterization of GMMAox and GMMAox conjugates

	Protein recovery	% oxidation	
GMMAox	68%	9%	
	Protein recovery	**Z-average d (nm)**	**glycan chain/ GMMA particle**
GMMAox-GAC	50%	127.4	1813
GMMAox-GAC-dimer	31%	107.50	2124

The resulting conjugates, GMMAox-GAC and GMMAox-GAC-dimer, were purified three times by UC to ensure the removal of all unreacted glycan. This time, the percentage of oxidation of GMMA was of 9%. This always resulted in high number of sugar chains linked: 1813 chains of GAC-ADH were introduced per GMMA particle, and 2124 of GAC-dimer **3** (Table 6).

3.6.2 Immunogenicity study in mice: GMMAox-GAC conjugate compared to CRM_{197}-GAC conjugate

In order to evaluate GMMA as alternative carrier to more traditional CRM_{197} carrier protein for GAS carbohydrate antigens, a preliminary study in mice was conducted to test GMMAox-GAC conjugate (paragraph 3.6.1, Figure 28) in comparison to GAC-CRM_{197} conjugate, already available in GVGH laboratory. Because of its higher glycan loading compared to the corresponding conjugate prepared by BS^3 chemistry (paragraph 3.6.1, Figure 27), the GMMA conjugate prepared by reductive amination chemistry was tested only.

Table 7: immunization scheme

Antigen	Rha dose per mouse per injection	Protein dose per mouse per injection	mol/mol glycan/CRM_{197}	n° GAC chains per GMMA particle
GMMAox-GAC + Alhydrogel (2 mg/mL)	2 µg	15.4 µg	nd	1198
GAC-CRM_{197} + Alhydrogel (2 mg/mL)	2 µg	12.1 µg	2	nd

Conjugates were formulated with Alhydrogel (2 mg/mL Al^{3+} in the final formulation) and compared at 2 µg Rha per dose (Table 7). CD1 female mice 5 weeks old were injected IP at days 0 and 28 and sera were collected at days -1, 14, 27 and 42. Sera were analyzed by ELISA assay for determining anti-GAC IgG and anti-OAg IgG titers (Figure 30).

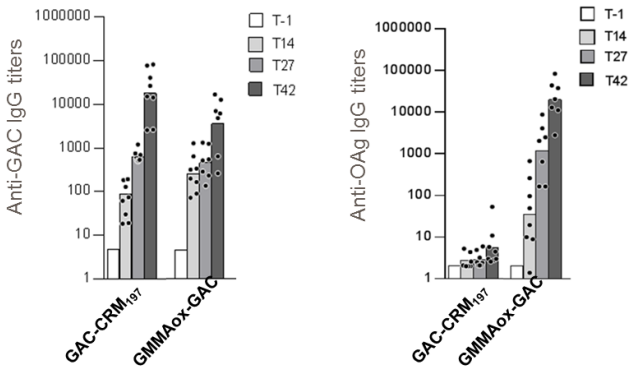

Figure 30: Anti-GAC and anti-OAg IgG titers (bars) induced in mice (dots) by GMMAox-GAC conjugate in comparison to GAC-CRM_{197} conjugate.

GMMAox-GAC was able to induce anti-GAC IgG titers comparable to GAC-CRM_{197} (p value = 0.07) confirming possibility to test GMMA as carrier for GAC antigen. Also, GMMAox-GAC induced high anti-OAg IgG titers meaning that this conjugate has the potential to result in a multivalent vaccine covering both GAS and bacterial diseases.

3.6.3 Synthesis, characterization and evaluation in competitive ELISA of glyco-AuNPs

AuNPs are suitable nanosystems to explore the effect of multivalent antigens presentation.[31] TetraRha **1** and hexaRha **2** were conjugated to two different types of AuNPs, spheres and stars, by using poly(ethylene glycol) 2-mercaptoethyl ether acetic acid PEG average M_n 5000, n=113, (HOOC-PEG_{5000}-SH) as a linker (Figure31). The AuNPs and the corresponding nanosystems with tetraRha **1** and hexaRha **2** were prepared by L. Polito (CNR–ISTM, Nanotechnology Lab.). The carboxyl group of HOOC-PEG_{5000}-SH was activated as pentafluoro phenyl ester and coupled with oligoRha **1** and **2** to give **1-PEG** and **2-PEG**. Sphere and star AuNPs were coated with **1-PEG** and **2-PEG** to give sphere-tetraRha, sphere-hexaRha, star-tetraRha and star-hexaRha.

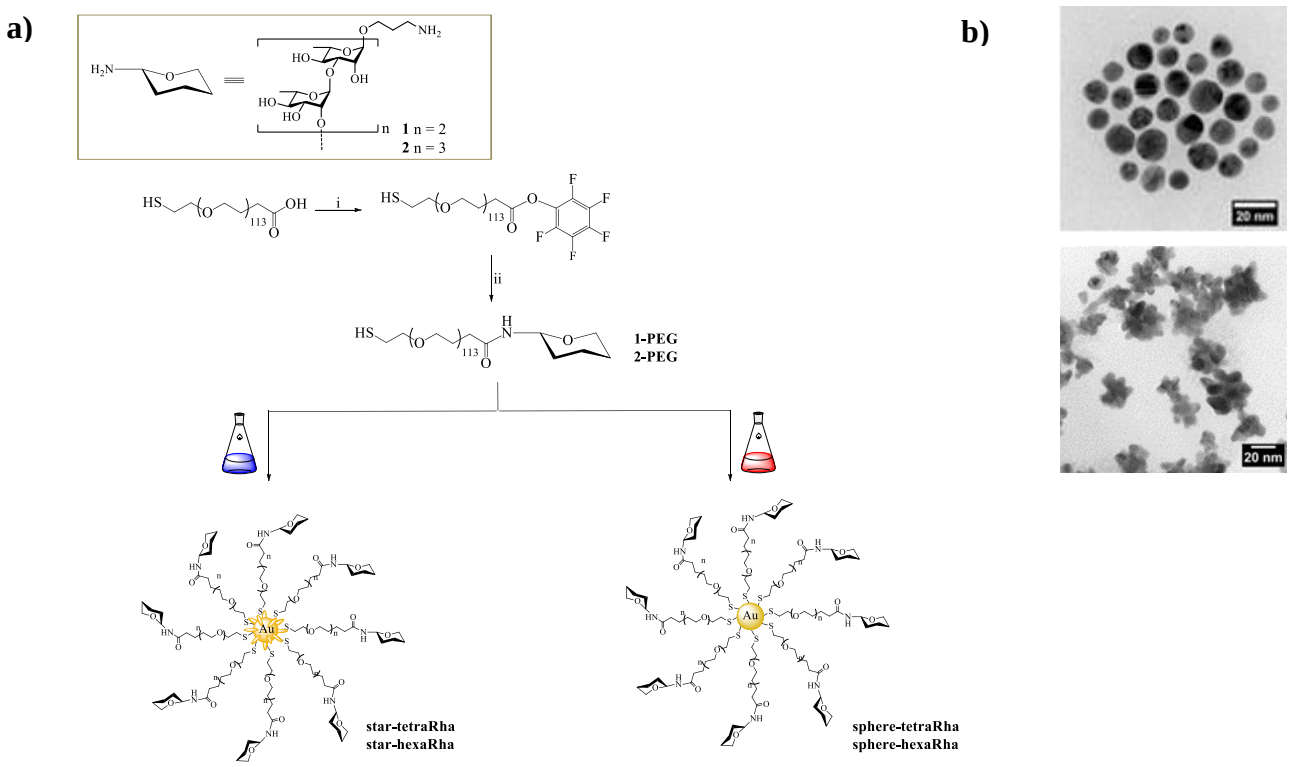

Figura 31: a) Synthesis of AuNPs coated with tetraRha **1** and hexaRha **2**. Reactions and conditions: i) pentafluorophenol, EDAC, DCM; ii) DIPEA, DCM; **b)** TEM imagines of sphere-hexaRha and star-hexaRha.

The resulting derivatized nanosystems were characterized by HPAEC-PAD, dynamic light scattering (DLS), transmission electron microscopy (TEM) and nanoparticle tracking analysis (NTA). Figure 31 show the TEM imagines (sphere-hexaRha and star-tetraRha as samples) where is clear the shape of the core, sphere and star, and the diameter of the Au core was 12 nm for sphere and 14 nm for star. The combination of HPAEC-PAD to quantify the total amount of sugar linked and NTA to count particles number allowed to calculate the number of oligoRha chains per

nanoparticle. Results obtained are summarized in Table 8. Data show that the number of oligoRha chains per nanoparticle increased with shorter oligomer. The morphology of the nanoparticles also influenced glycan loading. Indeed, star NPs were characterized by a lower loading than sphere NPs, probably meaning that anisotropic NPs have a decreased surface area available to bind oligoRha chains.

Table 8: Characterization of oligoRha-AuNPs				
Sample	**Diameter (Mode nm)**	**Z-potential**	**number of NPs/mL**	**n° oligoRha chains/ NP**
Sphere-tetraRha	44.1±0.5	-23.74±0.72	3.12E+12	4890
Star-tetraRha	53.9±0.2	-25.66±0.81	3.06E+12	2120
Sphere-hexaRha	45.9±0.3	-22.47±1.67	2.45E+12	3325
Star-hexaRha	55.4±0.3	-24.31±0.97	1.85E+12	1640

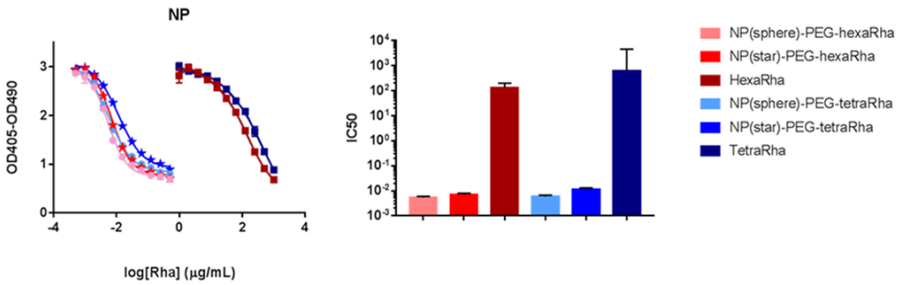

Sample	IC50 (Rha µg/mL)	Number of oligoRha/NPs
ExaRha	$1{,}34*10^{2}$	
NP(star)-PEG-hexaRha	$7{,}13*10^{-3}$	1640
NP(sphere)-PEG-hexaRha	$5{,}42*10^{-3}$	3325
TetraRha	$6{,}20*10^{2}$	
NP(star)-PEG-tetraRha	$1{,}18*10^{-2}$	2120
NP(sphere)-PEG-tetraRha	$5{,}90*10^{-3}$	4890

Figura 32: Competitive ELISA of AuNPs coated with tetraRha **1** and hexaRha **2**. Coating antigen: triRha-BSA. Sera: anti-triRha.

Obtained nanosystems were evaluated by competitive ELISA in comparison with unconjugated tetraRha **1** and hexaRha **2** chains for their ability to bind anti-Rha Abs (Figure 32). IC50 values (concentration of antigens needed to reduce to half serum standard ELISA titer), were almost in the same range for all nanosystems and lower compared to unconjugated tetraRha **1** and hexaRha **2**, even if characterized by different antigen length and loading. We can conclude that there is a correlation between antigen chain length and density for these nanosystems. The same antibody binding affinity was obtained with the nanosystem that present high density loading and the shorter antigen (sphere-tetraRha) and with the nanosystem that present low density loading and the longer antigen (star-hexaRha).

4 MATERIALS AND METHODS

4.1 General method for the synthesis of CRM_{197} conjugates with SIDEA linker

TetraRha and hexaRha (10 mg/mL) were dissolved in 300 μL of DMSO/H_2O 9:1. TEA (5 eq) and SIDEA (12 eq) were added. Reactions occurred for 1 h, then an aqueous solution of HCl 82.5 ppm was added (50 ppm in the final solutions) to precipitate the SIDEA in excess. The mixtures were centrifugated for three times and the supernatants were lyophilized. The derivatized oligomers were characterized by HPAEC-PAD for sugar quantification and TNBS assay for amino groups quantification,[77] allowing to calculate the % of derivatization of oligomers with SIDEA. Derivatized oligomers were conjugated to CRM_{197} in NaPi 100mM pH 7.5 working with a CRM_{197} concentration of 5 mg/mL and a weight ratio oligoRha-SIDEA to CRM_{197} of 1:1. Conjugations occurred at room temperature in 3 h. Reaction mixtures were purified by HiPrep™ 16/60 Sephacryl® S-100 HR column. Samples were diluted to 1 mL of PBS, loaded and eluted in PBS with a flow rate of 0.5 mL/min. Pooled fractions corresponding to pure conjugates were concentrated by Vivaspin 10k. Conjugates were characterized by micro BCA, SDS-PAGE and HPAEC-PAD.

A different purification procedure was then followed to prepare SIDEA intermediates for hexaRha and GAC-dimer. Oligomers were derivatized with SIDEA linker as previous described and purified by prepacked single-use PD MidiTrap G-10. Reaction mixtures were loaded in DMSO/H_2O 1:1 and eluted with water, according to manufacturer instructions. Eluted hexaRha-SIDEA and GAC-dimer-SIDEA were dried in SpeedVac Concentrator®, then conjugated to CRM_{197} in NaPi 100mM pH 7.2 working with CRM_{197} concentration of 5 mg/mL and a ratio glycan/CRM_{197} of 2:1 in weight. Conjugation occurred overnight at room temperature. Reaction mixtures were purified and characterized as previously described.

4.2 General method for the synthesis of CRM_{197} conjugates with malemido chemistry

4.2.1 Derivatization of oligomers with N-acetyl homocysteine linker

TetraRha and hexaRha were derivatized with N-acetyl homocysteine. Oligomers (80 mM) were dissolved in DMSO/H_2O 9:1. TEA (5 eq) and N-acetyl homocysteine (20 eq) were added. Reaction occurred in 4 h at room temperature. Derivatized oligomers were purified by prepacked single-use PD MidiTrap G-10. Reaction mixtures were loaded in water and eluted with water according to

manufacturer instructions. Eluted oligomers were dried in SpeedVac Concentrator® then characterized by Dische assay and ESI-MS.

4.2.2 Derivatization of oligomers with EMCS linker

TetraRha and hexaRha were derivatized with EMCS linker. Oligomers (80 mM) were dissolved in DMSO/H_2O 9:1. TEA (5 eq) and EMCS (20 eq) were added. Reaction occurred in 4 h at room temperature. Derivatied oligomers were purified by prepacked single-use PD MidiTrap G-10. Reaction mixtures were loaded in water and eluted with water according to manufacturer instructions. Eluted oligomers were dried in SpeedVac Concentrator® then characterized by Dische assay and ESI-MS.

4.2.3 Derivatization of tetraRha with SATA linker

TetraRha was derivatized with SATA linker. TetraRha (50 mM) was dissolved in DMSO/H_2O 9:1. TEA (5 eq) and SATA (20 eq) were added. Reaction occurred in 4 h at room temperature. Derivatized oligomers were purified by prepacked single-use PD MidiTrap G-10. Reaction mixtures were loaded in water and eluted with water according to manufactures instructions. Eluted oligomers were concentrated in SpeedVac Concentrator® then characterized by Dische assay and ESI-MS.

TetraRha-SATA (10 mg/mL) was deprotected from acetate groups in 500 mM hydroxylamine + 25 mM EDTA in PBS for 3 h at room temperature. Resulting tetraRha-SH was purified by prepacked single-use PD MidiTrap G-10. Reaction mixture was loaded in NaPi 50 mM pH 7.2 + 20 mM EDTA and eluted with the same buffer according to manufacturer instructions. Eluted oligomer was concentrated in SpeedVac Concentrator® then characterized by Dische assay and ESI-MS.

4.2.4 Derivatization of CRM_{197} with N-acetyl homocysteine linker

N-acetyl homocysteine was added to a solution of CRM_{197} protein (5 mg/mL) in borate 100 mM pH 11 + 45 mM EDTA + 16 mM DTT, with a molar ratio linker/Lys of 6.6. Reaction occurred in 4 h at room temperature. CRM_{197}-SH was purified by Amikon 10k with conjugation buffer and characterized by micro-BCA, MALDI-MS, SEC-HPLC and SDS-PAGE.

4.2.5 Derivatization of CRM_{197} with EMCS linker

EMCS dissolved in DMSO (4 mg/mL) was added to a solution of CRM_{197} protein (4.7 mg/mL) in NaPi 100 mM pH 8 + 1 mM EDTA, with a molar ratio linker/Lys of 0.3. Reaction occurred in 4 h

at room temperature. CRM_{197}-EMCS was purified by Amikon 10k with conjugation buffer and characterized by micro-BCA, MALDI-MS, SEC-HPLC and SDS-PAGE.

4.2.6 Conjugation reactions with CRM_{197}-SH and oligoRha-EMCS

CRM_{197}-SH (4.6 mg/mL) in MES 100 mM pH 6.2 + 1 mM EDTA was added to dried hexaRha-EMCS in weight ratio hexaRha/CRM_{197} 1:1. Conjugation occurred overnight at room temperature. Protein precipitation was observed.

CRM_{197}-SH (10 mg/mL) in NaPi 100 mM pH 7.2 + 1 mM EDTA was added to dried tetraRha-EMCS in weight ratio tetraRha/CRM_{197} 1:1. Conjugation occurred overnight at room temperature. Protein precipitation was observed.

4.2.7 Conjugation reactions with CRM_{197}-EMCS and hexaRha-SH

CRM_{197}-EMCS (45 mg/mL or 10 mg/mL) in NaPi 100 mM pH 7.2 + 1 mM EDTA was added to dried hexaRha-SH in weight ratio hexaRha/CRM_{197} 1:1. Conjugation reactions occurred overnight at room temperature. Reaction mixtures were purified by HiPrep™ 16/60 Sephacryl® S-100 HR column. Sample was diluted to 1 mL of PBS, loaded and eluted in PBS with a flow rate of 0.5 mL/min. Pooled fractions corresponding to pure conjugates were concentrated by Amikon 10k. Conjugates were characterized by micro BCA, SDS-PAGE and Dische assay, SEC-HPLC. No conjugate formation was observed with tetraRha-SH.

4.2.8 Conjugation reactions with CRM_{197}-EMCS and hexaRha-SH

CRM_{197}-EMCS (10 mg/mL) in NaPi 50 mM pH 7.2 + 20mM EDTA was added to dried tetraRha-SH in weight ratio tetraRha/CRM_{197} 1:1. Conjugation reaction occurred overnight at room No conjugate formation was observed by SEC-HPLC.

4.3 General method for the synthesis of CRM_{197} conjugates with SBAP linker

TetraRha and hexaRha were derivatized with SBAP linker. Oligomers (100 mM) were dissolved in DMSO/H_2O 9:1. TEA (5 eq) and SBAP (20 eq) were added. Reaction occurred in 4 h at room temperature. Derivatized oligomers were purified by prepacked single-use PD MidiTrap G-10. Reaction mixtures were eluted with water according to manufacturer instructions. Eluted oligomers were dried in SpeedVac Concentrator® then characterized by Dische assay and ESI-MS.

CRM-SH (10 mg/mL) in NaPi 100 mM pH 7.2 + 1 mM EDTA was added to dried oligomers working in a weight ratio oligomers/CRM_{197} 1:1. Conjugation reactions occurred overnight at room temperature. Reaction mixtures were purified by HiPrep™ 16/60 Sephacryl® S-100 HR column. Sample was diluted to 1 mL of PBS, loaded and eluted in PBS with a flow rate of 0.5 mL/min. Pooled fractions corresponding to pure conjugates were concentrated by Amikon 10k. Conjugates were characterized by micro BCA, SDS-PAGE and Dische assay, SEC-HPLC.

4.4 Synthesis of GAC-ADH

GAC polysaccharide (30 mg/mL) was dissolved in NaOAc 20 mM pH 4.5, then ADH linker and $NaCNBH_3$ were added working in a weight ratio GAC/ADH/$NaCNBH_3$ 1:1:1. Reaction occurred in 5 days at 30 °C. GAC-ADH was purified by prepacked single-use PD10 desalting column twice: GAC-ADH was diluted to 2.5 mL total volume to have final NaCl concentration of 3 M and eluted in NaCl 3M, collecting 3.5 mL of foregoing product. GAC-ADH was then dried in SpeedVac Concentrator®. Dried GAC-ADH was then dissolved in 2.5 mL of water and loaded in prepacked single-use PD10 desalting column. Elution was performed in water according to manufacturer instructions.

GAC-ADH was characterized by HPAEC-PAD, and TNBS assay[77]. Free ADH was detected by reversed Phase-Ultra High-Performance Liquid Chromatography (RP-UHPLC). A 600 nmol/mL solution of ADH was used to create a calibration curve in the 0.8-20 nmol/mL of amino groups range in a final volume of 250 µL. Samples were diluted with MilliQ water in order to obtain amino groups concentration in the range of calibration curve. A volume of 250 µL of 70 mM Sodium Phosphate pH 7.5 solution and a volume of 250 µL of 0.1% solution of TNBS were added to

standards and samples, then incubated for 2 h at 40 °C. Samples (10 μL injected) were eluted on a Kinetex reversed-phase column (2.6 μm, 50x4.6 mm, Phenomenex) on a Waters Alliance UPLC system with in-line UV, fluorescence emission, dRI detectors. Samples were eluted with a flow rate of 1.0 mL/min and eluent mixture was generated by the pump system. The eluent program (total run time 50 minutes) was: 90% water, 10% ACN in isocratic condition for 10 min; linear gradient 10% water, 90% ACN in 10 min; 10% water, 90% ACN in isocratic condition for 10 min; 90% water, 10% ACN in isocratic condition for 20 min (column re-equilibration). Detection was done at 425 nm. The amount of free ADH in the samples was calculated using the calibration curve built with the peak areas of derivatized ADH standards at 425 nm. The percentage of activated GAC was calculate as % of linked ADH moles/GAC moles.

4.5 General method for the synthesis of GMMA conjugates with BS^3 linker

GMMA were derivatized with BS^3 linker. GMMA were suspended in MES 100 mM pH 6 at concentration of 4 mg/mL and BS^3 (50 mg/mL) was added. Reaction occurred for 30 min at 25°C controlled temperature. Derivatized GMMA-BS^3 were purified by ultracentrifuge (UC) at 110K rpm for 16 minutes. A small portion of GMMA-BS^3 was resuspended in PBS for characterization by micro BCA for total protein content, and TNBS assay[77] to estimate % of NH2 groups on GMMA derivatised with BS3 linker. Total active esters groups introduced were quantified by RP-HPLC as sulfo N-hydroxysuccinimide (sulfo NHS) groups. A 1000 nmol/mL solution of sulfo NHS was used to create a calibration curve in the 5-300 nmol/mL range. GMMA-BS^3 were diluted with MilliQ water in order to obtain sample sulfo NHS concentration in the range of the calibration curve. Samples and calibration curve were prepared in 200 μL total volume and hydrolyzed with 400 μL of ammonia (NH_4OH) 0.17% for 1 h at room temperature. Samples were concentrated in SpeedVac Concentrator® and re-suspended in 200 μL of MilliQ water.

A volume of 200 μL for samples and calibration curve was injected and analyzed on TSK 3000. GAC-ADH, tetraRha and hexaRha in PBS were respectively added to GMMA-BS^3 pellets to have GMMA concentration of 10 mg/mL and weight ratio of GMMA to glycan of 1:3. Reactions were mixed overnight at room temperature. The resulting conjugates GMMA-GAC, GMMA-tetraRha and GMMA-hexaRha were purified by two UC steps (110K rpm for 30 min) and re-suspended in PBS. Full characterization was done by micro BCA, HPAEC-PAD and DLS.

4.6 General method for the synthesis of GMMA conjugates with reductive amination chemistry

GMMA suspended in NaOAc 100 mM pH 5 (GMMA concentration 2.38 mg/mL) were oxidized with $NaIO_4$ 10 mM for 2 h at room temperature in the dark. Oxidized GMMA were purified by UC at 110K rpm for 30 min. A small portion of GMMAox was re-suspended in PBS for characterization by micro BCA (total protein recovery) and HPAEC-PAD (for estimating % OAg oxidation). The % OAg oxidation was calculated on Rha, considering that the un-oxidized GMMA has a molar ratio Rha:Man of 1:1.

The oxidation step was also performed by using different reaction conditions. GMMA 2192 ΔtolR ΔPagP ΔmsbB suspended in NaPi 100 mM pH 6.5 (GMMA concentration 2 mg/mL) were oxidized with NaIO4 5 mM for 30 min at 25°C in the dark.

GAC-ADH in NaOAc 100 mM pH 4.5 and tetraRha and hexaRha or GAC-dimer in NaPi 100 mM pH 7.2 were respectively added to GMMAox pellets to have GMMAox concentration of 5 mg/mL. The reducent agent $NaCNBH_3$ was added (weight ratio GMMA/glycan/$NaCNBH_3$ 1:1:1 or 1:3:3) and reaction mixtures were stirred overnight at room temperature. Resulting conjugates GMMAox-GAC, GMMAox-tetraRha, GMMAox-hexaRha were purified twice by UC (110K rpm for 30 min) and characterized by micro BCA (total protein content), HPAEC-PAD (total sugar content) and DLS (average particle size determination).

4.7 General method for the synthesis of glycol-gold nanoparticles

Two different shape of gold nanoparticles (AuNPs), sphere (12 nm from Transmissio Electron Microscopy, TEM) and star (14 nm from TEM), were prepared by Laura Polito (CNR-ISTM, Nanotechnology Lab, Milan). That AuNPs were coated with TetraRha and hexaRha by meand PEG_{5000} linker.

The carboxylic acid group of HOOC-PEG_{5000}-SH was activated as pentafluoro phenyl ester. HOOC-PEG_{5000}-SH (80 mg, 0.016 mmol) was dissolved in 800 μL of DCM dry. Pentafluorophenol (6.1 mg, 0.033 mmol) and ethyl-3-(3-dimethylaminopropyl)carbodiimide (6.3 mg, 0.33 mmol) were added. Reaction mixture was stirred for 24 h, when TLC (DCM/MeOH 80:20) showed the disappearance of starting material. The solvent was concentrated under reduced pressure and product was precipitated from cooled Et_2O and filtered.

The filtered PFP-PEG_{5000}-SH (30 mg, 0.006 mmol) was dissolved in 400 μL of dried DCM and solution was degassed for 1 h. DIPEA (3.10 mg, 0.024 mmol) was added. A solution of oligoRha (tetraRha or hexaRha) in dried DMF (400 μL, 0.012 mmol) was added to the reaction mixture drop

by drop. The reaction occurred for 36 h, when TLC (DCM/MeOH 80:20) showed the disappearance of starting material. Solvent was removed under vacuum. The crude was dissolved in water and purified by G25 Sephadex. The yield was 30 % after two steps for both tetraRha-PEG (30.7 mg) and hexaRha-PEG (30.2 mg).

OligoRha-PEG were characterized by HPAEC-PAD to quantify tetraRha (313 μg) and hexaRha (246 μg).

Under argon atmosphere, 30 mg of the suitable oligoRha-PEG_{5000}-SH were dissolved in 5 mL of water containing 9 mg of NaOH. Au NPs were prepared by L. Polito (CNR-ISTM, Nanotechnology Lab, Milan) with a reported procedure[78]. Then, the oligoRha-PEG_{5000}-SH solution was added to the colloidal solution containing citrate-capped AuNPs (sphere or star) while Argon was bubbling inside the solution (for 5 minutes) and the reaction mixture stirred for further 48 h at room temperature. Functionalized sphere-oligoRha and star-oligoRha were then purified by means of Amikon centrifugal Filter units to a volume of 5 mL.

Nanosystems were characterized by DLS (Z-average), TEM (determination of diameter of core shape), NTA (nanoparticle quantification in NP/mL) and HPAEC-PAD (tetraRha or hexaRha quantification). The combination of NTA analysis with HPAEC-PAD analysis allowed to calculate the number of oligoRha chains per NP.

4.8 General methods for glycoconjugates characterization

4.8.1 Glycan quantification

Total saccharide concentration was determined by HPAEC-PAD analysis (ICS-3000 dionex system). Conjugates (450 µL) were hydrolyzed in 4M trifluoroacetic acid in a final volume of 600 µL for 4h at 100 °C, dried and dissolved in water. Samples of 25 µL were injected in CarboPac PA10 analytical column (4 x 250 mm) with CarboPac PA10 guard column (4 x 250 mm). Isocratic separations were performed using 50 mM NaOH followed by 500 mM NaOH regeneration step and re-equilibration, set to a flow rate of 1.0 mL/min. Monosaccharide peaks were detected directly using quadruple-potential waveform pulsed amperometry on a gold electrode and an Ag/AgCl reference electrode. Raw data were elaborated with Chromeleon software (Dionex) with 0.5-10 µg/mL calibration curves of Rha, GlcNAc for CRM_{197} conjugates and with 0.5-10 µg/mL calibration curve of Rha, GlcNAc, Gal, Glc, Man for GMMA conjugates.

Fast quantification of glycans on CRM_{197} conjugates or derivatized oligosaccharides was achieved by Dische assay. Samples were hydrolyzed in sulfuric acid 100% at 100 °C: methyl furfural (from rhamnose) was formed and made reacted with cysteine. Absorbance was measured at 396 nm and 427 nm before and after cysteine addition. Rhamnose concentration was calculated by subtracting the 427 nm contribute to 396 nm methyl pentose contribute in the range 2-32 µg/mL calibration curve of fucose.

4.8.2 Protein quantification

Total protein quantification was performed by micro BCA (Thermo Scientifics). A 2 mg/mL solution of serum bovine albumin (BSA) was used to create a calibration curve in the range 5-20 µg/mL. Samples were diluted with MilliQ water in order to obtain sample protein concentration in the range of the calibration curve with a final volume of 500 µL. The micro BCA reagent was prepared according to manufacturer instructions and 500 µL were added to each sample, then incubated for 1 h at 60°C. Absorbance at 562 nm was measured by spectrophotometer per each samples and protein concentration was calculated.

4.8.3 SDS-PAGE analysis

SDS-PAGE was performed on pre-casted polyacrylamide gels (NuPAGE®Invitrogen). 3-8% gradient or 7%. Gel were used. Electrophoretic runs were performed in Tris-Acetate SDS running buffer (NuPAGE®Invitrogen) loading 2.5- 5µg of protein per sample, using the electrophoretic

chamber with a voltage of 150V for 45 minutes. After electrophoretic running, the gel was washed in water for 3 times and then stained with dye comassie (TermoFisher).

4.8.3 Size Exclusion High Performance Liquid Chromatography (SEC-HPLC)

SEC-HPLC was performed on Waters Alliance (system, eluting the samples on a TSK 3000. with 0.1M NaCl 0.1M NaPi 5% CH_3CN pH 7.2 on SWXL (Tosoh Bioscience) at flow rate of 0.5 mL/min, with 80 µL of injection volume loading 50 µg of sample in protein content. The resulting chromatographic data were processed using Empower 3 software.
This analysis was performed to analyze glycoconjugate reaction mixtures in comparison to free CRM_{197} to verify glycoconjugate formation and, eventually, the presence of unreacted CRM_{197}.

4.9 STD NMR experiments

NMR experiments were carried out on a Bruker 600 MHz NMR instrument equipped with a TBI cooled probe at controlled temperature (± 0.1 K). Data acquisition and processing were performed using TOPSPIN 3.1 software. Proton-Carbon Saccharides resonances were assigned collecting both 1D (^1H and ^{13}C) and 2D (COSY, HSQC, HMBC, NOESY) experiments, using standard pulse sequences. STD-NMR experiments were acquired with 96 scans over 96 accumulations and spectral width of 8000 Hz (12 ppm) at 298 K; a saturation transfer of 2/4 sec. was applied to enhance the saturation transfer effect, irradiating at a frequency of 8.0 and -2.0 ppm (4000 and -1000 Hz respectively). Spectra acquired irradiating at a frequency of 8.0 ppm provide better signal/noise ration. To avoid pitfalls in the interpretation of STD-NMR spectra, a negative control spectrum was always recorded in absence of mAb (ligand and buffer only at the same molar concentration and pH of the protein-saccharide sample). The STD negative controls were always subtracted to the relative protein-saccharide STD spectrum, obtaining the STDD experiments.
Monoclonal antibody (anti-GAC from Abnova) was exchanged in the working buffer (Tris d-11 50 mM in D_2O at pH 7.2 +/- 0.1) through 2mL Zeba Spin desalting column pre-equilibrated with 3 cycles of working buffer. Oligomers were dissolved in the working buffer too. 200 µg of mAb were prepared in a final volume of 510 µL of buffer with 100 equivalents of GAC-dimer. Tetrarhamnose and N-acetyl glucosamine samples were prepared using the same Rha and the same GlcNAc molar concentration contained in GAC-dimer, respectively, and mixed with 200 µg of mAb in 510 µL of buffer.

4.10 Particles size distribution characterization

4.10.1 Dynamic Light Scattering (DLS)

DLS measurements of GMMA conjugates were performed with a Malvern Zetasizer Nano ZS (Malvern, Herremberg, Germany) equipped with a 663 nm He-Ne laser and operating at an angle of 173°. Scattering light detected at 173° was automatically adjusted by laser attenuation filters.

DLS measurements of gold glyco-nanoparticles were performed by L. Polito (CNR-STM, Nanotechnology Lab, Milan) with a Brookhaven instrument equipped with a 632.8 nm He-Ne laser and operating at an angle of 173°. Scattering light detected at 173° was automatically adjusted by laser attenuation filters.

For data analysis the viscosity and refractive index (RI) of PBS buffer solution (at 25°C) were used for GMMA conjugates, while water was used for glyco-gold nanoparticles.

The software used to collect and analyze the data was the Zetasizer software version 7.11. Temperature was set at 25 °C. 60 μL of each sample at 50 μg/mL protein content were measured in single-use polystyrene micro cuvette (ZEN0040, Alfatest) with a path length of 10 mm. The hydrodynamic diameter of GMMA conjugates and glycol-gold nanoparticles was expressed by a Z-average value of three measurements for each replicate.

4.10.2 Nanoparticle Tracking Analysis (NTA)

NS300 Nanosight instrument (Nanosight Ltd, Salisbury, UK) equipped with CMOS camera and 488 nm monochromatic laser beam was used. Data acquisition and processing were performed using NTA software 3.2. Automatic settings for the minimum track length, the minimal expected particle size and blur setting were applied. Viscosity settings for water were applied and automatically corrected for the temperature used (25 °C). Particle movement was analyzed by NTA software with camera level at 16, slider shutter at 1300 and slider gain at 512. Different detection threshold values were tested, adjusted for the sample appearance after dilution. Five movies of 30s at 25 frames per second were recorded, generating five replicate histograms that were averaged. Several dilutions of the samples were analysed and duplicates were recorded for every diluted sample.

Samples were slowly injected in the sample chamber using a 1 mL syringe in 5 to 10 seconds under controlled flow, using NanoSight syringe pump (speed 20). Each video was then analyzed to determine the respective mean and mode particle size. Concentrations of the sample are reported in nanoparticle per mL and particle frame.

4.11 Immunogenicity of conjugates in mice

Animal studies were performed at Toscana Life Science Animal Care Facility and were approved by the Italian Ministry of Health (Approval number 479/2017-PR of 09/06/2017). The groups of eight five weeks old female CD1 mice were immunized by intraperitoneal injection. All conjugates were compared at same rhamnose dose (2 μg Rha) formulated on Alhydrogel as adjuvant at 2 mg/mL Al^{3+} concentration. Mice received the vaccines at days 0 and 28. Sera were bled at days -1 (and pooled for each gorup), 14, 27 and 42. Sera were analyzed by ELISA from GVGH Immunoassay unit.

5 CONCLUSIONS

GAS causes autoimmune responses that can lead to RHD and, consequently, to the death of about 350,000 people worldwide annually and no vaccine is available against this pathogen. GAS clinical isolates express the GAC, a conserved surface polysaccharide comprising of α-L -Rhap(1→3)-α-L-Rhap(1→2)-β-D-GlcpNAc-(1→3) repeats. Although the main driver of GAS autoimmune responses is the so-called M protein; some studies have linked GlcNAc side chain of GAC with cross-reactive epitopes that might also be responsible for rheumatic diseases. On the other hand, the polyrhamnose backbone could be an alternative to GAC for a broadly conserved vaccine candidate against GAS infections.

Here, the chemical synthesis for producing fragments of GAC polysaccharide was developed with the final aim to investigate the role of structural features of GAC on the immune response induced by the corresponding glycoconjugate vaccine. TetraRha, hexaRha and GAC dimer were synthesized and fully characterized. For the first time well-defined synthetic structures were available to immunize mice and look at the role of GlcNAc on the immune response induced by GAC polysaccharide.

Different conjugation chemistries were tested for linking oligosaccharides produced to CRM_{197}. Among the chemistries tested, the use of SIDEA homo-bifunctional linker resulted in higher glycosylation degree and the process of intermediate SIDEA derivative was optimized to avoid protein crosslinking and to obtain well defined sun-like structure conjugates.

By immunizing mice with hexaRha-CRM_{197} and GAC-CRM_{197} conjugates we clarified that hexaRha is able to induce anti-Rha specific Abs, similar to those induced by GAC-CRM conjugate, but is not able to induce anti-GAC Abs. Anti-Rha Abs produced do not recognize GAC on GAS bacterial surface, as shown by FACS analysis. Such results were also confirmed by competitive ELISA experiments: anti-GAC Abs were not able to bind oligoRha independently of oligosaccharides chain length, while anti-Rha Abs showed dose-dependent binding, and affinity for the antibodies increased with oligosaccharides chain length. Finally, STD-NMR of tetraRha, GAC-dimer and GlcNAc suggested that the rhamnose backbone plays an important role in the presentation of GlcNAc side chain which is involved in a strong binding with mAbs, while GlcNAc alone is not recognized.

An immunogenicity study is ongoing to test also GAC dimer-CRM_{197} conjugate in mice, with the aim to verify possibility to use the synthetic oligosaccharide as alternative to native GAC in the development of a conjugate vaccine against GAS and to corroborate the concept that GlcNAc plays a dominant role on the immune response induced by GAC. STD-NMR results seem to indicate that GlcNAc residue is recognized in the context of GAC polysaccharide structure removing concerns

related to autoimmunity. To further support this finding, a competitive ELISA is ongoing by testing different structures that contain GlcNAc residues (GAC-dimer, GlcNAc alone and GBS III fragment).

In this study GMMA were also tested as carrier for GAC, showing ability to induce similar anti-GAC Abs response compared to the traditional CRM_{197} carrier protein. Presence of GAC on GMMA did not interfere with the immune response induced by GMMA itself, supporting the use of GMMA for the development of multivalent vaccines.

The opportunity to decorate spherical and anisotropic AuNPs with oligoRha has been also verified. Sphere and star AuNPs were used and for analytical methods were put in place to quantify number of oligosaccharide chains per nanoparticle. Different loading of oligoRha per AuNP was obtained according to oligosaccharides chain length and NP shape. As expected, these nanosystems confirmed much higher Abs binding affinity compared to free oligosaccharides (multivalency effect).

6 EXPERIMENTAL SESSION

General Methods for chemical synthesis of oligosaccharides

All chemicals were of reagent grade and were used without further purification. Reactions were monitored by thin-layer chromatography (TLC) on Silica Gel 60 F_{254} (Sigma Aldrich) or with high performance thin-layer chromatography (HPTLC); after examination under UV light, compounds were visualized by heating with 10% (v/v) ethanolic H_2SO_4. In the work up procedures, organic solutions were washed with the amounts of the indicated aqueous solutions, then dried with anhydrous Na_2SO_4, and concentrated under reduced pressure at 30-50ºC on a water bath. Column chromatography was performed using Silica Gel 200-400 mesh or Biotage SNAP Ultra.

^{1}H NMR spectra were measured at 400 MHz (except where otherwise specified) and 298 K with a Bruker Avance^{III} spectrometer; δ_H values were reported in ppm, relative to the internal standard Me_4Si (δ_H = 0.00, $CDCl_3$) or the water signal (δ_H = 4.79 ppm, D_2O). ^{13}C NMR spectra were measured at 100 MHz (except where otherwise specified) and 298 K with a Bruker Avance^{III} spectrometer; δ_C values are reported in ppm relative to the signal of $CDCl_3$ (δ_C = 77.0, $CDCl_3$). NMR signals were assigned by homonuclear and heteronuclear 2-dimensional correlation spectroscopy (COSY, HSQC).

Mass was measured by Electron Spray Ionization (ESI) or Matrix-Assisted Laser Ionization (MALDI) spectroscopy. Optical rotation was measured with a P-2000 Jasco polarimeter at 25°C.

Synthesis of oligorhamnoses: tetrarhamnose and hexarhamnose

2-O-acetyl-3,4-di-O-benzyl-α-rhamnopyranosyl trichloroacetimidate [6].

A solution of allyl monosaccharide **5** (3 g, 7.04 mmol) in THF (150 mL) containing 1,5-cyclooctadienebis(methyldiphenylphosphine)-Iridium(I)-hexafluorophosphate (297 mg, 0.352 mmol) was degassed for 1 h, then hydrogen was flown for 10 min. The mixture was stirred for 30 min, when ^{1}HNMR showed isomerization of the double bond. Water (51 mL) and I_2 (3.57 g, 14.08 mmol) were added. The mixture was stirred for 15 min, then partitioned with 10% NaS_2O_3 (30 mL) and DCM (100 mL for 3 times). Organic layers were unified, washed with 5% $NaHCO_3$ (150 mL), H_2O (150 mL) and brine (150 mL), then dried with Na_2SO_4 and concentrated under vacuum. The deallylated intermediate was purified by flash chromatography (hexane/AcOEt 80:20→60:40) to afford 2.63g of foregoing product, which was dissolved in DCM (50 mL), then CCl_3CN (4 mL, 41.16 mmol) and DBU (0.3 mL, 2.06 mmol) were added. The mixture was stirred for 1.5 h, concentrated under vacuum and purified on silica gel (hexane/AcOEt + 1% TEA 80:20→60:40). Compound **6** was recovered in 95% yield after two steps and checked by ^{1}HNMR and used in the next step to preserve the trichloroacetimidate from hydrolysis.

^{1}HNMR: ($CDCl_3$, 400 MHz): δ = 8.68 (s, 1H, NH), 7.41-7.30 (m, 10 H, Ph), 6.22 (d, 1H, $J_{1,2}$= 1.6 Hz, H-1), 5.52 (dd, 1H, $J_{1,2}$= 2.0 Hz, $J_{2,3}$= 2.8 Hz, H-2), 4.96 (d, 1H, *J* = 10.4 Hz, PhC*H*H), 4.76 (d, 1H, *J* = 10.8 Hz, PhC*H*H), 4.66 (d, 1H, *J* = 10.8 Hz, PhC*H*H), 4.61 (d, 1H, *J* = 11.2 Hz, PhC*H*H), 4.03 (dd, 1H, $J_{2,3}$= 3.2 Hz, $J_{3,4}$= 9.2 Hz, H-3), 4.00-3.93 (m, 1H, H-5), 3.56 (t, 1H, $J_{3,4}$= 9.6 Hz, H-4), 2.22 (s, 3H, CH_3CO), 1.38 (d, 3H, $J_{5,6}$= 6.4 Hz, H-6).

Allyl (2-O-acetyl-3,4-di-O-benzyl-α-rhamnopyranosyl)-(1-3)-2,4-di-O-benzyl-α-rhamnopyranoside [7].

To a stirred solution of acceptor allyl 2,4-di-O-benzyl-α-L-rhamnopyranoside **4** (2.03 g, 5.28 mmol) and donor **6** (3.35 g, 6.34 mmol) in DCM (50 mL) containing activated 4 Å molecular sieves (2.03 g), TMSOTf (1.19 mL, 0.528 mmol) was added at 0°C. The mixture was stirred at 0°C for 30 min. After neutralization with TEA, the mixture was concentrated and purified by flash chromatography (hexane/AcOEt 85:15) to afford product **7** in 75% yield.

^{1}HNMR: ($CDCl_3$, 400 MHz): δ = 7.42-7.23 (m, 20H, Ph), 5.92-5.82 (m, 1H, CH_2-C*H*=CH_2), 5.55 (dd, 1H, $J_{1,2}$= 1.6 Hz, $J_{2,3}$= 3.2 Hz, H-2^{II}), 5.25 (ddd, 1H, J_1= 1.6 Hz, J_2 = 3.2 Hz, CH_2-CH=C*H*H), 5.17 (ddd, 1H, J_1= 1.2 Hz, J_2 = 2.8 Hz, CH_2-CH=C*H*H), 5.13 (d, 1H, $J_{1,2}$= 1.2 Hz, H-1^{II}), 4.96 (d, 1H, *J* = 10.8 Hz, PhC*H*H), 4.84 (d, 1H, *J* = 10.8 Hz, PhC*H*H), 4.80 (d, 1H, $J_{1,2}$= 1.6 Hz, H-1^{I}), 4.70 (s, 2H, PhC*H*H), 4.67-4.62 (3 d, 3H, PhC*H*H), 4,48 (d, 1H, *J* = 10.4 Hz, PhC*H*H), 4.18-4.12 (m,

2H, C*H*H-CH=CH_2, H-3^{II}), 4.00-3.84 (m, 3H, C*H*H-CH=CH_2, H-3^{I}, H-5^{II}), 3.77-3.69 (m, 2H, H-2^{I}, H-5^{I}), 3.65 (t, 1H, $J_{3,4}$ = 9.6 Hz, H-4^{I}), 3.45 (t, 1H, $J_{3,4}$ = 9.6 Hz, H-4^{II}), 2.11 (s, 3H, CH_3CO), 1.33 (d, 3H, $J_{5,6}$ = 6.0 Hz, H-6^{I}), 1.30 (d, 3H, $J_{5,6}$ = 6.4 Hz, H-6^{II}).

Characterization in agreement to J.Zhang, J. Mao, H. Chen, M. Cain, *Tetrahedron Asymmetry*, **1994**, 5, 2283.

2-O-acetyl-3,4-di-O-benzyl-α-rhamnopyranosyl-(1-3)-2,4-di-O-benzyl-α-rhamnopyranosyl trichloroacetimidate [8].

A solution of disaccharide **7** (2.95 g, 3.92 mmol) in THF (150 mL) containing 1,5-cyclooctadienebis(methyldiphenylphosphine)-Iridium(I)-hexafluorophosphate (330 mg, 0.390 mmol) was degassed for 1 h, then hydrogen was flown for 10 min. The mixture was stirred for 30 min, when ^{1}HNMR showed isomerization of the double bond. Water (50 mL) and I_2 (2.0 g, 7.84 mmol) were added. The mixture was stirred for 15 min, then partitioned with 10% NaS_2O_3 (30 mL) and DCM (100 mL for 3 times). Organic layers were unified, washed with 5% $NaHCO_3$ (150 mL), H_2O (150 mL) and brine (150 mL), then dried with Na_2SO_4 and concentrated. The deallylated intermediate was purified on silica gel (hexane/AcOEt 80:20→60:40) to afford 2.8 g of foregoing product, which was dissolved in DCM (40 mL), then CCl_3CN (2.4 mL, 23.58 mmol) and DBU (0.176 mL, 1.18 mmol) were added. The mixture was stirred for 2 h, concentrated and purified by flash chromatography (hexane/AcOEt + 1% TEA 70:30). Compound **8** was recovered in 95% yield after two steps. The presence of trichloroacetimidate was confirmed by ^{1}HNMR with typical NH signal at 8.46 ppm. Compound **8** has been used immediately in the next step to preserve the trichloroacetimidate from hydrolysis.

^{1}HNMR: ($CDCl_3$, 400 MHz): δ = 8.46 (s, 1H, NH), 7.33-7.21 (m, 20H, Ph), 6.19 (d, 1H, $J_{1,2}$ = 1.3 Hz, H-1^{I}), 5.46 (dd, 1H, $J_{1,2}$ = 1.5 Hz, $J_{2,3}$ = 2.7 Hz, H-2^{II}), 5.04 (s, 1H, H-1^{II}), 4.85 (d, 1H, J = 11.0 Hz, PhC*H*H), 4.74 (d, 1H, J = 10.9 Hz, PhC*H*H), 4.69-4.49 (m, 5H, PhC*H*H), 4.42 (d, 1H, J = 10.9 Hz, PhC*H*H), 4.05 (dd, 1H, $J_{2,3}$= 3.2 Hz, $J_{3,4}$= 9.8 Hz, H-3^{II}), 3.86-3.81 (m, 3H, H-3^{I}, H-5^{I}, H-5^{II}), 3.70-3.61 (m, 2H, H-2^{I}, H-4^{I}), 3.34 (t, 1H, $J_{3,4}$ = 8.8 Hz, H-4^{II}), 2.07 (s, 3H, CH_3CO), 1.27 (d, 3H, $J_{5,6}$ = 6.2 Hz, H-6^{I}), 1.13 (d, 3H, $J_{5,6}$ = 6.4 Hz, H-6^{II}).

Characterization in agreement to S. Crotti, H. Zhai, J. Zhou, M. Allan, D. Proietti, W. Pansegrau, Q.Y. Hu, F. Berti, R. Adamo, *ChemBioChem*, **2014**, 15, 836.

3-(benzyloxycarbonyl)aminopropyl (2-O-acetyl-3,4-di-O-benzyl-α-rhamnopyranosyl)-(1-3)-2,4-di-O-benzyl- α-rhamnopyranoside [9].

To a stirred solution of 3-(benzyloxycarbonyl)aminopropanol (732 mg, 3.5 mmol) and disaccharide **8** (1.5 g, 1.75 mmol) in DCM (17 mL) containing activated 4 Å molecular sieves (732 mg), TMSOTf (0.397 mL, 0.175 mmol) was added at 0°C. The mixture was stirred at 0°C for 2 h. After neutralization with TEA, the mixture was concentrated and purified by flash chromatography (hexane/AcOEt 90:10→70:30). Compound **9** was recovered in 60% yield.

^{1}HNMR: ($CDCl_3$, 400 MHz): δ = 7.41-7.21 (m, 25H, Ph), 5.53 (dd, 1H, $J_{1,2}$ = 1.6 Hz, $J_{2,3}$ = 3.2 Hz, H-2^{II}), 5.10 (s, 2H, CH_2Cbz), 4.95 (d, 1H, *J* = 10.4 Hz, PhC*H*H), 4.82 (d, 1H, *J* = 10.5 Hz, PhC*H*H), 4-75-4.60 (m, 7H, PhC*H*H, H-1^{I}, H-1^{II}), 4.47 (d, 1H, *J* = 11.6 Hz, PhC*H*H), 4.07 (dd, 1H, $J_{2,3}$ = 3.6 Hz, $J_{3,4}$ = 9.2, H-3^{I}), 3.97 (dd, 1H, $J_{2,3}$ = 3.2 Hz, $J_{3,4}$ = 9.2, H-3^{II}), 3.92-3.83 (m, 1H, H-5^{II}), 3.75-3.59 (m, 4H, H-2^{I}, H-4^{I}, H-5^{I}, O-C*H*H-CH_2-CH_2-NH), 3.47-3.37 (m, 2H, H-4^{II}, O-C*H*H-CH_2-CH_2-NH), 3.32-3.22 (m, 2H, O-CH_2-CH_2-CH_2-NH), 2.10 (s, 3H, CH_3CO), 1.80-1.74 (m, 2H O-CH_2-CH_2-CH_2-NH), 1.31 (d, 3H, , $J_{5,6}$ = 6.0 Hz, H-6^{I}), 1.28 (d, 3H, $J_{5,6}$ = 6.0 Hz, H-6^{II}).

Characterization in agreement to S. Crotti, H. Zhai, J. Zhou, M. Allan, D. Proietti, W. Pansegrau, Q.Y. Hu, F. Berti, R. Adamo, *ChemBioChem*, **2014**, 15, 836.

3-(benzyloxycarbonyl)aminopropyl (3,4-di-O-benzyl-α-rhamnopyranosyl)-(1-3)-2,4-di-O-benzyl- α-rhamnopyranoside [10].

Compound **9** (950 mg, 1.05 mmol) was dissolved in MeOH (10 mL) and a solution 0.1M of NaOMe/MeOH was added until pH 9. The mixture was stirred for 1h, then neutralized with Amberlite resin (H^+ form). After filtration, compound **10** was concentrated and recovered in quantitative yield.

^{1}HNMR: ($CDCl_3$, 400 MHz): δ = 7.40-7.24 (m, 25H, Ph), 5.14 (d, 1H, , $J_{1,2}$ = 1.2 Hz, H-1^{II}), 5.10 (s, 2H, CH_2Cbz), 4.91 (d, 1H, *J* = 10.8, PhC*H*H), 4.76-4.59 (m, 7H, PhC*H*H, H-1^{I}), 4.05 (dd, 1H, $J_{2,3}$ = 3.2 Hz, $J_{3,4}$ = 9.2, H-3^{I}), 4.01 (dd, 1H, $J_{1,2}$ = 1.6 Hz, $J_{2,3}$ = 2.8, H-2^{II}), 3.89-3.83 (m, 2H, H-3^{II}, H-5^{II}), 3.74-3.63 (m, 3H, H-2^{I}, H-5^{I}, O-C*H*H-CH_2-CH_2-NH), 3.58 (t, 1H, $J_{3,4}$ = 9.2 Hz, H-4^{I}), 3.51-3.38 (m, 2H, H-4^{II}, O-C*H*H-CH_2-CH_2-NH), 3.32-3.22 (m, 2H, O-CH_2-CH_2-CH_2-NH), 1.81-1.75 (m, 2H, O-CH_2-CH_2-CH_2-NH), 1.31 (d, 3H, $J_{5,6}$ = 6.0 Hz, H-6^{I}), 1.26 (d, 3H, $J_{5,6}$ = 6.0 Hz, H-6^{II}).

Characterization in agreement to S. Crotti, H. Zhai, J. Zhou, M. Allan, D. Proietti, W. Pansegrau, Q.Y. Hu, F. Berti, R. Adamo, *ChemBioChem*, **2014**, 15, 836.

3-(benzyloxycarbonyl)aminopropyl (2-O-acetyl-3,4-di-O-benzyl-α-rhamnopyranosyl)-(1-3)-(2,4-di-O-benzyl-α-rhamnopyranosyl)-(1-2)-(3,4-di-O-benzyl-α-rhamnopyranosyl)-(1-3)-2,4-di-O-benzyl- α-rhamnopyranoside [11].

To a stirred solution of acceptor **10** (904 mg, 1.05 mmol) and donor **8** (1.0 g, 1.26 mmol) in DCM (11 mL) containing activated 4 Å molecular sieves (904 mg), TMSOTf (0.238 mL, 0.105 mmol) was added at 0°C. The mixture was stirred at 0°C for 30 min. After neutralization with TEA, the mixture was concentrated and purified by flash chromatography (hexane/AcOEt 80:20→60:40) to afford the product **11** in 86% yield.

^{1}HNMR: ($CDCl_3$, 400 MHz): δ = 4.42-7.15 (m, 45H, Ph), 5.55 (dd, 1H, $J_{1,2}$ = 1.6 Hz, $J_{2,3}$ = 2.7 Hz, H-2^{IV}), 5.14-5.03 (m, 4H, H-1^{II}, H-1^{III}, CH_2Cbz), 4.97-4.77 (m, 4H, H-1^{IV}, PhC*H*H, H-1^{I}), 4.74-4.43 (m, 14H, PhC*H*H), 4.18-4.11 (m, 2H, H-2^{III}, H-3^{IV}), 4.05 (s, 1H, H-2^{II}), 4.00 (dd, 1H, $J_{2,3}$ = 3.2 Hz, $J_{3,4}$ = 9.2, H-3^{I}), 3.94 (dd, 1H, $J_{2,3}$ = 3.6 Hz, $J_{3,4}$ = 9.6, H-3^{II}), 3.91-3.83 (m, 2H, H-3^{III}, H-5^{I}), 3.82-3.51 (m, 8H, H-2^{I}, H-4^{I}, H-4^{II}, H-5^{II}, H-5^{III}, H-5^{IV}, O-C*H*H-CH_2-CH_2-NH), 3.46-3.36 (m, 3H, H-4^{III}, H-4^{IV}, O-C*H*H-CH_2-CH_2-NH), 3.31-3.21 (m, 2H, O-CH_2-CH_2-C*H*$_2$-NH), 2.10 (s, 3H, CH_3CO), 1.82-1.74 (m, 2H, O-CH_2-C*H*$_2$-CH_2-NH), 1.31-1.16 (m, 12H, H-6^{I}, H-6^{II}, H-6^{III}, H-6^{IV}).

Characterization in agreement to S. Crotti, H. Zhai, J. Zhou, M. Allan, D. Proietti, W. Pansegrau, Q.Y. Hu, F. Berti, R. Adamo, *ChemBioChem*, **2014**, 15, 836.

3-(benzyloxycarbonyl)aminopropyl (3,4-di-O-benzyl-α-rhamnopyranosyl)-(1-3)-(2,4-di-O-benzyl-α-rhamnopyranosyl)-(1-2)-(3,4-di-O-benzyl-α-rhamnopyranosyl-(1-3)-2,4-di-O-benzyl-α-rhamnopyranoside [12].

Compound **11** (1.4 g, 0.903 mmol) was dissolved in MeOH (8 mL) and a solution 0.1M of NaOMe/MeOH was added until pH 9. The mixture was stirred for 1h, when ^{1}HNMR showed the disappearance of the acetate signal at 2.10 ppm. the reaction was neutralized with Amberlite (H^+ form). After filtration, compound **12** was concentrated and used in the next step without other purification.

3-aminopropyl α-rhamnopyranosyl-(1-3)-α-rhamnopyranosyl-(1-2)-α-rhamnopyranosyl-(1-3)-α-rhamnopyranoside [1].

Compound **12** (630 mg, 0.416 mmol) was dissolved in a mixture EtOH/H_2O 1:1 + HCl 5% (8mL) and 10% Pd/C (100 mg) was added. The hydrogenation was performed with appropriate reactor using high H_2 pressure (20 bar). The mixture was stirred overnight, then filtered through a celite pad

and the filtered was concentrated under vacuum. The residue was lyophilized to afford tetraRha **1** in 90% yield.

^{1}HNMR: (D_2O, 400 MHz): δ = 5.18 (s, 1H, H-1^{II}), 5.04 (s, 1H, H-1^{III}), 4.94 (s, 1H, H-1^{IV}), 4.80 (s, 1H, H-1^{I}), 4.15 (s, 1H,), 4.06 (s, 2H,), 4.00 (s, 1H,), 3.90 (dd, $J_{2,3}$ = 2.8 Hz, $J_{3,4}$ = 9.6, H-3^{III}), 3.8-3.6 (m, 9H), 3.57-3.39 (m, 6H), 3.09-3.01 (m, 2H, O-CH_2-CH_2-CH_2-NH), 1.97-1.89 (m, 2H, O-CH_2-CH_2-CH_2-NH), 1.28-1.19 (m, 12H, H-6^{I}, H-6^{II}, H-6^{III}, H-6^{IV}).

Characterization in agreement to S. Crotti, H. Zhai, J. Zhou, M. Allan, D. Proietti, W. Pansegrau, Q.Y. Hu, F. Berti, R. Adamo, *ChemBioChem*, **2014**, 15, 836.

3-(benzyloxycarbonyl)aminopropyl (2-O-acetyl-3,4-di-O-benzyl-α-rhamnopyranosyl)-(1-3)-(2,4-di-O-benzyl-α-rhamnopyranosyl)-(1-2)-(3,4-di-O-benzyl-α-rhamnopyranosil)-(1-3)-(2,4-di-O-benzyl-α-rhamnopyranosyl)-(1-2)-(2,4-di-O-benzyl-α-rhamnopyranosyl)-(1-3)-3,4-di-O-benzyl-α-rhamnopyranoside [13].

To a stirred solution of acceptor **12** (1.0 g, 0.66 mmol) and donor **8** (677 mg, 0.792 mmol) in DCM (7 mL) containing activated 4 Å molecular sieves (1.0 g), TMSOTf (0.149 mL, 0.066 mmol) was added at 0°C. The mixture was stirred at 0°C for 1h. After neutralization with TEA, the mixture was concentrated and purified with Biotage SNAP 50g column (hexane/AcOEt 0→100%) to afford product **11** in 86% yield.

^{1}HNMR: ($CDCl_3$, 400 MHz): δ = 7.41-7.20 (m, 65H, Ph), 5.57 (dd, 1H, $J_{1,2}$ = 1.6 Hz, $J_{2,3}$ = 3.2 Hz, H-2^{VI}), 5.16-5.02 (m, 7H, H-1^{VI}, H-1^{V}, H-1^{IV}, H-1^{III}, H-1^{II}, CH_2Cbz), 4.97-4.77 (m, 7H, H-1^{I}, PhC*H*H), 4.75-4.43 (m, 20H, PhC*H*H), 4.19 (dd, 1H, $J_{2,3}$ = 2.8 Hz, $J_{3,4}$ = 9.2, H-3^{VI}), 4.12 (dd, 1H, $J_{2,3}$ = 3.2 Hz, $J_{3,4}$ = 9.6, H-3^{V}), 4.07 (dd, 1H, $J_{1,2}$ = 2.0 Hz, H-2^{V}), 4.02 (dd, 1H, $J_{2,3}$ = 3.2 Hz, $J_{3,4}$ = 9.2, H-3^{IV}), 3.95 (dd, 1H, $J_{2,3}$ = 3.6 Hz, $J_{3,4}$ = 9.6, H-3^{III}), 3.93-3.51 (m, 17H), 3.50-3.39 (m, 4.51), 3.33-3.25 (m, 2H, O-CH_2-CH_2-CH_2-NH), 2.11 (s, 3H, CH_3CO), 1.82-1.70 (m, 2H, O-CH_2-CH_2-CH_2-NH), 1.31-1.22 (m, 12H, H-6^{VI}, H-6^{V}, H-6^{IV}, H-6^{III}), 1.19 (d, 3H, $J_{5,6}$ = 6.4 Hz, H-6^{II}), 1.11 (d, 3H, $J_{5,6}$ = 6.0 Hz, H-6^{I}). ^{13}CNMR ($CDCl_3$, 100MHz): δ = 169.88 (CO), 156.37 (CONH), 138.79, 138.29, 138.03, 128.39, 128.30, 128.15, 127.74, 127.56 (Ph), 100.96, 100.64, 99.71, 99.46, 99.103, 97.53 (C-1), 81.16, 80.69, 80.65, 80.34, 79.99, 79.82, 78.17, 78.05, 77.85, 76.53, 75.51, 75.20, 74.72, 72.72, 72.41, 72.27, 71.75, 69.00, 68.76, 68.53, 68.30, 66.63, 65.17, 38.50, 29.65, 21.02 (*C*H_3CO), 18.04. MALDI: $[M+Na]^+$= 2232.13.

3-aminopropyl α-rhamnopyranosyl-(1-3)-α-rhamnopyranosyl-(1-2)-α-rhamnopyranosyl-(1-3)-α-rhamnopyranosyl-(1-2)-α-rhamnopyranosyl-(1-3)-α-rhamnopyranoside [2].

Compound **13** (1.2 g, 0.543 mmol) was dissolved in MeOH (5mL) and a solution 0.1M NaOMe/MeOH was added until pH 9. The mixture was stirred for 2h, when the ^{1}HNMR showed the disappearance of the acetate signal at 2.11 ppm. The reaction was neutralized with Amberlite (H^+ form), filtered and concentrated. The resulting intermediate **14** was dissolved in EtOH/H_2O 1:1 + HCl 5% in presence of 10% Pd/C (100 mg) to perform hydrogenation at high pressure of H_2 (20 bar). The reaction was stirred overnight, then filtered through a celite pad. The filtrated was concentrated under vacuum and lyophilized to afford hexaRha **2** in 90% yield.

^{1}HNMR: (D_2O, 400 MHz): δ = 5.16 (bs, 2H, H-1^{VI}, H-1^{V}), 5.02 (s, 1H, H-1^{IV}), 4.93 (bs, 2H, H-1^{III}, H-1^{II}), 4.81-4.66 (H-1^{I}), 4.17-3.88 (m, 8H, H-3^{VI}, H-3^{V}, H-3^{IV}, H-3^{III}, H-4^{VI}, H-4^{V}, H-4^{IV}, H-4^{III}), 3.87-3.64(m, 25H, O-C*H*H-CH_2-CH_2-NH, H-2^{VI}, H-2^{V}, H-2^{IV}, H-2^{III}, H-2^{II}, H-2^{I}, H-3^{II}, H-3^{I}, H-4^{II}, H-5^{VI}, H-5^{V}, OH), 3.62-3.42 (m, 6H, O-C*H*H-CH_2-CH_2-NH, H-4^{II}, H-5^{IV}, H-5^{III}, H-5^{II}, H-5^{I}), 3.10 (bs, 2H, O-CH_2-CH_2-C*H*$_2$-NH), 1.97 (bs, 2H, O-CH_2-C*H*$_2$-CH_2-NH), 1.34-1.20 (m, 18H, H-6^{VI}, H-6^{V}, H-6^{IV}, H-6^{III}, H-6^{II}, H-6^{I}). ^{13}CNMR (D_2O, 100MHz): δ = 102.23, 101.92, 101.86, 100.71, 100.70, 99.50, 77.97, 77.86, 77.75, 72.05, 71.87, 71.59, 71.50, 71.19, 70.00, 69.77, 69.76, 69.18, 69.17, 69.16, 69.15, 69.10, 69.00, 64.68, 37.38, 26.47, 16.58, 16.57, 16.55, 16.53, 15.51, 16.49. ESI: $[M+Na]^+$= 974.48. $[\alpha]_D^{25}$ = -32.40° (c 0.5, D_2O).

Synthesis of GAC-dimer

1,2,3,4-tetra-O-acetyl-α-rhamnopyranose [15].

In a solution of Ac_2O (250 mL) and I_2 (2.4 g, 9.60 mmol) at 0 °C, L-rhamnose (50 g, 274 mmol) was added. The mixture was stirred for 15min, then a solution of 10% NaS_2O_3 (100 mL) was added and product was extracted with DCM (120 mL) for three times. Organic layers were unified and washed with a solution of 5% $NaHCO_3$ (200 mL), H_2O (200 mL) and brine (200 mL), dried and concentrated under vacuum. The product **15** was recovered in α/β mixture (40% β from NMR) in quantitative yield.

^{1}HNMR: ($CDCl_3$, 400 MHz): δ = 6.02 (s, 1H, H-1α), 5.84 (s, 1H, H-1β), 5.48 (bs,1H, H-3 β), 5.31 (dd, 1H, $J_{2,3}$ = 3.6 Hz, $J_{3,4}$ = 10.4 Hz, H-3α), 5.26-5.24 (m, 1H, H-2α), 5.16-5.07 (m, 3H, $J_{3,4}$ = 10.0 Hz, H-4α, H-2β, H- 4β), 3.98-3.91 (m, 1H, H-5α), 3.71-3.64 (m, 1H, H-5β), 2.23 (s, 3H, CH_3CO), 2.21 (s, 3H, CH_3CO), 2.17 (s, 3H, CH_3CO), 2.16 (s, 3H, CH_3CO), 2.10 (s, 3H, CH_3CO), 2.07 (s, 3H, CH_3CO), 2.01 (s, 3H, CH_3CO), 1.3 (d, 1H, $J_{5,6}$ = 6.4 Hz, H-6β), 1.24 (d, 1H, $J_{5,6}$ = 6.0 Hz, H-6α). ^{13}CNMR ($CDCl_3$, 100 MHz): δ = 170.06, 169.83, 168.36, 90.58 (C-1α), 90.27 (C-1β), 71.40 (C-5β), 70.67, 70.42, 70.20, 68.72 (C-5α),68.65, 68.60, 68.47, 22.12, 20.81, 20.73, 20.60, 17.40(C-6α), 17.32 (C-6β). ESI: $[M+Na]^+$= 355.12. $[\alpha]_D^{25}$ = -57.87° (c 1.1, $CHCl_3$).

3-(benzyloxycarbonyl) aminopropyl 2,3,4-tri-O-acetyl-α-rhamnopyranoside [16].

3-(benzyloxycarbonil)aminopropanol (37.80 g, 180.66 mmol) and compound **15** (20 g, 60.22 mmol) were dissolved in DCM (250 mL). The reaction mixture was cooled at 0°C and $BF_3{\cdot}Et_2O$ (22.3 mL, 180.66 mmol) was added slowly. After 30 min, the reaction was left to warm at room temperature, then stirred overnight at 40°C. The reaction was neutralized with TEA at 0°C, concentrated under reduced pressure and purified by flash chromatography (hexane/AcOEt 1:1). The α-product **16** was recovered in 62% yield.

^{1}HNMR: ($CDCl_3$, 400 MHz): δ = 7.39-7.32 (m, 5H, Ph), 5.29 (dd, 1H, $J_{2,3}$ = 3.2 Hz, $J_{3,4}$ = 9.6 Hz, H-3), 5.25 (dd, 1H, $J_{1,2}$ = 1.6 Hz, $J_{2,3}$ = 3.6 Hz, H-2), 5.13 (s, 2H, CH_2Cbz), 5.08 (t, 1H, $J_{3,4}$ = 10.0 Hz, H-4), 4.9 (bs, 1H, NH), 4.73 (d, $J_{1,2}$ = 1.6 Hz, H-1), 3.91-3.83 (m, 1H, H-5), 3.80-3.75 (m, 1H, O-C*H*H-CH_2-CH_2-NH), 3.54-3.48 (m, 1H, O-C*H*H-CH_2-CH_2-NH), 3.36-3.31 (m, 2H, O-CH_2-CH_2-C*H*$_2$-NH), 2.17 (s, 3H, CH_3CO), 2.06 (s, 3H, CH_3CO), 2.01 (s, 3H, CH_3CO), 1.90-1.80 (m, 2H O-CH_2-C*H*$_2$-CH_2-NH), 1.24 (d, 3H, $J_{5,6}$ = 6.0 Hz, H-6). ^{13}CNMR ($CDCl_3$, 100 MHz): δ = 170.16, 169.84, 156.46, 128.51, 128.08, 97.54 (C-1), 71.05 (C-4), 69.89 (C-2), 69.12 (C-3), 66.70 (*C*H_2Cbz), 66.51 (C-5), 65.79 (O-*C*H_2-CH_2-CH_2-NH), 38.47 (O-CH_2-CH_2-*C*H_2-NH), 29.68 (O-CH_2-*C*H_2-CH_2-NH), 20.91, 20.81, 20.72, 17.44 (C-6). ESI: $[M+Na]^+$= 504.41. $[\alpha]_D^{25}$ = - 25.20° (c 0.5, $CHCl_3$).

3-(benzyloxycarbonyl) aminopropyl 2,3-O-isopropylidene-α-rhamnopyranoside [17].

Compound **16** (15 g, 31.17 mmol) was dissolved in MeOH (200 mL) and a solution 0.1M of NaOMe/MeOH was added until pH 9. The mixture was stirred overnight, then neutralized with Amberlite (H^+ form), filtered and concentrated. The crude was dissolved in 2,2-dimethoxypropane/DCM 4:1 (200 mL) and *p*-TsOH (1.48 g, 7.79 mmol) was added. The mixture was stirred overnight at room temperature, then neutralized with TEA at 0 °C and concentrated. Product **17** was recovered in 87% yield after purification by flash chromatography (hexane/AcOEt 50:50).

^{1}HNMR: ($CDCl_3$, 400 MHz): δ = 7.39-7.32 (m, 5H, Ph), 5.13 (CH_2Cbz), 4.95 (s, 1H, H-1), 4.92 (bs, 1H, NH), 4.14 (d, 1H, $J_{2,3}$ = 2.8 Hz, H-2), 4.08 (t, 1H, $J_{3,4}$ = 7.2 Hz, H-3), 3.83-3.77 (m, 1H, O-C*H*H-CH_2-CH_2-NH), 3.68-3.61 (m, 1H, H-5), 3.54-3.48 (m, 1H, O-C*H*H-CH_2-CH_2-NH), 3.41 (dd, 1H, $J_{3,4}$ = 7.2 Hz, $J_{4,5}$ = 9.2 Hz, H-4), 3.36-3.18 (m, 2H, O-CH_2-CH_2-CH_2-NH), 1.88-1.79 (m, 3H, OH, O-CH_2-CH_2-CH_2-NH), 1.54 (s, 3H, OCH_3), 1.37 (s, 3H, OCH_3), 1.30 (d, 3H, $J_{5,6}$ = 6.0 Hz, H-6). ^{13}CNMR ($CDCl_3$, 100 MHz): δ = 128.56, 128.55, 128.18, 128.14, 97.33 (C-1), 78.31 (C-2), 75.85 (C-3), 74.51 (C-4), 66.77 (*C*H_2Cbz), 66.01 (C-5), 65.36, 38.62, 29.55, 27.96 (O*C*H_3), 26.25 (O*C*H_3), 17.48. ESI: $[M+Na]^+$= 418.39. $[\alpha]_D^{25}$ = -25.20˚ (c 0.5, $CHCl_3$).

3-(benzyloxycarbonyl)-3-N-benzyl aminopropyl 4-O-benzyl-2,3-O-isopropylidene- -α-rhamnopyranoside [18].

To a solution of compound **17** (5 g, 8.68 mmol) in DMF (80 mL) at 0°C, NaH (1.25 g, 52.08 mmol) was added. Benzyl bromide (4 mL, 34.72 mmol) was introduced dropwise. The mixture was stirred overnight at room temperature, then concentrated to the minimum amount of solvent (~20 mL) and cooled at 0°C. H_2O (20 mL) was added slowly and the product was extracted with DCM (20 mL for five times). Organic layers were unified and washed with brine (40 mL), dried and concentrated under vacuum. The product **18** was recovered in 72% yield after purification by flash chromatography (hexane/AcOEt 90:10→60:40).

^{1}HNMR: ($CDCl_3$, 400 MHz): δ = 7.40-7.22 (m, 15H, Ph), 5.21 (bs, 2H, CH_2Cbz), 4.90 (d, bs, 2H, *J* = 11.2 Hz, PhC*H*H, H-1), 4.65 (d, 1H, *J* = 11.2 Hz, PhC*H*H), 4.53 (s, 2H, $PhCH_2$), 4.25 (bs, 1H, H-2), 4.10 (bs, 1H, H-3), 3.67 (bs, 2H, H-5, O-C*H*H-CH_2-CH_2-NH), 3.38 (bs, 3H, O-C*H*H-CH_2-CH_2-NH, O-CH_2-CH_2-CH_2-NH), 3.22 (dd, 1H, $J_{3,4}$ = 6.8 Hz, $J_{4,5}$ = 9.2 Hz, H-4), 1.82 (bs, 2H, O-CH_2-CH_2-CH_2-NH), 1.53 (s, 3H, OCH_3), 1.39 (s, 3H, OCH_3), 1.27 (d, 3H, $J_{5,6}$ = 6.2 Hz, H-6). ^{13}CNMR ($CDCl_3$, 100 MHz): δ = 138.31, 137.77, 136.68, 128.56, 128.49, 128.25, 127.87, 127.67, 127,66, 127.40, 127.23, 109.29, 96.99 (C-1), 80.96 (C-4), 78.56, 76.67, 72.84, 67.32, 64.51, 50.76, 50.75, 27.94, 26.42, 17.77. ESI: $[M+Na]^+$= 598.60. $[\alpha]_D^{25}$ = -25.70˚ (c 1.2, $CHCl_3$).

3-(benzyloxycarbonyl)-3-N-benzyl aminopropyl 4-O-benzyl-α-rhamnopyranoside [19].

Compound **18** (5 g, 8.68 mmol) was dissolved in DCM (50 mL) and cooled at 0°C. A solution of TFA 50% in DCM was added (13 mL) and the mixture was stirred for 2h, when NMR showed the disappearance of methoxy signals (1.53 ppm and 1.39 ppm). The reaction was treated with a saturated solution of K_2CO_3 (20 mL). The organic layer was washed with H_2O (20 mL) and brine (20 mL), dried and concentrated. The product was used in the next step without other purification.

3-(benzyloxycarbonyl)-3-N-benzyl-aminopropyl 4-O-benzyl-3-O-naphthylmethyl- -α-rhamnopyranoside [20].

To a solution of compound **19** (4.6 g, 8.68 mmol) in toluene (50 mL) 4Å activated molecular sieves (2.3 g) and Bu_2SnO (2.58 g, 10.42 mmol) were added. The reaction was stirred for 4h at reflux, then it was cooled at 45°C and NapBr (2.16 g, 10.42 mmol) and TBAI (3.8 g, 10.42 mmol) were introduced. The mixture was stirred overnight, then filtered on a celite pad, concentrated and purified by flash chromatography (hexane/AcOEt 90:10→50:50) to afford product **20** in 54% yield. ^{1}HNMR: ($CDCl_3$, 400 MHz): δ = 7.87-7.76 (m, 4H, Ph-Nap), 7.52-7.46 (m, 3H, Ph-Nap), 7.39-7.19 (m, 15H, Ph), 5.21 (s, 2H, CH_2Cbz), 4.95 (d, 1H, *J* = 11.2, PhC*H*H), 4.87-7.19 (bs, 3H, $PhCH_2$, H-1), 4.69 (d, 1H, *J* = 11.2, PhC*H*H), 4.51 (bs, 2H, $PhCH_2$), 4.02 (bs, 1H, H-2), 3.88 (bs, 1H, H-3), 3.70 (bs, 2H, O-C*H*H-CH_2-CH_2-NH, H-5), 3.49 (t, 1H, $J_{3,4}$ = 9.6 Hz), 3.35 (bs, 3H, O-C*H*H-CH_2-CH_2-NH, O-CH_2-CH_2-CH_2-NH), 2.19 (bs, 1H, OH), 1.80 (bs, 2H, O-CH_2-CH_2-CH_2-NH), 1.33 (d, 3H, $J_{5,6}$ = 6.4 Hz, H-6). ^{13}CNMR ($CDCl_3$, 100 MHz): δ = 156.68, 138.40, 137.78, 136.71, 135.33, 133.25, 133.05, 128.59, 128.42, 127.95, 127.70, 127.40, 127.24, 126.61, 126.20, 126.04, 125.76, 98.95, 75.41, 72.09, 68.64, 67.42, 67.26, 65.15, 50.59, 27.81, 17.85. ESI: $[M+Na]^+$= 698.74. $[\alpha]_D^{25}$ = -16.76˚ (c 0.6, $CHCl_3$).

3-(benzyloxycarbonyl)-3-N-benzyl-aminopropyl 2,4-di-O-benzyl-3-O-naphthylmethyl-α-rhamnopyranoside [21].

To a solution of compound **20** (3.16 g, 4.67 mmol) in DMF (46 mL) at 0°C, NaH (224 mg, 9.34 mmol) was added. Benzyl bromide (1.11 mL, 9.34 mmol) was introduced dropwise. The mixture was stirred overnight at room temperature, then concentrated to the minimum amount of solvent (~15 mL) and cooled at 0°C. H_2O (10 mL) was added slowly and the product was extracted with DCM (15 mL for five times). Organic layers were unified and washed with brine (30 mL), dried, concentrated under vacuum and purified by flash chromatography (hexane/AcOEt 70:30) to afford product **21** in 78% yield.

^{1}HNMR: ($CDCl_3$, 400 MHz): δ = 7.84-7.69 (m, 4H, Ph-Nap), 7.48-7.43 (m, 3H, Ph-Nap), 7.39-7.17 (m, 20H, Ph), 5.12 (s, 2H, CH_2Cbz), 4.91 (d, 1H, *J* = 10.8, PhC*H*H), 4.79-4.62 (m, 6H, PhC*H*H, $PhCH_2$, H-1), 4.44 (bs, 2H, $PhCH_2$), 3.81 (bs, 2H, H-2, H-3), 3.59 (bs, 2H, O-C*H*H-CH_2-CH_2-NH, H-5), 3.50 (t, 1H, $J_{3,4}$ = 8.8 Hz, H-4), 3.37-3.24 (m, 3H, O-C*H*H-CH_2-CH_2-NH, O-CH_2-CH_2-CH_2-NH), 1.75-1.69 (m, 2H, O-CH_2-CH_2-CH_2-NH), 1.24 (d, 3H, $J_{5,6}$ = 6.4 Hz, H-6). ^{13}CNMR ($CDCl_3$, 100 MHz): δ = 128.57, 128.38, 127.97, 127.86, 127.66, 127.33, 126.21, 126.05, 125.76, 97.93, 80.54, 80.17, 75.46, 74.99, 72.74, 72.22, 68.08, 67.29, 64.98, 50.66, 29.91, 18.16. ESI: $[M+Na]^+$= 788.70. $[\alpha]_D^{25}$ = -20.66˚ (c 2.3, $CHCl_3$).

3-(benzyloxycarbonyl)-3-N-benzyl-aminopropyl 2,4-di-O-benzyl-α-rhamnopyranoside [22].

To a solution of compound **21** (2.78 g, 3.63 mmol) in MeOH/DCM 4:1 (35 mL) DDQ (1.64 g, 7.26 mmol) freshly crystallized from $CHCl_3$ was added. The mixture was stirred for 2h, then quenched with a solution of 15% $NaHCO_3$ (25 mL). Product **22** was extracted three times with DCM (20 mL). Organic layers were unified and washed with H_2O (25 mL) and brine (25 mL), dried with Na_2SO_4 and concentrated under reduced pressure. The mixture was purified by flash chromatography (hexane/AcOEt 90:10→60:40) to afford compound **22** in 82% yield.

^{1}HNMR: ($CDCl_3$, 400 MHz): δ = 7.30-7.13 (m, 20H, Ph), 5.10 (s, 2H, CH_2Cbz), 4.82 (d, 1H, *J* = 10.8 Hz, PhC*H*H), 4.70-4.53 (m, 3H, PhC*H*H, H-1), 4.51-4.37 (m, 3H, PhC*H*H, $PhCH_2$), 3.8 (bs, 1H, H-2), 3.62-3.48 (m, 3H, O-C*H*H-CH_2-CH_2-NH, H-3, H-5), 3.33-3.13 (m, 4H, $J_{3,4}$ = 8.8 Hz, O-C*H*H-CH_2-CH_2-NH, O-CH_2-CH_2-CH_2-NH, H-4), 2.19 (d, 1H, *J* = 8.4, OH), 1.67 (bs, 2H, O-CH_2-CH_2-CH_2-NH), 1.22 (d, 3H, $J_{5,6}$ = 6.0 Hz, H-6). ^{13}CNMR ($CDCl_3$, 100 MHz): δ = 128.64, 128.37, 127.94, 127.75, 127.36, 97.00, 82.39, 78.68, 75.14, 72.94, 71.70, 67.21, 67.11, 65.02, 28.21, 17.92. ESI: $[M+Na]^+$= 648.72. $[\alpha]_D^{25}$ = -29.81˚ (c 1.2, $CHCl_3$).

Allyl 2,3,4- tri-O-acetyl-α-rhamnopyranoside [23].

Allyl alcohol (6.16 mL, 90.33 mmol) and compound **15** (20 g, 60.22 mmol) were dissolved in DCM (200 mL). The reaction mixture was cooled at 0°C and BF_3·Et_2O (11.14 mL, 90.33 mmol) was added slowly. After 30 min, the reaction was left to warm at room temperature, then stirred for 5h at 40°C. The reaction was neutralized with TEA at 0°C, concentrated under reduced pressure and purified by flash chromatography(hexane/AcOEt 1:1). The α-product **23** was recovered in 60% yield.

^{1}HNMR: ($CDCl_3$, 400 MHz): δ = 5.95-5.85 (m, 1H, CH_2-C*H*=CH_2), 5.35-5.29 (m, 2H, CH_2-CH=C*H*H, H-3), 5.26 (dd, 1H, $J_{1,2}$= 1.2 Hz, $J_{2,3}$= 3.2 Hz, H-2), 5.23 (dt, 1H, J_1= 1.6 Hz, J_2 = 2.8 Hz, CH_2-CH=C*H*H), 5.07 (t, 1H, $J_{3,4}$ = 10.0 Hz, H-4), 4.78 (d, 1H, $J_{1,2}$= 1.2 Hz, H-1), 4.18 (ddt, 1H,

J_1= 1.6 Hz, J_2= 5.2 Hz, J_3= 7.2 Hz, C*H*H-CH=CH_2), 4.01 (ddt, 1H, J_1= 1.6 Hz, J_2= 5.2 Hz, J_3= 7.2 Hz, C*H*H-CH=CH_2), 3.93-3.86 (m, 1H, H-5), 2.15 (s, 3H, CH_3CO), 2.05 (s, 3H, CH_3CO), 1.99 (s, 3H, CH_3CO), 1.23 (d, 3H, $J_{5,6}$ = 6.4 Hz, H-6). ^{13}CNMR ($CDCl_3$, 100 MHz): δ = 170.11(CO), 169.99(CO), 169.93 (CO), 133.25 (CH_2-*C*H=CH_2), 118.00 (CH_2-CH=*C*H_2), 96.46 (C-1), 71.17 (C-4), 69.94 (C-2), 69.13 (C-3), 68.36 (*C*H_2-CH=CH_2), 66.41 (C-5), 20.91 (CH_3CO), 20.77 (CH_3CO), 20.70 (CH_3CO), 17.38 (C-6). ESI: $[M+Na]^+$= 353.73. $[\alpha]_D^{25}$ = -58.94˚ (c 1.2, $CHCl_3$).

Allyl 2,3-O-isopropylidene-α-rhamnopyranoside [24].

Compound **23** (15 g, 45.4 mmol) was dissolved in MeOH (200 mL) and a solution 0.1M of NaOMe/MeOH was added until pH 9. The mixture was stirred overnight, then neutralized with Amberlite (H^+ form), filtered and concentrated. The crude was dissolved in 2,2-dimethoxypropane/DCM 4:1 (200 mL) and *p*-TsOH (2.15 g, 11.35 mmol) was added. The mixture was stirred overnight at room temperature, then neutralized with TEA at 0°C and concentrated. Product **24** was recovered in 85% yield after purification by flash chromatography (hexane/AcOEt 60:40).

^{1}HNMR: ($CDCl_3$, 400 MHz): δ = 5.98-5.87 (m, 1H, CH_2-C*H*=CH_2), 5.35-5.21 (dt, 2H, J_1= 1.6 Hz, J_2 = 2.8 Hz, CH_2-CH=C*H*$_2$), 5.02 (s, 1H, H-1), 4.23-4.17 (m, 2H, C*H*H-CH=CH_2, H-2), 4.12 (t, 1H, $J_{3,4}$ = 8.4 Hz, H-3), 4.05-3.97 (m, 1H, C*H*H-CH=CH), 3.74-3.67 (m, 1H, H-5), 3.42 (t, 1H, $J_{3,4}$ = 8.0 Hz, H-4), 2.47 (bs, 1H, OH), 1.55 (s, 3H, OCH_3), 138 (s, 3H, OCH_3), 1.31 (d, 3H, $J_{5,6}$ = 6.4 Hz, H-6). ^{13}CNMR ($CDCl_3$, 100 MHz): δ = 133.29 (CH_2-*C*H=CH_2), 117.69 (CH_2-CH=*C*H_2), 95.61 (C-1), 78-17 (C-3), 75.88 (C-2), 73.96 (C-4), 67.56 (*C*H_2-CH=CH_2), 66.13 (C-5), 27.65 (OCH_3), 25.52 (OCH_3), 16.46 (C-6). ESI $[M+Na]^+$= 267.35. $[\alpha]_D^{25}$ = -55.34˚ (c 1.1, $CHCl_3$).

Allyl 4-O-benzyl-2,3-O-isopropylidene-α-rhamnopyranoside [25].

To a solution of compound **24** (4 g, 16.37 mmol) in DMF (150 mL) at 0°C, NaH (785 mg, 32.74 mmol) was added. Benzyl bromide (3.89 mL, 32.74 mmol) was introduced dropwise. The mixture was stirred for 6h at room temperature, then concentrated to the minimum amount of solvent (~20 mL) and cooled at 0°C. H_2O (40 mL) was added slowly and the product was extracted with DCM (30 mL for five times). Organic layers were unified and washed with brine (70 mL), dried with Na_2SO_4, concentrated under vacuum and purified by flash chromatography(hexane/AcOEt 70:30) to afford compound **25** in 95% yield.

^{1}HNMR: ($CDCl_3$, 400 MHz): δ = 7.42-7.28 (m, 5H, Ph), 5.98-5.88 (m, 1H, CH_2-C*H*=CH_2), 5.32 (dt, 1H, J_1= 1.6 Hz, J_2= 2.8 Hz, CH_2-CH=C*H*H), 5.23 (dt, 1H, J_1= 1.6 Hz, J_2= 2.8 Hz, CH_2-CH=C*H*H), 5.04 (s, 1H, H-1), 4.93 (d, 1H, *J* = 12.4, PhC*H*H), 4.65 (d, 1H, *J* = 12.4 Hz, PhC*H*H),

4.31 (t, 1H, $J_{3,4}$ =7.2 Hz, H-3), 4.22-4.16 (m, 2H, C*H*H-CH=CH_2, H-2), 4.02 (ddt, 1H, J_1= 1.6 Hz, J_2= 5.2 Hz, J_3= 7.2 Hz, C*H*H-CH=CH_2), 3.78-3.71 (m, 1H, H-5), 3.25 (dd, 1H, $J_{3,4}$ = 7.2 Hz, $J_{4,5}$ = 10.0 Hz, H-4), 1.54 (s, 3H, OCH_3), 1.40 (s, 3H, OCH_3), 1.31 (d, 3H, $J_{5,6}$ = 6.4 Hz, H-6). ^{13}CNMR ($CDCl_3$, 100 MHz): δ = 127.91, 133.95, 117.45, 95.64 (C-1), 80.70 (C-4), 78.09 (C-3), 76.35 (C-2), 72.17, 67.35, 64.86 (C-5), 28.45, 26.36, 17.18.

Allyl 4-O-benzyl-α-rhamnopyranoside [26].

Compound **25** (5.2 g, 15.54 mmol) was dissolved in DCM (70 mL) and cooled at 0°C. A solution of TFA 50% in DCM was added (16 mL) and the mixture was stirred for 2h, when NMR showed the disappearance of methoxy signals (1.54 ppm and 1.40 ppm). The reaction was treated with a saturated solution of K_2CO_3 (35 mL). The organic layer was washed with H_2O (30 mL) and brine (30 mL), dried with Na_2SO_4 and concentrated. The product **26** was used in the next step without other purification.

Allyl 4-O-benzyl-3-O-naphthylmethyl-α-rhamnopyranoside [27].

To a solution of compound **26** (4.5 g, 15.54 mmol) in toluene (70 mL) 4Å activated molecular sieves (2.2 g) and Bu_2SnO (4.6 g, 18.65 mmol) were added. The reaction was stirred for 4h at reflux, then it was cooled at 45°C and NapBr (3.8 g, 18.65 mmol) and TBAI (6.8 g, 18.65 mmol) were introduced. The mixture was stirred overnight, then filtered on a celite pad, concentrated and purified by flash chromatography (hexane/AcOEt 90:10→50:50) to afford product **27** in 58% yield. ^{1}HNMR: ($CDCl_3$, 400 MHz): δ = 7.89-7.78 (m, 4H, Ph-Nap), 7.53-7.49 (m, 3H, Ph-Nap), 7.40-7.30 (m, 5H, Ph), 5.96-5.87 (m, 1H, CH_2-C*H*=CH_2), 5.30 (dt, 1H, J_1= 1.6 Hz, J_2= 2.8 Hz, CH_2-CH=C*H*H), 5.22 (dt, 1H, J_1= 1.6 Hz, J_2= 2.8 Hz, CH_2-CH=C*H*H), 4.96 (d, 1H, J = 11.2 Hz, PhC*H*H), 4.91-4.85 (m, 3H, $PhCH_2$, H-1), 4.70 (d, 1H, J = 11.2 Hz, PhC*H*H), 4.22-4.13 (m, 2H, CH_2-CH=C*H*H, H-2), 4.03-3.96 (m, 2H, CH_2-CH=C*H*H, H-3), 3.85-3.78 (m, 1H, H-5), 3.54 (t, 1H, $J_{3,4}$ = 9.2 Hz, H-4), 1,37 (d, 3H, $J_{5,6}$ = 6.0 Hz, H-6). ^{13}CNMR ($CDCl_3$, 100 MHz): δ = 138.45, 135.42, 133.76, 133.32, 133.11, 128.43, 128.37, 128.32, 127.96, 127.76, 127.72, 126.66, 126.24, 126.20, 126.08, 125.90, 125.80, 125.42, 125.19, 117.48, 98,21 (C-1), 80.14 (C-3), 80.10 (C-4), 75.49, 72.20, 68.66 (C-2), 67.91, 67.49 (C-5), 17.91 (C-6). $[\alpha]_D^{25}$ = -50.09˚ (c 1.1, $CHCl_3$).

Allyl 2-O-acetyl-4-O-benzyl-3-O-naphthylmethyl-α-rhamnopyranoside [28].

Compound **27** (5 g, 11.50 mmol) was dissolved in pyridine (25 mL) and cooled at 0°C. Ac_2O (25 mL) was added dropwise and the mixture was stirred overnight at room temperature in presence of DMAP (14 mg, 0,115 mmol). The reaction was concentrated at minimum amount of solvent,

diluted with DCM (100 mL) and washed with a solution of 5% HCl (40 mL), H_2O (40 mL) and brine (40 mL). Organic layer was dried with Na_2SO_4, concentrated under reduced pressure and purified by flash chromatography (hexane/AcOEt 70:30). Yield 98%.

^{1}HNMR: ($CDCl_3$, 400 MHz): δ = 7.88-7.74 (m, 4H, Ph-Nap), 7.53-7.46 (m, 3H, Ph-Nap), 7.38-7.31 (m, 5H, Ph), 5.95-5.86 (m, 1H, CH_2-C*H*=CH_2), 5.49 (dd, 1H, $J_{1,2}$ = 2.0 Hz, $J_{2,3}$ = 3.2 Hz, H-2), 5.29 (dt, 1H, J_1= 1.6 Hz, J_2= 2.8 Hz, CH_2-CH=C*H*H), 5.21 (dt, 1H, J_1= 1.6 Hz, J_2= 2.8 Hz, CH_2-CH=C*H*H), 4.99 (d, 1H, *J* = 10.8 Hz, PhC*H*H), 4.90 (d, 1H, *J* = 11.2 Hz, PhC*H*H), 4.83 (d, 1H, $J_{1,2}$ = 2.0 Hz, H-1), 4.73 (d, 1H, *J* = 11.2 Hz, PhC*H*H), 4.68 (d, 1H, *J* = 10.8 Hz, PhC*H*H), 4.18 (ddt, 1H, J_1 = 1.6 Hz, J_2 = 5.2 Hz, J_3 = 7.6 Hz, C*H*H-CH=CH_2), 4.06 (dd, 1H, $J_{2,3}$ = 3.2 Hz, $J_{3,4}$ = 9.2 Hz, H-3), 4.00 (ddt, 1H, J_1 = 1.6 Hz, J_2 = 5.2 Hz, J_3 = 7.6 Hz, C*H*H-CH=CH_2), 3.86-3.80 (m, 1H, H-5), 3.51 (t, 1H, $J_{3,4}$ = 9.2 Hz, H-4), 2.20 (s, 3H, CH_3CO), 1.38 (d, 3H, $J_{5,6}$ = 6.4 Hz, H-6). ^{13}CNMR ($CDCl_3$, 100 MHz): δ = 170.43, 138.66, 135.64, 133.64, 133.45, 132.93, 128.40, 128.14, 127.93, 127.70, 126.84, 126.14, 126.01, 125.87, 117.81, 96.99 (C-1), 80.18 (C-4), 78.17 (C-3), 75.47, 71.82, 69.08 (C-2), 68.06, 67.82 (C-5), 21.31, 18.10. $[\alpha]_D^{25}$ = -52.14˚ (c 1.4, $CHCl_3$).

Allyl 2,4-di-O-benzyl-3-O-naphthylmethyl-α-rhamnopyranoside [29].

To a solution of compound **28** (5 g, 11.50 mmol) in DMF (115 mL) at 0°C, NaH (552 mg, 23 mmol) was added. Benzyl bromide (2.7 mL, 23 mmol) was introduced dropwise. The mixture was stirred for 2h at room temperature, then concentrated to the minimum amount of solvent (~25 mL) and cooled at 0°C. H_2O (50 mL) was added slowly and the product was extracted with DCM (40 mL for five times). Organic layers were unified and washed with brine (100 mL), dried with Na_2SO_4, concentrated under vacuum and purified by flash chromatography (hexane/AcOEt 70:30) to afford compound **29** in 95% yield.

^{1}HNMR: ($CDCl_3$, 400 MHz): δ = 7.9-7.72 (m, 4H, Ph-Nap), 7.54-7.28 (m, 18H, Ph), 5.90-5.79 (m, 1H, CH_2-C*H*=CH_2), 5.25-5.14 (m, 2H, CH_2-CH=CH_2), 5.01 (dd, 1H), 4.89-4.59 (m, 7H, PhC*H*H, H-1, H-2), 4.15 (bs, 1H, H-3), 4.01-3.91 (m, 2H, C*H*H-CH=CH_2, H-5), 3.79-3.65 (m, 2H, C*H*H-CH=CH_2, H-4), 1.38 (d, 3H, $J_{5,6}$ = 6.4 Hz, H-6).

Allyl 2,4-di-O-benzyl-α-rhamnopyranoside [30].

To a solution of compound **29** (5.73 g, 14.90 mmol) in MeOH/DCM 4:1 (30 mL) DDQ (6.76 g, 29.8 mmol) freshly crystallized from $CHCl_3$ was added. The mixture was stirred for 2h, then quenched with a solution of 15% $NaHCO_3$ (15 mL). Product **30** was extracted three times with DCM (25 mL). Organic layers were unified and washed with H_2O (35 mL) and brine (35 mL), dried

with Na_2SO_4 and concentrated under reduced pressure. The mixture was purified by flash chromatography (hexane/AcOEt 90:10→60:40) to afford compound **30** in 82% yield.

^{1}HNMR: ($CDCl_3$, 400 MHz): δ = 7.42-7.29 (m, 10H, Ph), 5.92-5.83 (m, 1H, CH_2-C*H*=CH_2), 5.27 (dt, 1H, J_1= 1.6 Hz, J_2= 2.8 Hz, CH_2-CH=C*H*H), 5.19 (dt, 1H, J_1= 1.6 Hz, J_2= 2.8 Hz, CH_2-CH=C*H*H), 4.93 (d, 1H, *J* = 11.2 Hz, PhC*H*H), 4.88 (d, 1H, $J_{1,2}$ = 1.2 Hz, H-1), 4.77 (d, 1H, *J* = 11.6 Hz, PhC*H*H), 4.68 (d, 1H, *J* = 11.2 Hz, PhC*H*H), 4.61 (d, 1H, *J* = 11.6 Hz, PhC*H*H), 4.16 (ddt, 1H, J_1 = 1.6 Hz, J_2 = 5.2 Hz, J_3 = 7.6 Hz, C*H*H-CH=CH_2), 4.01-3.93 (m, 2H, C*H*H-CH=CH_2, H-3), 3.77 (dd, 1H, $J_{1,2}$ =1.2 Hz, $J_{2,3}$ = 3.6 Hz, H-2), 3.75-3.69 (m, 1H, H-5), 3.55 (t, 1H, $J_{3,4}$ = 10 Hz, H-4), 1.92 (bs, 1H, OH), 1.35 (d, 3H, $J_{5,6}$ = 6.4 Hz, H-6). ^{13}CNMR ($CDCl_3$, 100 MHz): δ = 127.75, 133.53, 117.23, 95.79 (C-1), 81.80 (C-4), 78.49 (C-2), 74.51, 72.60, 71.63 (C-3), 67.84, 67.19 (C-5), 18.36 (C-6).

2-O-acetyl-4-O-benzyl-3-O-naphthylmethyl-α-rhamnopyranosyl trichloroacetimidate [32].

A solution of compound **28** (5.37 g, 11.2 mmol) in THF (112 mL) containing 1,5-cyclooctadienebis(methyldiphenylphosphine)-Iridium(I)-hexafluorophosphate (946.4 mg, 1.12 mmol) was degassed for 1h, then hydrogen was flown for 10 min. The mixture was stirred for 30 min, when ^{1}HNMR showed isomerization of the double bond. Water (55 mL) and I_2 (5.66 g, 22.4 mmol) were added. The mixture was stirred for 15 min, then 10% aq. NaS_2O_3 (80 mL) was added and the product was extracted with DCM (120 mL for 3 times). Organic layers were unified, washed with 5% $NaHCO_3$ (150 mL), H_2O (150 mL) and brine (150 mL), then dried with Na_2SO_4 and concentrated under vacuum. The deallyled intermediate was purified on silica gel (hexane/AcOEt 80:20→60:40) to afford 4.05g of foregoing product, which was dissolved in DCM (90 mL), then CCl_3CN (5.5 mL, 55.67 mmol) and DBU (0.41 mL, 2.78 mmol) were added. The mixture was stirred for 3h, concentrated under vacuum and purified by flash chromatography (hexane/AcOEt + 1% TEA 70:30). Compound **32** was recovered in 85% yield after two steps. The insertion of trichloroacetimidate was confirmed by ^{1}HNMR and the compound was immediately used in the next step to preserve the trichloroacetimidate from hydrolysis.

^{1}HNMR: ($CDCl_3$, 400 MHz): δ = 8.65 (s, 1H, NH), 7.85-7.75 (m, 4H, Ph-Nap), 7.51-7.47 (m, 3H, Ph-Nap), 7.38-7.31 (m, 5H, Ph), 6.20 (d, 1H, $J_{1,2}$ = 1.6 Hz, H-1), 5.53 (dd, 1H, $J_{1,2}$ = 2.0 Hz, $J_{2,3}$ = 3.2 Hz, H-2), 4.99 (d, 1H, *J* = 10.0 Hz, PhC*H*H), 4.91 (d, 1H, *J* = 10.8 Hz, PhC*H*H), 4.76 99 (d, 1H, *J* = 11.2 Hz, PhC*H*H), 4.69 99 (d, 1H, *J* = 10.8 Hz, PhC*H*H),4.06 (dd, 1H, $J_{2,3}$ = 2.4 Hz, $J_{3,4}$ = 9.2 Hz, H-3), 3.99-3.92 (m, 1H, H-5), 3.57 (t, 1H, $J_{3,4}$ = 9.2 Hz, H-4), 2.23 (s, 3H, CH_3CO), 1.38 (d, 3H, $J_{5,6}$ = 6.0 Hz, H-6).

3-(benzyloxycarbonyl)-3-N-benzyl-aminopropyl (2-O-acetyl-4-O-benzyl-3-O-naphthylmethyl-α-rhamnopyranosyl)-(1-3)-2,4-di-O-benzyl-α-rhamnopyranoside [33].

To a stirred solution of acceptor **22** (1.86 g, 2.97 mmol) and donor **32** (1.29 g, 2.23 mmol) in DCM (29 mL) containing activated 4 Å molecular sieves (1.86 g), TMSOTf (53.75 μL, 0.297 mmol) was added at 0°C. The reaction was stirred at 0°C for 30 min. After neutralization with TEA, the mixture was concentrated and purified by flash chromatography (hexane/AcOEt 80:20) to afford product **33** in 85% yield.

^{1}HNMR: ($CDCl_3$, 400 MHz): δ = 7.79-7.73 (m, 3H, Ph-Nap), 7.68-7.63 (m, 1H, Ph-Nap), 7.44-7.40 (m, 3H, Ph-Nap), 7.38-7.19 (m, 25H, Ph), 5.56 (dd, 1H, $J_{1,2}$ = 1.6 Hz, $J_{2,3}$ = 3.2 Hz, H-2^{II}), 5.18 (s, 2H, CH_2Cbz), 5.11 (d, 1H, $J_{1,2}$ = 1.2 Hz, H-1^{II}), 5.00 (d, 1H, J = 10.8 Hz, PhC*H*H), 4.84 (d, 1H, J = 11.6 Hz, PhC*H*H), 4.77 (d, 1H, J = 10.8 Hz, PhC*H*H), 4.69-4.34 (m, 8H, PhC*H*H, $PhCH_2$, H-1^{I}), 4.08-4.01 (m, 2H, H-3^{I}, H-3^{II}), 3.90-3.84 (m, 1H, H-5^{II}), 3.71-3.56 (m, 4H, O-C*H*H-CH_2-CH_2-NH, H-2^{I}, H-4^{I}, H-5^{I}), 3.38-3.23 (m, 3H, O-C*H*H-CH_2-CH_2-NH, O-CH_2-CH_2-CH_2-NH), 2.13 (s, 3H, CH_3CO), 1.76 (bs, 2H, O-CH_2-CH_2-CH_2-NH), 1.29 (d, 3H, $J_{5,6}$ = 6.0 Hz, H-6^{I}), 1.26 (d, 3H, $J_{5,6}$ = 6.4 Hz, H-6^{II}). ^{13}CNMR ($CDCl_3$, 100 MHz): δ = 170.11, 138.81, 138.14, 137.78, 136.74, 135.51, 133.25, 132.95, 128.59, 128.40, 128.29, 128.09, 127.90, 127.65, 127.35, 126.85, 126.13, 125.96, 125.82, 99.28 (C-1^{II}), 97.56 (C-1^{I}), 80.91 (C-4^{I}), 80.03 (C-4^{II}), 77.84 (C-2^{I}), 77.74 (C-3^{I}), 77.52 (C-3^{II}), 75.22, 72.67, 71.82, 69.08 (C-2^{II}), 68.39 (C-5^{II}), 68.21 (C-5^{I}), 67.22, 65.07, 28.37, 21,16, 18.12. ESI $[M+Na]^+$= 1024.47. $[\alpha]_D^{25}$ = -49.61˚ (c 1.3, $CHCl_3$).

3-(benzyloxycarbonyl)-3-N-benzyl-aminopropyl (4-O-benzyl-3-O-naphthylmethyl-α-rhamnopyranosyl-(1-3)-2,4-di-O-benzyl-α-rhamnopyranoside [34].

Compound **33** (1.13 g, 1.08 mmol) was dissolved in DCM (10 mL) and a solution 0.1M of NaOMe/MeOH was added until pH 9. The mixture was stirred overnight, then neutralized with Amberlite (H^+ form), filtered and concentrated to afford product **34** in 95% yield. ^{1}HNMR confirmed the disappearance of signal at 2.13 ppm.

Allyl (2-O-acetyl-4-O-benzyl-3-O-naphthylmethyl-α-rhamnopyranosyl)-(1-3)-2,4-di-O-benzyl-α-rhamnopyranoside [35].

To a stirred solution of acceptor **30** (2 g, 5.20 mmol) and donor **32** (3.6 g, 6.24 mmol) in DCM (52 mL) containing activated 4 Å molecular sieves (2 g), TMSOTf (94.11 μL, 0.520 mmol) was added at 0°C. The reaction was stirred at 0°C for 30 min. After neutralization with TEA, the mixture was concentrated and purified by flash chromatography (hexane/AcOEt 90:10→70:30) to afford product **35** in 72% yield.

^{1}HNMR: ($CDCl_3$, 400 MHz): δ = 7.78-7.71 (m, 3H, Ph-Nap), 7.68-7.63 (m, 1H, Ph-Nap), 7.46-7.40 (m, 3H,Ph-Nap), 7.39-7.21 (m, 15H, Ph), 5.90-5.80 (m, 1H, CH_2-C*H*=CH_2), 5.56 (dd, 1H, $J_{1,2}$ = 2.0 Hz, $J_{2,3}$ = 3.2 Hz, H-2^{II}), 5.24 (dt, 1H, J_1= 1.6 Hz, J_2= 2.8 Hz, CH_2-CH=C*H*H), 5.16 (dt, 1H, J_1= 1.6 Hz, J_2= 2.8 Hz, CH_2-CH=C*H*H), 5.13 (d, 1H, $J_{1,2}$ = 1.2 Hz, H-1^{II}), 4.99 (d, 1H, *J* = 11.2 Hz, PhC*H*H), 4.85-4.76 (m, 3H, PhC*H*H, H-1^{I}), 4.67-4.56 (m, 5H, PhC*H*H), 4.16-4.10 (m, 2H, C*H*H-CH=CH_2, H-3^{I}), 4.04 (dd, 1H, $J_{2,3}$ = 3.6 Hz, $J_{3.4}$ = 9.2 Hz, H-3^{II}), 3.95-3.85 (m, 2H, C*H*H-CH=CH_2, H-5^{II}), 3.75-3.67 (m, 2H, H-2^{I}, H-5^{I}), 3.60 (t, 1H, $J_{3.4}$ = 9.0 Hz, H-4^{I}), 3.47 (t, 1H, $J_{3.4}$ = 9.2 Hz, H-4^{II}), 2.12 (s, 3H, CH_3CO), 1.33-1.28 (m, 6H, H-6^{I}, H-6^{II}). ^{13}CNMR ($CDCl_3$, 100 MHz): δ = 169.92, 135.39, 133.81, 128.39, 128.30, 128.10, 127.92, 127.86, 127.84, 127.68, 127.67, 127.63, 127.53, 126.85, 126.12, 125.95, 125.83, 117.00, 99.34 (C-1^{II}), 96.80 (C-1^{I}), 80.97 (C-4^{I}), 80.00 (C-4^{II}), 77.85 (C-3^{I}), 77.77 (C-3^{II}), 77.55 (C-2^{I}), 75.24, 75.16, 72.71, 71.81, 69.08 (C-2^{II}), 68.37 (C-5^{II}), 68.18 (C-5^{I}), 67.71, 21.03, 18.02 (C-6^{I}), 17.94 (C-6^{II}). ESI: $[M+Na]^+$= 825.99. $[\alpha]_D^{25}$ = +34.66° (c 1.5, $CHCl_3$).

(2-O-acetyl-4-O-benzyl-3-O-naphthylmethyl-α-rhamnopyranosyl)-(1-3)-2,4-di-O-benzyl-α-rhamnopyranosyl trichloroacetimidate [36].

A solution of compound **35** (3 g, 3.74 mmol) in THF (38 mL) containing 1,5-cyclooctadienebis(methyldiphenylphosphine)-Iridium(I)-hexafluorophosphate (316 mg, 0.374 mmol) was degassed for 1h, then hydrogen was flown for 10 min. The mixture was stirred for 30 min, when ^{1}HNMR showed isomerization of the double bond. Water (16 mL) and I_2 (1.8 g, 7.48 mmol) were added. The mixture was stirred for 20 min, then partitioned with 10% NaS_2O_3 (15 mL) and DCM (35 mL for 3 times). Organic layers were unified, washed with 5% $NaHCO_3$ (45 mL), H_2O (45 mL) and brine (45 mL), then dried with Na_2SO_4 and concentrated under vacuum. The deallyled intermediate was purified on silica gel (hexane/AcOEt 70:30) to afford 2.5g of foregoing product, which was dissolved in DCM (32 mL), then CCl_3CN (1.97 mL, 19.67 mmol) and DBU (0.49 mL, 3.27 mmol) were added. The mixture was stirred for 5h, concentrated under vacuum and purified by flash chromatography (hexane/AcOEt + 1% TEA 70:30). Compound **36** was recovered in 85% yield after two steps. The insertion of trichloroacetimidate was confirmed by ^{1}HNMR and the compound was immediately used in the next step to preserve the trichloroacetimidate from hydrolysis.

^{1}HNMR: ($CDCl_3$, 400 MHz): δ = 8.56 (s, 1H, NH), 7.80-7.66 (m, 4H, Ph-Nap), 7.47-7.41 (m, 3H, Ph-Nap), 7.38-7.22 (m, 15H, Ph), 6.28 (d, 1H, $J_{1,2}$ = 1.6 Hz, H-1^{I}), 5.58 (dd, 1H, $J_{1,2}$ = 2.0 Hz, $J_{2,3}$ = 3.2 Hz, H-2^{II}), 5.14 (s, 1H-H-1^{II}), 4.99 (d, 1H, *J* = 11.2 Hz, PhC*H*H), 4.87 (d, 1H, *J* = 10.8 Hz, PhC*H*H), 4.81-4.57 (m, 6H, PhC*H*H), 4.18 (m, 2H, $J_{2,3}$ = 2.8 Hz, $J_{3.4}$ = 9.2 Hz H-3^{I},), 4.01 (dd, 1H,

$J_{2,3}$ = 3.6 Hz, $J_{3.4}$ = 9.2 Hz, H-3^{II}), 3.95-3.89 (m, 2H, H-2^{I}, H-5^{II}), 3.83-3.76 (m, 1H, H-5^{II}), 3.71 (t, 1H, $J_{3.4}$ = 9.0 Hz, H-4^{I}), 3.47 (t, 1H, $J_{3.4}$ = 9.2 Hz, H-4^{II}), 2.13 (s, 3H, CH_3CO), 1.36 (s, 3H, $J_{5,6}$ = 6.4 Hz, H-6^{I}), 1.24 (s, 3H, $J_{5,6}$ = 6.0 Hz, H-6^{I}).

3-(benzyloxycarbonyl)-3-N-benzyl-aminopropyl (2-O-acetyl-4-O-benzyl-3-O-naphthylmethyl-α-rhamnopyranosyl)-(1-3)-(2,4-di-O-benzyl-α-rhamnopyranosyl)-(1-2)-(4-O-benzyl-3-O-naphthylmethyl-α-rhamnopyranosyl)-(1-3)-2,4-di-O-benzyl-α-rhamnopyranoside [37].

To a stirred solution of disaccharide acceptor **34** (1.27 g, 1.26 mmol) and disaccharide donor **36** (1.36 g, 1.51 mmol) in DCM (12.6 mL) containing activated 4 Å molecular sieves (1 g), TMSOTf (22.8 μL, 0.126 mmol) was added at 0°C. The reaction was stirred at 0°C for 1h. After neutralization with TEA, the mixture was concentrated and purified with Biotage SNAP 50g column (hexane/AcOEt 0→100%) to afford tetrasaccharide **37** in 87% yield.

^{1}HNMR: ($CDCl_3$, 400 MHz): δ = 7.79-7.60 (m, 4H, Ph-Nap), 7.46-7.12 (m, 46 H, Ph-Nap, Ph), 5.58 (dd, 1H, $J_{1,2}$ = 1.6 Hz, $J_{2,3}$ = 3.2 Hz, H-2^{IV}), 5.17 (s, 2H, CH_2Cbz), 5.13 (d, 1H, $J_{1,2}$ = 1.6 Hz, H-1^{IV}), 5.08 (d, 1H, $J_{1,2}$ = 1.6 Hz, H-1^{III}), 5.02 (d, 1H, $J_{1,2}$ = 1.6 Hz, H-1^{II}), 4.95 (dd, 1H, J_1 = 4.4 Hz, J_1 = 10.8 Hz, $PhCH_2$), 4.85-4.51 (m, 14H, $PhCH_2$, H-1^{I}), 4.48-4.34 (m, 5H, $PhCH_2$), 4.15 (dd, 1H, , $J_{2,3}$ = 3.2 Hz, $J_{3.4}$ = 9.6 Hz, H-3^{III}), 4.03-3.93 (m, 4H, H-2^{II}, H-3^{II}, H-3^{IV}, H-5^{III}) 3.89-3.67 (m, 5H, H-2^{III}, H-2^{I}, H-3^{I}, H-5^{II}, H-5^{IV}), 3.66-3.52 (m, 3H, O-C*H*H-CH_2-CH_2-NH, H-4^{III}, H-5^{I}), 3.51-3.40 (m, 3H, H-4^{II}, H-4^{I}, H-4^{IV}), 3.37-3.20 (m, 3H, O-C*H*H-CH_2-CH_2-NH, O-CH_2-CH_2-CH_2-NH), 2.11 (s, 3H, CH_3CO), 1.76 (bs, 2H, O-CH_2-CH_2-CH_2-NH), 1.27 (s, 3H, $J_{5,6}$ = 6.4 Hz, H-6^{IV}), 1.23 (s, 3H, $J_{5,6}$ = 6.4 Hz, H-6^{III}), 1.18 (s, 3H, $J_{5,6}$ = 6.0 Hz, H-6^{I}), 1.12 (s, 3H, $J_{5,6}$ = 6.0 Hz, H-6^{II}). ^{13}CNMR ($CDCl_3$, 100 MHz): δ = 170.07, 138.86, 138.76, 138.34, 138.18, 138.05, 137.80, 135.62, 135.49, 133.32, 133.24, 133.05, 129.99, 128.68, 128.65, 128.46, 128.40, 128.37, 128.31, 128.26, 128.16, 127.99, 127.95, 127.81, 127.80, 127.74, 127.68, 127.62, 127.60, 127.46, 127.40, 126.91, 126.65, 126.21, 126.02, 125.98, 125.90, 125.89, 100.90, 99.25, 99.02, 97.45, 81.05, 80.78, 80.54, 80.02, 79.78, 78.66, 78.19, 78.09, 77.89, 76.70, 75.40, 75.28, 75.24, 75.09, 72.64, 72.25, 71.91, 69.10, 69.83, 69.84, 68.30, 68.18, 67.27, 65.12, 43.84, 28.35, 21.11, 18.19, 18.04, 18.02, 8.01. ESI $[M+Na]^+$= 1768.89. $[\alpha]_D^{25}$ = -53.40˚ (c 1.0, $CHCl_3$).

3-(benzyloxycarbonyl)-3-N-benzyl-aminopropyl (2-O-acetyl-4-O-benzyl-α-rhamnopyranosyl)-(1-3)-(2,4-di-O-benzyl-α-rhamnopyranosyl)-(1-2)-(4-O-benzyl-α-rhamnopyranosyl)-(1-3)-2,4-di-O-benzyl- α-rhamnopyranoside [38].

To a solution of compound **37** (1.91 g, 1.09 mmol) in MeOH/DCM 4:1 (11 mL) DDQ (989 mg, 4.36 mmol) freshly crystallized from $CHCl_3$ was added. The mixture was stirred for 6h, then

quenched with a solution of 15% $NaHCO_3$ (5 mL). Product **37** was extracted three times with DCM (10 mL). Organic layers were unified and washed with H_2O (10 mL) and brine (10 mL), dried with Na_2SO_4 and concentrated under reduced pressure. The mixture was purified with Biotage SNAP 50g column (hexane/AcOEt 0→100%). Yield = 78%.

^{1}HNMR: ($CDCl_3$, 400 MHz): δ = 7.39-7.22 (m, 40H, Ph), 5.26 (dd, 1H, $J_{1,2}$ = 1.6 Hz, $J_{2,3}$ = 3.2 Hz, H-2^{IV}), 5.18 (s, 2H, CH_2Cbz), 5.13 (s, 1H, H-1^{III}) 5.09 (s, 1H, H-1^{IV}) 4.96 (d, 1H, $J_{1,2}$ = 1.6 Hz, H-1^{II}) 4.86-4.77 (m, 3H, PhC*H*H), 4.73-4.53 (m, 12H, PhC*H*H, H-1^{I}), 4.15-4.09 (m, 2H, H-3^{II}, H-3^{IV}), 4.02-3.97 (m, 2H, H-3^{I} H-3^{III}), 3.90 (bs, 1H, H-2^{III}), 3.87-3.77 (m, 4H, H-2^{II}, H-5^{I}, H-5^{II}, H-5^{IV}), 3.69 (bs, 1H, H-2^{I}), 3.65-3.51 (m, 4H, O-C*H*H-CH_2-CH_2-NH, H-4^{II}, H-4^{III}, H-5^{III}), 3.38-3.20 (m, 5H, O-C*H*H-CH_2-CH_2-NH, O-CH_2-CH_2-C*H*$_2$-NH, H-4^{I}, H-4^{IV}) 2.11 (s, 3H, CH_3CO), 1.77 (bs, 2H, O-CH_2-C*H*$_2$-CH_2-NH), 1.30 (s, 3H, $J_{5,6}$ = 6.4 Hz, H-6^{IV}), 1.23 (s, 3H, $J_{5,6}$ = 6.4 Hz, H-6^{I}), 1.20 (s, 3H, $J_{5,6}$ = 6.0 Hz, H-6^{III}), 1.15 (s, 3H, $J_{5,6}$ = 6.0 Hz, H-6^{II}). ^{13}CNMR ($CDCl_3$, 100 MHz): δ = 170.55, 139.53, 138.39, 138.14, 138.12, 137.91, 137.74, 128.58, 128.44, 128.41, 128.37, 128.36, 127.86, 127.81, 127.75, 127.72, 127.67, 127.60, 100.55, 99.67, 98.57, 97.42, 82.34, 81.50, 80.96, 80.57, 79.27, 78.12, 77.67, 75.00, 74.81, 72.67, 72.57, 72.35, 71.39, 70.42, 68.83, 68.15, 67.93, 67.92, 67.19, 65.21, 20.94, 18.13, 18.12, 18.03, 17.96. ESI: $[M+Na]^+$= 1488.97. [α]D25 = -30.28° (c 2.5, $CHCl_3$).

1,3,4,6-tetra-O-acetyl-2-deoxy-2-phthalimido-β-D-glucopyranose [43]

D-Glucosamine hydrochloride (50g, 231.8 mmol) was dissolved in MeOH (500 mL). The solution was cooled down to 0°C and NaOMe (13.6 g, 251 mmol) was added. The mixture was stirred for 10min, then phthalic anhydride (20 g, 135.0 mmol) was introduced slowly. After 20min at 0°C, TEA (25 mL) was added and the mixture was stirred overnight at room temperature.

The solution was cooled down to 0°C, phthalic anhydride (20 g, 135.0 mmol) was added slowly and the mixture was stirred overnight at room temperature.

The reaction was co-evaporated with toluene for three time. The crude was dissolved in pyridine (350 mL), cooled down to 0°C and acetic anhydride (150mL) was added slowly. The reaction was stirred overnight at room temperature. The mixture was concentrated under vacuum and partionated from $CHCl_3$ (300 mL) and HCl 5% (120 mL). The organic layer was washed with brine (120 mL), concentrated, dried with Na_2SO_4 and purified by flash chromatography (hexane/AcOEt 60:40). The product **43** was obtained in α/β mixture (40% α-anomer) in yield = 47%.

^{1}HNMR: ($CDCl_3$, 400 MHz): δ = 7.82-7.76 (m, 2H, Phth), 7.71-7.67 (m, 2H, Phth), 6.44 (d, 1H, $J_{1,2}$ = 9.2 Hz, H-1), 5.82 (dd, 1H, $J_{1,2}$ = 9.2 Hz, $J_{2,3}$ = 10.8 Hz, H-2), 5.14 (t, 1H, $J_{3,4}$ = 10.0 Hz, H-4), 4.40 (dd, 1H, $J_{2,3}$ = 10.7 Hz, $J_{3,4}$ = 10.2 Hz, H-3), 4.29 (dd, 1H, $J_{5,6}$ = 4.0 Hz, $J_{6,6}$ = 12.0 Hz, H-6a),

4.05 (dd, 1H, $J_{5,6}$ = 4.0 Hz, $J_{6,6}$ = 12.0 Hz, H-6b), 3.97-3.94 (m, 1H, H-5), 2.04 (s, 3H, CH_3CO), 1.97 (s, 3H, CH_3CO), 1.92 (s, 3H, CH_3CO), 1.79 (s, 3H, CH_3CO).

Characterization in agreement to D. Bednarcyk et al. *Carbohydrate Research*, **2013**, 367, 10-17.

p-Methoxyphenyl 3,4,6-tri-O-acetyl-2-deoxy-2-phthalimido-β-D-glucopyranoside [44].

Compound **43** (17 g, 35.6 mmol) was dissolved in DCM (60.0 mL) at 0°C with 4Å activated molecular sieves (40 g) and stirred for 10 min under nitrogen. Para-methoxyphenol (25 g, 201.4 mmol) and $BF_3{\cdot}Et_2O$ (24 mL, 194.5 mmol) were added at 0°C. After 1 h, the mixture was allowed to warm up to room temperature. Stirring was continued for further 24 h. TEA was added, solid was filtered off and the solvent removed at reduced pressure. The crude was purified with Biotage SNAP 100g column (hexane/AcOEt (0→100%); yield = 89%.

^{1}HNMR (400 MHz, CDCl3): δ = 7.80-6.66 (m, 8H, Ar), 5.81 (m, 2H, H-1, H-3) , 5.19 (t, 1H, $J_{3,4}$ = 9.7 Hz, H-4), 4.50 (dd, 1H, $J_{1,2}$ = 8.6 Hz, $J_{2,3}$ = 10.6 Hz, H-2), 4.29 (dd, 1H, $J_{5,6}$ = 5.3 Hz, $J_{6,6}$ = 12.3 Hz, H-6a) , 4.16 (dd, 1H, $J_{5,6}$ = 1.9 Hz, $J_{6,6}$ = 12.3 Hz, H-6b), 3.90-3.86 (m, 1H, H-5), 3.66 (s, 3H, OCH3), 2.04 (s, 3H, CH_3CO), 1.98(s, 3H, CH_3CO), 1.82 (s, 3H, CH_3CO), ^{13}CNMR (100 MHz, $CDCl_3$): δ = 134.4-114.4 (C-Ar), 97.5 (C-1), 72.0 (C-5), 70.7 (C-3), 68.9 (C-4), 62.0 (C-6), 55.6 (O*C*H_3), 54.5 (C-2), 20.8, 20.7, 20.5. ESI MS m/z $[M+Na]^+$ = 564.14. $[\alpha]_D^{25}$ = +63.04° (c 1.3, $CHCl_3$).

p-Methoxyphenyl 4,6-O-benzylidene-2-deoxy-2-phthalimido-β-D-glucopyranoside [45].

Sodium methoxide (until pH 9) was added to a stirred mixture of compound **44** (18.0 g, 35.6 mmol) in methanol (40 mL). After 20 hours the reaction was quenched with Dowex 50WX2. After the filtration of the resin, the filtrate was evaporated under reduced pressure.

To the crude material acetonitrile (30 mL), benzaldehyde dimethyl acetal (6.9 mL, 68 mmol) and para-toluenesulfonic acid (0.470 g, 2.73 mmol) were added. After 3 h the reaction was quenched with triethylamine (4.7 mL), and the mixture was evaporated under reduced pressure. The crude was purified by flash chromatography (hexane/AcOEt 50:50) to afford **45** in, 84 % yield

^{1}HNMR (400 MHz, $CDCl_3$) δ 7.95-6.77(m, 13H, H-Ar), 5.84 (d, 1H, $J_{1,2}$ = 8.5 Hz, H-1), 5.62 (s, 1H, PhCH), 4.74 (dd, 1H, $J_{2,3}$ =8.5 Hz, $J_{3,4}$ = 10.3 Hz, H-3), 4.54 (dd, 1H, $J_{1,2}$ =8.5 Hz, $J_{2,3}$ = 10.7 Hz, H-2), 4.44 (dd, 1H, $J_{5,6}$ = 4.5 Hz, $J_{6,6}$ = 10.7 Hz, H-6a), 3.90 (t, 1H, $J_{6,6}$ = 9.8 Hz, H-6), 3.81-3.66 (m, 5H, H-4, H-5, O*C*H_3).^{13}CNMR (100 MHz, $CDCl_3$): δ = 134.4-112.8 (C-Ar), 102.07 (*C*HPh), 98.10 (C-1), 82.04 (C-4), 68.69 (C-3), 68.63 (C-6), 66.32 (C-5), 56.47 (C-2), 55.70 (O*C*H_3). $[\alpha]_D^{25}$ = +64.10° (c 1.2, $CHCl_3$).

3-O-benzyl-4,6-O-benzylidene-2-deoxy-2-phthalimido-β-D-glucopyranosil trichloroacetimidate [46].

Sodium hydride (285 mg, 11.91 mmol) was added to a stirred solution of compound **45** (5 g, 9.93 mmol) in DMF (20 mL) at 0°C under argon. After 15 min benzyl bromide (2.08 mL, 13.90 mmol) was added, and the mixture was allowed warming to room temperature. After 2 h methanol (15 mL) was added, and the mixture was evaporated under reduced pressure. The product was dissolved in AcOEt (30 mL) and washed with $NaHCO_3$ (15 mL) and brine (15 mL), dried with Na_2SO_4 and evaporated under reduced pressure. The crude was purified with Biotage SNAP 50g column (hexane/AcOEt 0→100%) to afford **46** in 82% yield.

^{1}HNMR (400 MHz, $CDCl_3$): δ = 7.78- 6.74 (m, 18H, H-Ar), 5.77 (d, 1H, $J_{1,2}$ = 7.9 Hz, H-1), 5.68 (s, 1H, C*H*Ph), 4.86 (d, 1H, *J* = 12.4 Hz, C*H*HPh), 4.57 (d, 1H, *J* = 12.4 Hz, CH*H*Ph), 4.53-4.48 (m, 2H, H-3, H-2), 4.45 (dd, 1H, $J_{5,6}$ = 4.9, $J_{6,6}$ = 10.4 Hz, H-6a), 3.98-3.88 (m, 2H, H-4, H-6), 3.80-3.74 (m, 1H, H-5), 3.73 (s, 3H, OCH_3). ^{13}CNMR (100 MHz, $CDCl_3$): δ = 134.00-114.53 (C-Ar), 101.40 (*C*HPh), 98.00 (H-1), 83.00 (C-4), 74.20 (*C*H_2Ph), 74.51 (C-3), 68.74 (C-6), 55.74 (C-2), 66.30 (C-5), 55.60 (O*C*H_3). ESI MS m/z $[M+Na]^+$ = 616.18. $[\alpha]_D^{25}$ = +65.17° (c 1.1, $CHCl_3$).

3-O-benzyl-4,6-O-benzylidene-2-deoxy-2-phthalimido-α,β-D-glucopyranosyl trichloroacetimidate [41].

Cerium ammonium nitrate (9.1 g, 16.68 mmol) was added to a stirred solution of compound **46** (4.9 g, 8.34 mmol) in acetonitrile/H_2O 4:1 (80 mL) at 0°C. After 3 h, TLC (hexane/AcOEt 60:40) showed the disappearance of the starting material and the formation of one major spot. The reaction was washed with a solution of 10% $NaHCO_3$ (40 mL two times) and brine (40 mL) and the combined organic phases were dried with Na_2SO_4 and evaporated under reduced pressure. The crude (3.65 g, 7.50 mmol) was dissolved in DCM (35 mL) and CCl_3CN (4.51 mL, 45.0 mmol) and DBU (0.335 mL, 2.25 mmol) were added. The mixture was stirred for 2h, then concentrated under reduced pressure and the crude was purified by flash chromatography (hexane/AcOEt 60:40) to afford **41** in 70% yield in 1:2 α/β ratio. The presence of trichloroacetimidate was confirmed by ^{1}HNMR and the product **41** was immediately used in the next step to preserve trichloroacetimidate from the hydrolysis.

^{1}HNMR (400 MHz, $CDCl_3$): δ = 8.5 (s, 1H, NH) 7.62-6.80 (m, 14H, H-Ar), 6.42 (d, 1H, $J_{1,2}$ = 8.4 Hz, H-1$_\beta$), 6.30 (d, $J_{1,2}$ =3.8 Hz, H-1$_\alpha$), 5.60 (s, C*H*Ph$_\alpha$), 5.57 (s, 1H, C*H*Ph$_\beta$), 5.46 (t, H-3$_\alpha$) , 4.95 (d, 1H, *J* = 11.1 Hz, C*H*HPh$_\alpha$), 4.75 (d, 1H, *J* = 12.4 Hz, C*H*HPh$_\beta$), 4.62 (d, 1H, *J* = 11.1 Hz, CH*H*Ph$_\alpha$), 4.56 (dd, H-2$_\alpha$), 4.94-4.36 (m, H-2$_\beta$, H-3$_\beta$, CH*H*Ph$_\beta$, H-6$_{a\beta}$), 4.31 (dd, H-6$_{a\alpha}$), 4.18-4.12 (m, H-5$_\alpha$), 3.86-3.76 (m, H-4$_\alpha$, H-6$_{b\alpha}$, H-4$_\beta$, H-5$_\beta$, H-6$_{b\beta}$).

3-(benzyloxycarbonyl)-3-N-benzyl-aminopropyl [(3-O-benzyl-4,6-O-benzylidene-2-deoxy-2-phthalimido-β-D-glucopyranosyl)]-(1-3)-(2-O-acetyl-4-O-benzyl-α-rhamnopyranosyl)-(1-3)-(2,4-di-O-benzyl-α-rhamnopyranosyl)-(1-2)-[(3-O-benzyl-4,6-O-benzylidene-2-deoxy-2-phthalimido-β-D-glucopyranosyl)]-(1-3)-(4-O-benzyl-α-rhamnopyranosyl)-(1-3)-2,4-di-O-benzyl-α-rhamnopyranoside [42].

To a stirred solution of tetrasaccharide acceptor **38** (367 mg, 0.250 mmol) and monosaccharide donor **41** (633 mg, 1.002 mmol) in DCM (2.5 mL) containing activated 4 Å molecular sieves (200 mg), TMSOTf (11.13 μL, 0.050 mmol) was added at 0°C. The reaction was stirred at 0°C for 6h. After neutralization with TEA, the mixture was concentrated and purified with Biotage SNAP 50g column (toluene/AcOEt 0→100%) and with a second Biotage SNAP 25g column (hexane/AcOEt 0→100%) to afford the hexasaccharide **42** in 47% yield.

^{1}HNMR (400 MHz, $CDCl_3$): δ = 7.58-6.66 (m, 68H, Ph), 5.53 (s, 1H, H-1, Rha), 5.41 (bs, 1H, H-2^{IV}, Rha), 5.38 (d, 1H $J_{1,2}$ =7.2 Hz, H-1, GlcN), 5.33 (d, 1H, $J_{1,2}$ =7.2 Hz, H-1, GlcN), 5.23 (s, 1H, H-1, Rha), 2.65 (s, 2H, CH_2Cbz), 5.03-4.95 (m, 3H, H-1, Rha, PhC*H*H), 4.87 (s, 1H, H-1, Rha),

4.81-4.58 (m, 7H, PhC*H*H), 4.49-3.84 (m, 22H, PhC*H*H, *H*Rha, *H*GlcN), 3.79-3.47 (m, 11H, O-C*H*H-CH_2-CH_2-NH, *H*Rha, *H*GlcN), 3.41-3.14 (m, 8H, O-C*H*H-CH_2-CH_2-NH, O-CH_2-CH_2-C*H*$_2$-NH, *H*Rha, *H*GlcN), 2.12 (s, 3H, CH_3CO), 1.72 (bs, 2H, O-CH_2-C*H*$_2$-CH_2-NH), 1.24-1.14 (m, 9H, H-6, Rha), 0.95 (d, $J_{5,6}$ = 6.0 Hz, H-6, Rha). ^{13}CNMR (100 MHz, $CDCl_3$): δ = 133.54, 133.39, 128.72, 128.53, 128.45, 128.27, 128.25, 128.14, 127.98, 127.97, 127.84, 127.71, 127.33, 127.28, 127.22, 126.47, 126.26, 126.22, 101.26, 100.92, 100.61, 99.03, 98.74, 98.02, 82.91, 82.67, 82.47, 82.32, 79.64, 79.60, 79.59, 79.55, 79.53, 79.51, 77.21, 77.01, 74.55, 74.30, 74.31, 74.02, 68.72, 68.07, 68.06, 68.05, 68.04, 65.45, 65.07, 56.09, 55.87, 20.74, 18.13, 17.97, 17.88, 17.84.
MALDI: $[M+Na]^+$= 2322.13. $[\alpha]_D^{25}$ = -20.86° (c 1.1, $CHCl_3$).

3-aminopropyl [(2-deoxy-2-acetamido-β-D-glucopyranosyl)]-(1-3)-(α-rhamnopyranosyl)-(1-3)-(α-rhamnopyranosyl)-(1-2)-[(2-deoxy-2-acetamido-β-D-glucopyranosyl)]-(1-3)-(α-L-rhamnopyranosyl)-(1-3)-α-L-rhamnopyranoside [3].

Compound **42** (282 mg, 0.118 mmol) was dissolved in EtOH (4 mL) and etylendiamine (400 μL) was added. The solution was stirred overnight at 100°C. HP-TLC (toluene/AcOEt 60:40 + 0.1% TEA) showed the disappearance of starting material and the formation of main spot (R_f = 0.5). the solvent was co-evaporated with toluene, then the crude was dissolved in pyridine (2 mL) and cooled at 0°C. Acetic anhydride (2 mL) was added slowly and the solution was stirred overnight at room temperature. The TLC (hexane/AcOEt 70:30) showed the formation of a main spot (R_f = 0.4). The solvent was co-evaporated with toluene and purified with Biotage SNAP 25g column (hexane/AcOEt 0→100%). The foregoing product (257 mg, 0.115 mmol) was dissolved in MeOH (2 mL) and NaOMe was added until pH 9. The mixture was stirred for 5h, then neutralized with Amberlite (H^+ form), filtered and concentrated under reduced pressure. The intermediate (114 mg) was hydrogenated (H_2 pressure: 3 bar) in H_2O/EtOH 4:1 (3 mL) in the presence of 10% Pd/C (100 mg). The reaction was stirred at room temperature for 2 weeks, when ^{1}HNMR showed the disappearance of aromatic signals. The mixture was filtered through a celite pad, concentrated under vacuum, then lyophilized to afford product **3** in 40% yield after three steps.
^{1}HNMR (400 MHz, $CDCl_3$): δ = 5.18 (s, 1H, H-1^{III}, Rha), 5.07 (s, 1H, H-1^{II}, Rha), 5.02 (s, 1H, H-1^{IV}, Rha), 4.76 (s, 1H, H-1^{I}, Rha), 4.71 (d, 1H, $J_{1,2}$ =7.2 Hz ,H-1, GlcN), 4.69 (d, 1H, $J_{1,2}$ =7.2 Hz ,H-1, GlcN), 4.29, 4.26 (m, 2H, H-2^{II}, H-2^{IV}, Rha), 4.07 (bs, 1H, H-2^{III}, Rha), 3.99-3.89 (m, 4H, H-3^{II}, H-3^{IV}, Rha, H-6^{I}, H-6^{II}, GlcNAc), 3.83-3.67 (m, 8H, *H*Rha, *H*GlcNAc), 3.57-3.42 (m, 8H, O-C*H*H-CH_2-CH_2-NH, *H*Rha, *H*GlcNAc), 3.21-3.05 (m, 3H, O-C*H*H-CH_2-CH_2-NH, O-CH_2-CH_2-C*H*$_2$-NH), 2.02 (s, 3H, CH_3NH), 2.01 (s, 3H, CH_3NH), 1.80 (bs, 2H, O-CH_2-C*H*$_2$-CH_2-NH), 1.30-1.25 (m, 12H, H-6, Rha).

Characterization in agreement to M. Johnson, M. Pinto, *J. Am. Chem. Soc.*, **2002**, 124, 15368-15374.

7 **REFERENCES**

1. Cooper NR, Nemerow GR. The role of antibody and complement in the control of viral infections. *J Invest Dermatol*. 1984. doi:10.1038/jid.1984.33.
2. Bacchetta R, Gregori S, Roncarolo MG. CD4+ regulatory T cells: mechanisms of induction and effector function. *Autoimmun Rev*. 2005. doi:10.1016/j.autrev.2005.04.005.
3. Igietseme JU, Eko FO, He Q, Black CM. Antibody regulation of T-cell immunity: Implications for vaccine strategies against intracellular pathogens. *Expert Rev Vaccines*. 2004. doi:10.1586/14760584.3.1.23.
4. Hoebe K, Janssen E, Beutler B. The interface between innate and adaptive immunity. *Nat Immunol*. 2004. doi:10.1038/ni1004-971.
5. Costantino P, Rappuoli R, Berti F. The design of semi-synthetic and synthetic glycoconjugate vaccines. *Expert Opin Drug Discov*. 2011. doi:10.1517/17460441.2011.609554.
6. MacLeod CM. PREVENTION OF PNEUMOCOCCAL PNEUMONIA BY IMMUNIZATION WITH SPECIFIC CAPSULAR POLYSACCHARIDES. *J Exp Med*. 1945. doi:10.1084/jem.82.6.445.
7. Gold R, Artenstein MS. Meningococcal infections. 2. Field trial of group C meningococcal polysaccharide vaccine in 1969-70. *Bull World Health Organ*. 1971.
8. Artenstein MS, Gold R, Zimmerly JG, Wyle FA, Schneider H, Harkins C. Prevention of Meningococcal Disease by Group C Polysaccharide Vaccine. *N Engl J Med*. 1970. doi:10.1056/NEJM197002192820803.
9. Peltola H, Kayhty H, Sivonen A, Makela H. Haemophilus influenzae type b capsular polysaccharide vaccine in children: a double-blind field study of 100,000 vaccinees 3 months to 5 years of age in Finland. *Pediatrics*. 1977.
10. Peltola H, Mäkelä H, Käyhty H, et al. Clinical efficacy of meningococcus group A capsular polysaccharide vaccine in children three months to five years of age. *N Engl J Med*. 1977. doi:10.1056/NEJM197709292971302.
11. Schneerson R, Barrera O, Sutton A, Robbins JB. Preparation, characterization, and immunogenicity of Haemophilus influenzae type b polysaccharide-protein conjugate. *J Exp Med*. 1980. doi:10.1128/IAI.73.12.7887-7893.2005.
12. Anderson PW, Pichichero ME, Insel R a, Betts R, Eby R, Smith DH. Vaccines consisting of periodate-cleaved oligosaccharides from the capsule of Haemophilus influenzae type b coupled to a protein carrier: structural and temporal requirements for priming in the human infant. *J Immunol*. 1986.
13. Adamo R. Advancing Homogeneous Antimicrobial Glycoconjugate Vaccines. *Acc Chem Res*. 2017. doi:10.1021/acs.accounts.7b00106.
14. Kelly J, Jarrell H, Millar L, et al. Biosynthesis of the N-linked glycan in Campylobacter jejuni and addition onto protein through block transfer. *J Bacteriol*. 2006. doi:10.1128/JB.188.7.2427-2434.2006.
15. Ihssen J, Kowarik M, Dilettoso S, Tanner C, Wacker M, Thöny-Meyer L. Production of glycoprotein vaccines in Escherichia coli. *Microb Cell Fact*. 2010. doi:10.1186/1475-2859-9-61.
16. Decker MD, Edwards KM, Bradley R, Palmer P. Comparative trial in infants of four conjugate Haemophilus influenzae type b vaccines. *J Pediatr*. 1992. doi:10.1016/S0022-3476(05)80424-X.
17. Granoff DM, Anderson EL, Osterholm MT, et al. Differences in the immunogenicity of three Haemophilus influenzae type b conjugate vaccines in infants. *J Pediatr*. 1992.
18. Halperin SA, Gupta A, Jeanfreau R, et al. Comparison of the safety and immunogenicity of an investigational

and a licensed quadrivalent meningococcal conjugate vaccine in children 2-10 years of age. *Vaccine*. 2010. doi:10.1016/j.vaccine.2010.09.092.

19. Jackson LA, Baxter R, Reisinger K, et al. Phase III Comparison of an Investigational Quadrivalent Meningococcal Conjugate Vaccine with the Licensed Meningococcal ACWY Conjugate Vaccine in Adolescents. *Clin Infect Dis*. 2009. doi:10.1086/599117.
20. Southern J, Borrow R, Andrews N, et al. Immunogenicity of a reduced schedule of meningococcal group C conjugate vaccine given concomitantly with the prevenar and pediacel vaccines in healthy infants in the United Kingdom. *Clin Vaccine Immunol*. 2009. doi:10.1128/CVI.00420-08.
21. Adamo R, Nilo A, Castagner B, Boutureira O, Berti F, Bernardes GJL. Synthetically defined glycoprotein vaccines: Current status and future directions. *Chem Sci*. 2013. doi:10.1039/c3sc50862e.
22. Crotti S, Zhai H, Zhou J, et al. Defined conjugation of glycans to the lysines of CRM197 guided by their reactivity mapping. *ChemBioChem*. 2014. doi:10.1002/cbic.201300785.
23. Möginger U, Resemann A, Martin CE, et al. Cross Reactive Material 197 glycoconjugate vaccines contain privileged conjugation sites. *Sci Rep*. 2016. doi:10.1038/srep20488.
24. Stefanetti G, Hu QY, Usera A, et al. Sugar-Protein Connectivity Impacts on the Immunogenicity of Site-Selective Salmonella O-Antigen Glycoconjugate Vaccines. *Angew Chemie - Int Ed*. 2015. doi:10.1002/anie.201506112.
25. Hu QY, Allan M, Adamo R, et al. Synthesis of a well-defined glycoconjugate vaccine by a tyrosine-selective conjugation strategy. *Chem Sci*. 2013. doi:10.1039/c3sc51694f.
26. Carboni F, Adamo R, Fabbrini M, et al. Structure of a protective epitope of group B Streptococcus type III capsular polysaccharide. *Proc Natl Acad Sci*. 2017. doi:10.1073/pnas.1701885114.
27. Colombo C, Pitirollo O, Lay L. Recent Advances in the Synthesis of Glycoconjugates for Vaccine Development. *Molecules*. 2018. doi:10.3390/molecules23071712.
28. Fernández-Santana V, Cardoso F, Rodriguez A, et al. Antigenicity and immunogenicity of a synthetic oligosaccharide-protein conjugate vaccine against Haemophilus influenzae type b. *Infect Immun*. 2004. doi:10.1128/IAI.72.12.7115-7123.2004.
29. Oldrini D, Fiebig T, Romano MR, et al. Combined Chemical Synthesis and Tailored Enzymatic Elongation Provide Fully Synthetic and Conjugation-Ready Neisseria meningitidis Serogroup X Vaccine Antigens. *ACS Chem Biol*. 2018. doi:10.1021/acschembio.7b01057.
30. Love JC, Estroff LA, Kriebel JK, Nuzzo RG, Whitesides GM. Self-assembled monolayers of thiolates on metals as a form of nanotechnology. *Chem Rev*. 2005. doi:10.1021/cr0300789.
31. Compostella F, Pitirollo O, Silvestri A, Polito L. Glyco-gold nanoparticles: Synthesis and applications. *Beilstein J Org Chem*. 2017. doi:10.3762/bjoc.13.100.
32. Vetro M, Safari D, Fallarini S, et al. Preparation and immunogenicity of gold glyco-nanoparticles as antipneumococcal vaccine model. *Nanomedicine*. 2017. doi:10.2217/nnm-2016-0306.
33. Fallarini S, Paoletti T, Battaglini CO, et al. Factors affecting T cell responses induced by fully synthetic glyco-gold-nanoparticles. *Nanoscale*. 2013. doi:10.1039/c2nr32338a.
34. Smit J, Kamio Y, Nikaido H. Outer membrane of Salmonella typhimurium: chemical analysis and freeze-fracture studies with lipopolysaccharide mutants. *J Bacteriol*. 1975.
35. Ellis TN, Kuehn MJ. Virulence and Immunomodulatory Roles of Bacterial Outer Membrane Vesicles. *Microbiol Mol Biol Rev*. 2010. doi:10.1128/MMBR.00031-09.

36. Berlanda Scorza F, Colucci AM, Maggiore L, et al. High yield production process for Shigella outer membrane particles. *PLoS One*. 2012. doi:10.1371/journal.pone.0035616.
37. Rossi O, Pesce I, Giannelli C, et al. Modulation of endotoxicity of Shigella Generalized Modules for Membrane Antigens (GMMA) by genetic lipid A modifications: Relative activation of TLR4 and TLR2 pathways in different mutants. *J Biol Chem*. 2014. doi:10.1074/jbc.M114.566570.
38. Roberts R, Moreno G, Bottero D, et al. Outer membrane vesicles as acellular vaccine against pertussis. *Vaccine*. 2008. doi:10.1016/j.vaccine.2008.07.004.
39. Lu R, Popov V, Patel J, Eaves-Pyles T. Burkholderia mallei and Burkholderia pseudomallei stimulate differential inflammatory responses from human alveolar type II cells (ATII) and macrophages. *Front Cell Infect Microbiol*. 2012. doi:10.3389/fcimb.2012.00165.
40. Choh L-C, Ong G-H, Vellasamy KM, et al. *Burkholderia* vaccines: are we moving forward? *Front Cell Infect Microbiol*. 2013. doi:10.3389/fcimb.2013.00005.
41. Schild S, Nelson EJ, Camilli A. Immunization with Vibrio cholerae outer membrane vesicles induces protective immunity in mice. *Infect Immun*. 2008. doi:10.1128/IAI.00532-08.
42. Schild S, Nelson EJ, Bishop AL, Camilli A. Characterization of Vibrio cholerae outer membrane vesicles as a candidate vaccine for cholera. *Infect Immun*. 2009. doi:10.1128/IAI.01139-08.
43. Gerke C, Colucci AM, Giannelli C, et al. Production of a Shigella sonnei vaccine based on generalized modules for membrane antigens (GMMA), 1790GAHB. *PLoS One*. 2015. doi:10.1371/journal.pone.0134478.
44. De Benedetto G, Alfini R, Cescutti P, et al. Characterization of O-antigen delivered by Generalized Modules for Membrane Antigens (GMMA) vaccine candidates against nontyphoidal Salmonella. *Vaccine*. 2017. doi:10.1016/j.vaccine.2016.11.089.
45. Di Benedetto R, Micoli F, Saul A. WO 2018/096013 Al. 2018;00(12).
46. Baron S. *Medical Microbiology. 4th Edition*.; 1996. doi:NBK8035 [bookaccession].
47. Lancefield RC. A SEROLOGICAL DIFFERENTIATION OF HUMAN AND OTHER GROUPS OF HEMOLYTIC STREPTOCOCCI. *J Exp Med*. 1933. doi:10.1084/jem.57.4.571.
48. Coligan JE, Kindt TJ, Krause RM. Structure of the streptococcal groups A, A-variant and C carbohydrates. *Mol Immunol*. 1978. doi:10.1016/0161-5890(78)90105-0.
49. Carapetis JR, Steer AC, Mulholland EK, Weber M. The global burden of group A streptococcal diseases. *Lancet Infect Dis*. 2005. doi:10.1016/S1473-3099(05)70267-X.
50. Walker MJ, Barnett TC, McArthur JD, et al. Disease manifestations and pathogenic mechanisms of group A Streptococcus. *Clin Microbiol Rev*. 2014. doi:10.1128/CMR.00101-13.
51. Steer AC, Law I, Matatolu L, Beall BW, Carapetis JR. Global emm type distribution of group A streptococci: systematic review and implications for vaccine development. *Lancet Infect Dis*. 2009. doi:10.1016/S1473-3099(09)70178-1.
52. Gillen CM, Towers RJ, McMillan DJ, et al. Immunological response mounted by Aboriginal Australians living in the Northern Territory of Australia against Streptococcus pyogenes serum opacity factor. *Microbiology*. 2002. doi:10.1099/00221287-148-1-169.
53. Smeesters PR, McMillan DJ, Sriprakash KS. The streptococcal M protein: A highly versatile molecule. *Trends Microbiol*. 2010. doi:10.1016/j.tim.2010.02.007.
54. D'Alessandri R, Plotkin G, Waldman RH, et al. Protective studies with group a streptococcal m protein vaccine. iii. challenge of volunteers after systemic or intranasal immunization with type 3 or type 12 group a

streptococcus. *J Infect Dis*. 1978. doi:10.1093/infdis/138.6.712.

55. McNeil S a, Halperin S a, Langley JM, et al. Safety and immunogenicity of 26-valent group a streptococcus vaccine in healthy adult volunteers. *Clin Infect Dis*. 2005. doi:10.1086/444458.
56. Dale JB, Penfound TA, Tamboura B, et al. Potential coverage of a multivalent M protein-based group A streptococcal vaccine. *Vaccine*. 2013. doi:10.1016/j.vaccine.2013.01.019.
57. Mannam P, Jones KF, Geller BL. Mucosal vaccine made from live, recombinant Lactococcus lactis protects mice against pharyngeal infection with Streptococcus pyogenes. *Infect Immun*. 2004. doi:10.1128/IAI.72.6.3444-3450.2004.
58. Batzloff MR, Hayman WA, Davies MR, et al. Protection against group A streptococcus by immunization with J8-diphtheria toxoid: contribution of J8- and diphtheria toxoid-specific antibodies to protection. *J Infect Dis*. 2003. doi:10.1086/374800.
59. Bauer MJ, Georgousakis MM, Vu T, et al. Evaluation of novel Streptococcus pyogenes vaccine candidates incorporating multiple conserved sequences from the C-repeat region of the M-protein. *Vaccine*. 2012. doi:10.1016/j.vaccine.2011.12.115.
60. Steer AC, Carapetis JR, Dale JB, et al. Status of research and development of vaccines for Streptococcus pyogenes. *Vaccine*. 2016. doi:10.1016/j.vaccine.2016.03.073.
61. Salvadori LG, Blake MS, Mc carty M, Tai JY, Zabriskie JB. Group a streptococcus-liposome elisa antibody titers to group a polysaccharide and opsonophagocytic capabilities of the antibodies. *J Infect Dis*. 1995. doi:10.1093/infdis/171.3.593.
62. Sabharwal H, Michon F, Nelson D, et al. Group A streptococcus (GAS) carbohydrate as an immunogen for protection against GAS infection. *JInfectDis*. 2006. doi:JID34910 [pii]\n10.1086/498618.
63. Reimer KB, Harris SL, Varma V, Mario Pinto B. Convergent synthesis of higher-order oligosaccharides corresponding to the cell-wall polysaccharide of the β-hemolytic streptococci group A. a branched hexasaccharide hapten. *Carbohydr Res*. 1992. doi:10.1016/0008-6215(92)84133-D.
64. Marino-Albernas JR, Harris SL, Varma V, Pinto BM. Convergent synthesis of an elusive hexasaccharide corresponding to the cell-wall polysaccharide of the β-hemolytic Streptococcus Group A. *Carbohydr Res*. 1993. doi:10.1016/0008-6215(93)80075-P.
65. Auzanneau FI, Pinto BM. Preparation of antigens and immunoadsorbents corresponding to the Streptococcus group A cell-wall polysaccharide. In: *Bioorganic and Medicinal Chemistry*. ; 1996. doi:10.1016/S0968-0896(96)00183-6.
66. Johnson MA, Pinto BM. NMR spectroscopic and molecular modeling studies of protein-carbohydrate and protein-peptide interactions. In: *Carbohydrate Research*. ; 2004. doi:10.1016/j.carres.2003.12.028.
67. Johnson MA, Pinto BM. Saturation transfer difference 1D-TOCSY experiments to map the topography of oligosaccharides recognized by a monoclonal antibody directed against the cell-wall polysaccharide of group a Streptococcus. *J Am Chem Soc*. 2002. doi:10.1021/ja020983v.
68. Kabanova A, Margarit I, Berti F, et al. Evaluation of a group a streptococcus synthetic oligosaccharide as vaccine candidate. *Vaccine*. 2010. doi:10.1016/j.vaccine.2010.09.018.
69. Auzanneau F-I, Borrelli S, Pinto BM. Synthesis and immunological activity of an oligosaccharide-conjugate as a vaccine candidate against Group A Streptococcus. *Bioorg Med Chem Lett*. 2013. doi:10.1016/j.bmcl.2013.09.042.
70. Malkiel S, Liao L, Cunningham MW, Diamond B. T-cell-dependent antibody response to the dominant epitope

of streptococcal polysaccharide, N-acetyl-glucosamine, is cross-reactive with cardiac myosin. *Infect Immun*. 2000. doi:10.1128/IAI.68.10.5803-5808.2000.

71. Van Sorge NM, Cole JN, Kuipers K, et al. The classical lancefield antigen of group A Streptococcus is a virulence determinant with implications for vaccine design. *Cell Host Microbe*. 2014. doi:10.1016/j.chom.2014.05.009.
72. Henningham A, Davies MR, Uchiyama S, et al. Virulence role of the glcnac side chain of the lancefield cell wall carbohydrate antigen in non-m1-serotype group a streptococcus. *MBio*. 2018. doi:10.1128/mBio.02294-17.
73. Michon F, Moore SL, Kim J, et al. Doubly branched hexasaccharide epitope on the cell wall polysaccharide of group A streptococci recognized by human and rabbit antisera. *Infect Immun*. 2005. doi:10.1128/IAI.73.10.6383-6389.2005.
74. Anderson W, Kozak D, Coleman VA, et al. Nanoparticles and microparticles for drug and vaccine delivery. *J Anat*. 2013. doi:10.1002/bit.
75. Riener CK, Kada G, Gruber HJ. Quick measurement of protein sulfhydryls with Ellman's reagent and with 4,4′-dithiodipyridine. *Anal Bioanal Chem*. 2002. doi:10.1007/s00216-002-1347-2.
76. Geert Volbeda A, Van Mechelen J, Meeuwenoord N, Overkleeft HS, Van Der Marel GA, Codée JDC. Cyanopivaloyl Ester in the Automated Solid-Phase Synthesis of Oligorhamnans. *J Org Chem*. 2017. doi:10.1021/acs.joc.7b02511.
77. Habeeb AFSA. Determination of free amino groups in proteins by trinitrobenzenesulfonic acid. *Anal Biochem*. 1966. doi:10.1016/0003-2697(66)90275-2.
78. Silvestri A, Zambelli V, Ferretti AM, Salerno D, Bellani G, Polito L. Design of functionalized gold nanoparticle probes for computed tomography imaging. *Contrast Media Mol Imaging*. 2016. doi:10.1002/cmmi.1704.

Acknowledgements

This work was sponsored by GlaxoSmithKline Vaccine in Siena. GSK Vaccine Institute for Global Health is an affiliate of GlaxoSmithKline. This thesis was realized in collaboration with University of Milan. Thanks to prof. L. Lay (Department of Chemistry, University of Milan); Dr. F. Micoli (GVGH); R. Adamo (GSK); L. Polito (CNR-ISTM, Nanotechnology Lab, Milan); D.Gomes Moriel (Project Leader, GVGH); A. Saul (Institute Director, GVGH). Thanks to all L. Lay's group (Department of Chemistry, University of Milan); all GVGH in Siena.